11-10-2010

The Conversion of Low-Grade Heat into Power Using Supercritical Rankine Cycles

Huijuan Chen
University of South Florida

The Conversion of Low-Grade Heat into Power Using Supercritical Rankine Cycles

by

Huijuan Chen

A dissertation submitted in partial fulfillment
of the requirements for the degree of
Doctor of Philosophy
Department of Chemical & Biomedical Engineering
College of Engineering
University of South Florida

Co-Major Professor: D. Yogi Goswami, Ph.D.
Co-Major Professor: Elias K. Stefanakos, Ph.D.
Muhammad M. Rahman Ph.D.
John T. Wolan, Ph.D.
Dale Johnson, Ph.D.

Date of Approval:
November 10, 2010

Keywords: Organic Rankine Cycle, Working Fluids, Heat Recovery, Efficiency, Optimization

DEDICATION

To the loving memory of my mother.

ACKNOWLEDGEMENTS

Looking back, I am grateful for all I have received throughout these years. It is my pleasure to acknowledge those people who have made this work possible.

I want to thank my advisor Dr. D. Yogi Goswami, for inspiring and encouraging me to be a researcher and engineer of innovative and critical thinking. His knowledge, zeal and dedication towards research have influenced me so much through my graduate study at the University of South Florida. I would be able to walk out of here with confidence if I have obtained a fraction of his knowledge and talent through the years. My co-advisor, Dr. Elias K. Stefanakos, has always been there to listen, support and give advice. My thanks go out to my committee members Dr. Muhammad M. Rahman, Dr. John T. Wolan, Dr. Dale Johnson and Dr. Babu Joseph for their valued suggestions and support in one way or another through my studies. Special thanks go to Dr. Amir Abtahi for his chairing my dissertation defense. I would like to acknowledge Dr. Aydin K. Sunol for his professional guidance. My friends and the whole CERC crew have made my life here so delightful and memorable.

My family to whom this dissertation is dedicated have been a constant source of love, concern, support and strength all these years and I would like to express my heart-felt gratitude to them.

TABLE OF CONTENTS

LIST OF TABLES

LIST OF FIGURES

LIST OF SYMBOLS

Nomenclature

e	Specific exergy (J)
E	Exergy (J)
$\dot{E}$	Rate of exergy (J/s)
h	Specific enthalpy (J/kg)
I	Irreversibility (J)
$\dot{I}$	Rate of irreversibility (J/s)
L	Latent heat (J)
$\dot{m}$	Flow rate (kg/s)
N_p	Power of the pump (J/s, W)
N_t	Power of the turbine (J/s, W)
P	Pressure (bar)
P_c	Critical pressure (MPa)
$\dot{q}$	Heat flow (J/s)
Q	Heat input (J)
q	Heat input per mass (J/kg)
R	Universal gas constant (J/ K–mol)
s	Salt concentration(%), entropy (J/K)
T	Temperature (K)
T_c	Critical temperature (K)
T_{rH}	Reduced evaporation temperature (K)
T_o	Temperature at dead state (K)
v_m	Mole volume (m^3/mol)
w	Work output (J)
z	Vertical coordinate (m)

ΔH	Enthalpy of vaporization (J)
ΔV	Volume change of the phase transition (m^3)
η	Efficiency
ξ	Ratio of entropy and temperature on a saturation curve (J/K^2)
ρ	Density (g/cm^3)

Subscripts

c	Condenser
cov	Energy conversion
ex	Exergy
f	Fluid
h	high temperature, heating process
in	Input
l	Low temperature
out	Output
p	pump
t	Turbine
th	Thermal
zeo	Zeotropic mixture

Superscripts

in	Input
out	Output

ABSTRACT

Low-grade heat sources, here defined as below 300 ºC, are abundantly available as industrial waste heat, solar thermal, and geothermal, to name a few. However, they are under-exploited for conversion to power because of the low efficiency of conversion. The utilization of low-grade heat is advantageous for many reasons. Technologies that allow the efficient conversion of low-grade heat into mechanical or electrical power are very important to develop.

This work investigates the potential of supercritical Rankine cycles in the conversion of low-grade heat into power. The performance of supercritical Rankine cycles is studied using ChemCAD linked with customized excel macros written in Visual Basic and programs written in C++.

The selection of working fluids for a supercritical Rankine cycle is of key importance. A rigorous investigation into the potential working fluids is carried out, and more than 30 substances are screened out from all the available fluid candidates. Zeotropic mixtures are innovatively proposed to be used in supercritical Rankine cycles to improve the system efficiency.

Supercritical Rankine cycles and organic Rankine cycles with pure working fluids as well as zeotropic mixtures are studied to optimize the conversion of low-grade heat into power. The results show that it is theoretically possible to extract and

convert more energy from such heat sources using the cycle developed in this research than the conventional organic Rankine cycles. A theory on the selection of appropriate working fluids for different heat source and heat sink profiles is developed to customize and maximize the thermodynamic cycle performance.

The outcomes of this research will eventually contribute to the utilization of low-grade waste heat more efficiently.

CHAPTER 1 INTRODUCTION AND OBJECTIVES

1.1 Overview

Currently, two-thirds of the world's electricity demand is met by non-renewable fossil fuels which has led to serious environmental problems and a widespread energy crisis. In trying to limit the emissions from the electricity generating sector, new energy resources as well as radically new technologies should be developed and/or current technologies be improved so that the power output per unit of pollution is reduced.

Renewable energy sources, such as solar thermal and geothermal, and vast amounts of industrial waste heat are potentially promising energy sources capable, in part, to meet the world electricity demand. However, the above mentioned energy sources are available largely at moderate temperatures. The conventional steam Rankine cycle works only efficiently at above 300 ºC, and the conversion efficiency becomes uneconomically low for the low-grade heat sources conversion [1-4].

In this context, developing other technologies that allow the efficient conversion of low-grade heat into mechanical or electrical power is of great significance.

1.2 Objectives

This research focuses on supercritical Rankine cycles for converting low-grade heat into mechanical or electrical power. This is a promising direction due to its simplicity in system configuration and advantage in cycle efficiency. The main objective of this project is to investigate the potential of a supercritical Rankine cycle to convert low-grade thermal energy by analyzing the desired properties of the working fluid candidates, studying the performance of the supercritical Rankine cycles, and optimizing the thermodynamic system. Other objectives of this work include screening the working fluids for supercritical Rankine cycles, comparing the performance of supercritical Rankine cycles with other thermodynamic cycles, and suggesting some feasible applications of the supercritical Rankine cycle.

CHAPTER 2 RESEARCH BACKGROUND

Low grade heat could be used to produce mechanical or electrical power and consequently reduce the burning of fossil fuels and emission of greenhouse gases. This chapter explores a variety of underutilized sustainable and waste low-grade heat sources that can be employed for power production as well as it reviews the thermodynamic technologies that have been proposed for the energy conversion.

2.1 Low-Grade Heat Sources

2.1.1 Solar Thermal

The solar radiation is incident on the earth's surface at a rate of approximately 1.7×10^{17} watts [5], more than 10,000 times the present world energy consumption [6]. In order to be more usable, however, the energy must be collected and converted to a suitable form. Solar thermal energy can be produced by using solar thermal collectors, solar ponds, etc.

Solar ponds are large-scale solar thermal energy collectors, which are pools filled with saltwater with a density gradient from the bottom to the top. A solar pond combines heat collection and storage. In a solar pond, the irradiation coming from the sun is transmitted through the water and captured by the dark-colored bottom of the

pond, where the saltwater concentration is maximum. Assuming that the density gradient follows the equation below, natural convection of heated water at the bottom is suppressed, which allows storage of heat in the bottom layer of the pond [5].

$$\frac{d\rho}{dz} = \frac{\partial \rho}{\partial s}\frac{ds}{dz} + \frac{\partial \rho}{\partial T}\frac{dT}{dz} \geq 0 \quad (2.1)$$

where s is the salt concentration, ρ is the density, T is the temperature, and z is the vertical coordinate, increasing downward.

With a 20°C ambient temperature, the thermal energy obtained from the solar ponds is in the form of low-grade heat at 70 to 80°C. The heat from the bottom layer of the brine can be extracted either by pumping out the brine itself or through a heat exchanger system.

There are not many commercial solar ponds existing to date that produce electricity and/or heat consistently. But there are a few examples running in the United States, Israel, and India. The EI Paso solar pond in Texas has been running since 1986, producing up to 10 kW electrical power using an organic Rankine cycle [7]; The Beith Ha'Avara Solar Pond located just north of the Dead Sea in Israel was the largest solar pond ever built and operated for electricity production, with an electrical output of 5 MW and surface area of 210000 m^2. However, the operation stopped in 1988 [8]. Other examples of solar pond are the Bhuj solar pond in India and the research ponds conjointly built by RMIT, Geo-Eng Australia Pty Ltd and

Pyramid Salt Pty Ltd in Australia. Below is a photo of a solar pond in Pyramid Hill, Victoria, Australia.

Figure 2.1 Solar pond in Pyramid Hill, Victoria, Australia [9]

There are low-, medium- and high- temperature solar thermal collectors, depending on their collecting temperature. Low temperature collectors are normally flat plate collectors with or without glazing. A flat plate collector basically consists of an absorber surface, a trap to reduce energy losses from the absorber surface, a heat transfer medium, and thermal insulation behind the absorber surface [5]. Temperatures around 80°C are normally obtained with such collectors, although higher temperatures can be obtained from higher efficiency collectors. Medium-temperature collectors are at a temperature levels of 80 - 250°C. This temperature can be reached by double glazed flat plate collectors, evacuated tube collectors, stationary concentrating collectors, and concentrating collectors with tracking.

Concentration of solar radiation is achieved by reflecting or refracting the flux incident on an aperture area A_a onto a smaller receiver/absorber area A_r [5]. There are parabolic trough concentrators, compound-curvature solar concentrators, central receiver collector, and Fresnel reflector concentrators. Recently, linear Fresnel reflector concentrator is attracting a lot of attention for medium temperature applications. It uses modular flat reflectors to focus the sunlight onto elevated receivers (See Figure 2.2). The heat transfer fluid in the tube is water, which is vaporized, and becomes high-pressure steam for direct conversion through steam turbines.

Figure 2.2 One dimensional moving flat detector or Fresnell reflector [10]

Parabolic trough solar collectors are the most common high-temperature collectors. Sunlight is concentrated on the focal line of the trough, where the heat is collected by a selective absorber material enclosed in an evacuated glass tube. With a

solar concentrating ratio of 40:1, the temperature of the solar collector can reach as high as 400°C. The world's largest parabolic trough power plant facilities are located in the Mojave Desert, which consist of nine plants producing 345 megawatts of power at peak output (See Figure 2.3).

Figure 2.3 Parabolic trough solar collectors [10]

2.1.2 Geothermal Energy

The Earth's internal heat flows to the surface by conduction at a rate of 44.2 terawatts (TW) [11]. Hot springs, hot geysers, and steam vents are examples of geothermal flux. Human extraction taps only an insignificant fraction of the natural outflow. Therefore, geothermal is considered to be a sustainable resource. Up to date, 10715 MW of geothermal power in 24 counties is online based on a report from the International Geothermal Association (IGA), and 67246 GWh of electricity is expected to be generated from geothermal energy in 2010 [12], of which 3086 MW is

generated in the United States. After the United States, Philippines is the second largest geothermal power producer, with 1904 MW of capacity online, making up about 18% of the country's electricity generation [13].

Present geothermal power generation is still mainly from hydrothermal reservoirs, and it is limited in geographic application to specific locations. Enhanced geothermal systems (EGS, also called engineered geothermal systems), on the other hand, do not require natural convective hydrothermal resources. By fracturing hot rock 3-10 km underground, circulating water through fractured hot rock, geothermal energy is drilled to the ground. Theoretically, EGS can be developed anywhere there is sufficiently hot rock. A 2006 report conducted by MIT, funded by the U.S. Department of Energy provides the most comprehensive analysis to date on the potential and technical status of EGS [14]. The report indicates the United States total EGS resources from 3000-10000m of depth to be over 200 zettajoules of extractable geothermal energy, 2000 zettajoules with technology improvements. That amount of energy is sufficient to provide the entire world's current energy need for several millennia. The histogram in Figure 2.4 shows the heat content in the continental United States as a function of depth of 1km slices. It indicates that there is a tremendous resource base of approximately 13 million EJ, between the depths of 3.5 to 7.5 km in the temperature range of 150°C to 250°C in the continental United States. Even if only 2% of the resource were to be developed, the thermal energy recovered

would be 260,000 EJ, which is roughly 2,600 times the annual primary energy consumption in the United States in 2006 [14]. However, it has to be mentioned that there are concerns of earthquakes caused by EGS, the Basel earthquakes in 2006 being an example, resulted in the cancellation of an EGS project in 2009.

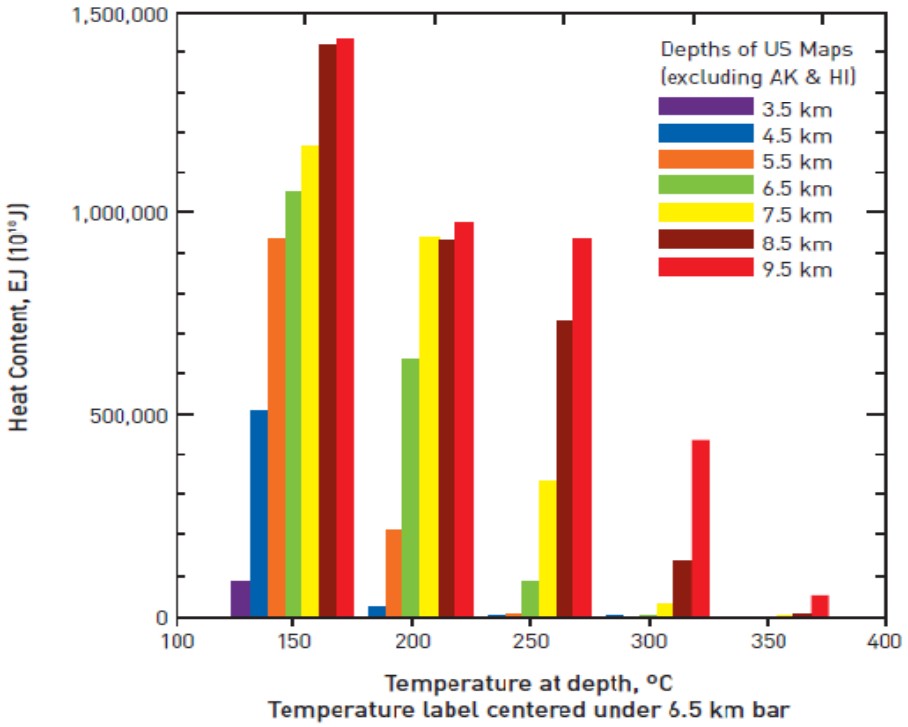

Figure 2.4 Histograms of heat content in EJ, as a function of depth for 1 km slices [14]

2.1.3 Industrial Waste Heat

Statistical investigations indicate that about 50% of all fuel burned by industrial sources becomes waste heat, mostly low-grade. This wasted heat is found at all stages of processes, such as inefficient generation, transmission, and during final use of the energy. Waste heat can be recovered directly and, more commonly,

indirectly. Direct heat recovery is often the cheaper option; however, its utilization is restricted by location, energy form, and contamination considerations. In indirect heat recovery systems, waste heat is passed on to another system through heat exchangers, from where heat is transferred and converted. In general, waste heat at temperatures of 300-400°C can be found in industries such as iron and steel, glass, nonferrous metals, bricks and ceramics processing. Medium temperature waste heat at the level of 150 °C is mainly identified in industries such as food, chemicals, refining, and building utilities. Low temperature waste heat is easily found in virtually all areas of industry. Although abundantly available, a large amount of the low-grade heat has not been efficiently utilized, and discarding it has become an environmental concern. The figure below shows the useful energy and the energy losses in major industrial sectors, indicating there are substantial energy losses in every section of the industry.

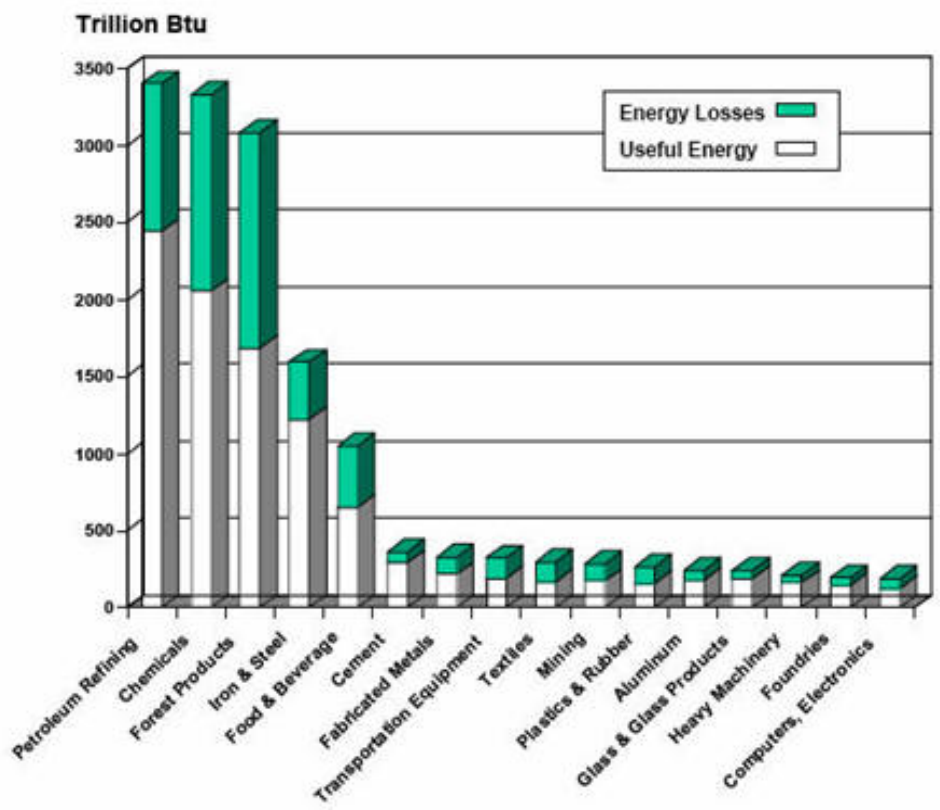

Figure 2.5 Useful energy and energy losses in major industrial sectors [15]

To sum up, low-grade heat resources are abundantly available, but not efficiently utilized. It leaves us a huge potential to explore. However, the moderate temperature heat from these sources cannot be converted efficiently to electrical power by conventional power generation methods. In this context, research on how to convert this low-grade heat is of great significance. Various thermodynamic cycles such as the organic Rankine cycle, supercritical Rankine cycle, Kalina cycle, Goswami cycle, and trilateral flash cycle have been proposed and studied for the conversion of low-grade heat sources into electricity. But there is still much to learn

to improve the performance and bring down the costs. The following section is a brief review of the thermodynamic cycles.

2.2 Thermodynamic Cycles for the Conversion of Low-Grade Heat

2.2.1 Kalina Cycle

The Kalina cycle was first developed by Aleksandr Kalina in the late 1970's and early 1980's [16]. Since then, several variations of the Kalina cycle have been proposed based on different applications. Kalina cycle uses a working fluid comprised of at least two different components, typically water and ammonia. The ratio between those components varies in different parts of the system to decrease thermodynamic irreversibility and therefore increase the overall thermodynamic efficiency. A basic configuration of the Kalina cycle is shown in Figure 2.6. In the Kalina cycle, the use of a mixture results in a good thermal match in the boiler due to the non-isothermal boiling created by the shifting mixture composition. Several studies have shown that the Kalina cycle performs substantially better than a steam Rankine cycle system [17-20]. A second law analysis showed that by using a binary fluid, the Kalina cycle reduced irreversibility in the boiler, resulting in 10 to 20% higher exergy efficiency than the conventional Rankine cycle [21].

The Kalina Cycle System No.12 is a modification of the Kalina cycle that was proposed for geothermal applications [22]. Kalina cycle system No.12 has a more complicated network of recovery heat exchangers but no distillation arrangement.

Desideri et al. [22] studied the Kalina cycle system No.12, and concluded that there is a potential for optimization of the performance by using feasible non-conventional fluids.

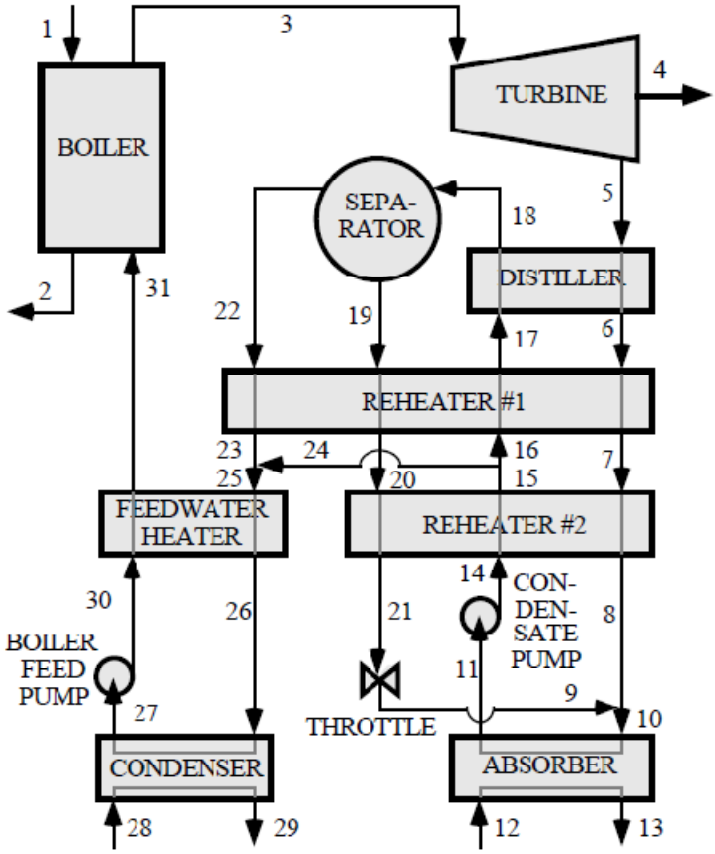

Figure 2.6 Basic configuration of the Kalina cycle [21]

The first bottoming cycle demonstration of the Kalina power plant was at the Energy Technology and Engineering Center, a DOE facility near Canoga Park, California, which is a 3MW demonstration plant constructed in 1992 and put into operation in 1996 [23]. The Kalina Cycle trademark and patents are now owned by Global Geothermal Ltd [24]. The Sumitomo Metal steelworks and Fuji Oil's refinery

in Tokyo Bay are using the Kalina cycle to recover their waste heat [25]. Kalina cycles also are in operation in gethermal power plants in Husavik, Iceland, and Untherhaching, Germany [25].

Dejfors et al. [20] investigated the thermodynamic advantages of using ammonia-water mixture cycles in small direct-fired biomass fueled cogeneration plants. Different configurations of the ammonia-water mixture cycle were compared to a Rankine steam cycle with a five-pressure turbine and three preheaters. With condensing power application, the ammonia-water cycle reaches higher power generation than the Rankine steam cycle.

Figure 2.7 Kalina cycle geothermal power plant in Iceland [26]

The above figure is the first Kalina cycle geothermal power plant in Iceland, built by Mannvit Engineering in 1999, and commissioned in the middle of 2000. The power plant generates two megawatts of electricity from the geothermal brine flow of 90 kg/s, at a temperature of 120°C. The two megawatt power generated from the

geothermal power plant fulfills up to 80% of the electricity demand of the Husavik town, where the plant is located [24]. The discharged brine is at 80°C, which can still be used for various purposes, such as district heating. The Kalina cycle based geothermal power station in a small town outside of Munich, Germany is the second plant of this kind. The plant is capable of generating 3.4 megawatts of electricity—or enough to power 10,000 homes, as the company claims [27].

One drawback of the Kalina cycle relates to the corrosivity of ammonia. Impurities in liquid ammonia such as air or carbon dioxide can cause stress corrosion cracking of mild steel and also ammonia is highly corrosive towards copper and zinc. Also it can be seen from the simplified schematic in Figure 2.6, there is still a very high level of complexity to build a Kalina cycle power plant. The extra capital costs may overweigh the benefit of the increased conversion efficiency.

2.2.2 Goswami Power and Cooling Cogeneration Cycle

Goswami cycle, proposed by Dr. Yogi Goswami (1998) is a novel thermodynamic cycle that uses a binary mixture to produce power and refrigeration simultaneously in one loop [26]. This cycle is a combination of the Rankine power cycle and an absorption cooling cycle. Its advantages include the production of power and cooling in the same cycle, the design flexibility to produce any combination of power and refrigeration, the efficient conversion of moderate temperature heat sources, and the possibility of improved resource utilization compared to separate

power and cooling systems [28]. The binary mixture first used was ammonia-water, and later on new binary fluids were proposed and studied. A configuration of the cycle is shown in Figure 2.8. The cycle can be described this way: the ammonia-strong saturated solution (1) from the absorber (AB) is pumped to a high pressure (2). It is then split into two streams; stream 2A and stream 2B, the former recovers the heat from the rectifier (RE), and the latter recovers the heat from the weak solution (10) from the generator (GE). The condensed liquid (5) from the rectifier (RE) and both 3A and 3B (i.e. 2A and 2B after the recovery, respectively) streams are mixed in a mixer (MX) and then fed to the generator (3). In the generator (GE), stream 3 is separated into the aforesaid weak ammonia-water solution (10) and ammonia-rich vapor by the heat from a low-grade heat source. The ammonia-rich vapor (4) is then purified in the above-mentioned rectifier (RE). The ammonia-rich vapor after the rectifier (6) can be superheated through heat exchanger HE-2 and then expanded through the turbine (VT) to produce power. The ammonia vapor leaving the turbine is at a temperature low enough to be used for cooling purposes. The ammonia-weak solution (11) coming from the recovery heat exchanger HE-1 passes through an expansion valve (TV) where it is throttled down to the cycle low pressure (12). Both stream 12 and stream 9 are fed to the absorber to produce the ammonia-strong saturated solution (1) completing the cycle.

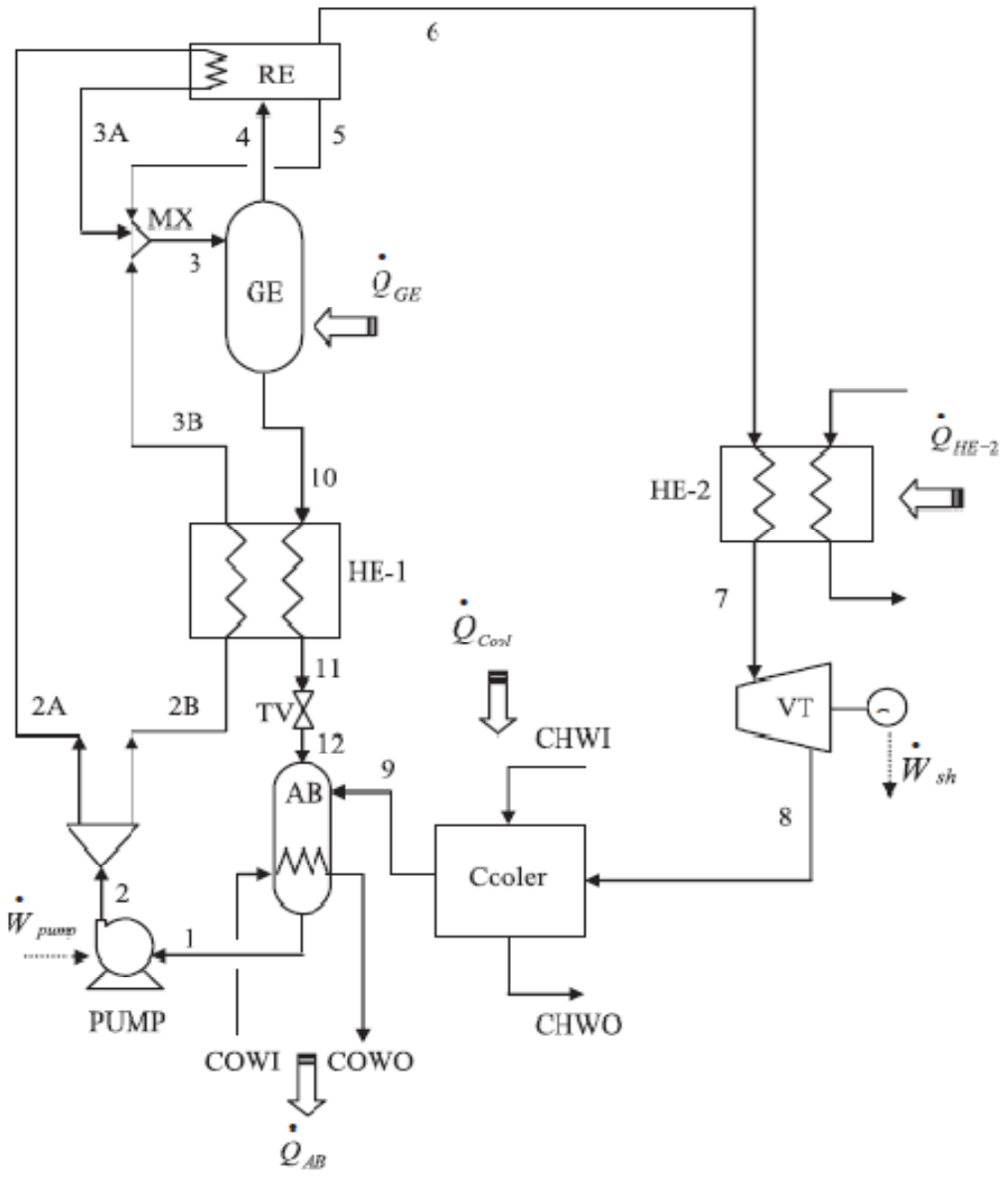

Figure 2.8 The basic configuration of the combined power and cooling cycle [29]

A parametric analysis of the cycle using a low temperature sensible heat source established the feasibility of the proposed configuration by Goswami and his group [30]. The parametric study also showed that there is an optimal operation of the cycle. Finding the optimum working condition is a non-linear problem, which was

handled by the optimization method of Generalized Reduced Gradient (GRG) algorithm in several studies of this cycle [16], [31], [32]. The lowest temperature that could be achieved using the Goswami cycle was found to be as low as 205K (-68ºC) with an ammonia-water working fluid [33]. However, it has to be mentioned that the requirement for a low absorber pressure and pure ammonia vapor become very stringent in order to get this low temperature refrigeration. As the system has two outputs, electricity and refrigeration, the optimization of the system is more complicated. Different analyses have been done on the optimized electricity output, optimized refrigeration output, and optimized first law efficiency, second law efficiency, and energy utilization efficiency. Modified configurations of the Goswami cycle were studied by adding a distillation process to improve the performance of the system [28]. Experimental studies were also done to verify the actual performance of the combined power and cooling cycle [34]. The results indicated that both power and cooling can be obtained simultaneously.

The Goswami cycle power system is still at a research stage. However, an experimental setup was built at the University of Florida in the 1990's, and now it is relocated to the Research Park of the University of South Florida. Below is a snapshot of the experimental setup.

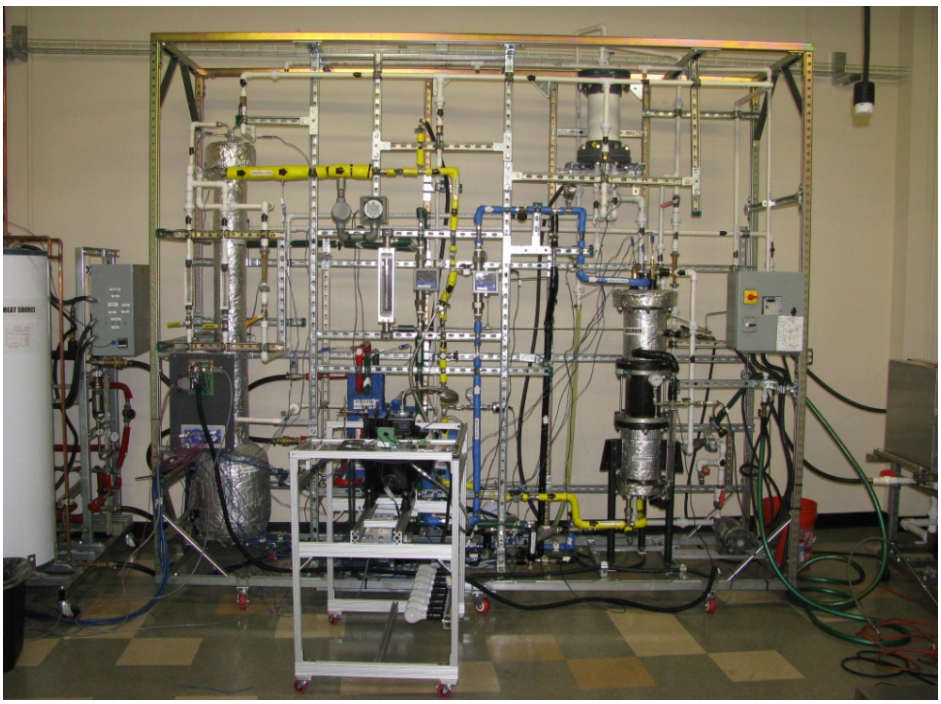

Figure 2.9 An experimental setup of the Goswami cycle

2.2.3 Trilateral Flash Cycle

Figure 2.10 is the configuration of a trilateral flash cycle and its process in a T-s diagram. A trilateral flash cycle (TFC) is a thermodynamic power cycle whose expansion starts from the saturated liquid rather than a vapor phase. By avoiding the boiling part, the heat transfer from a heat source to a liquid working fluid is achieved with almost perfect temperature matching. Irreversibilities are thereby minimized. According to Stiedel et al. [35], its potential power recovery could be 14 - 85% more than from ORC or flash steam systems provided that the two-phase expansion process is efficient.

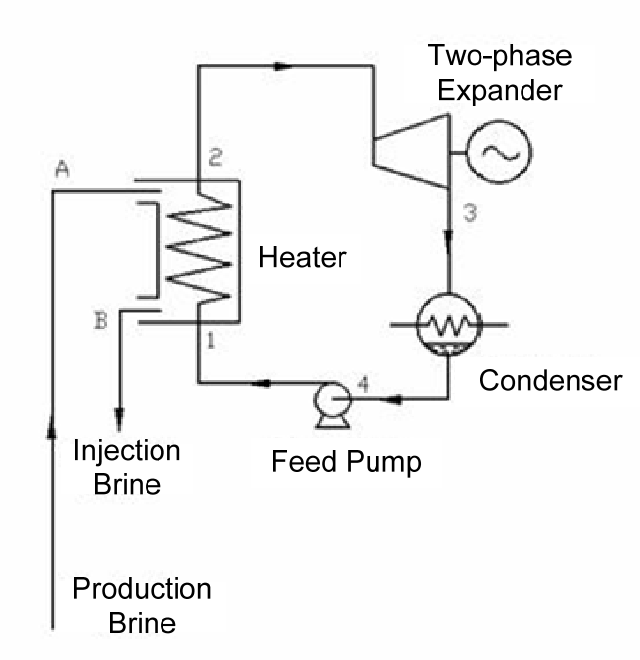

(a) The configuration

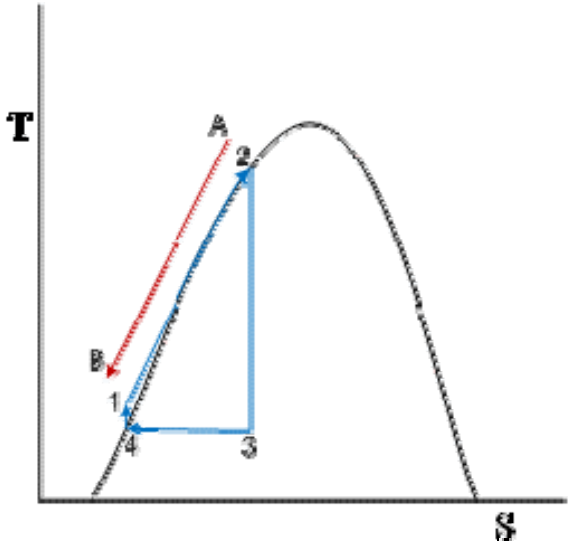

(b) The process in a T-s diagram

Figure 2.10 A trilateral flash cycle

Although this system has been considered for over 30 years, a lack of suitable two-phase expanders with high adiabatic efficiencies is the main obstacle for it to become reality and only a small scale demonstration unit has been built. Two-phase expanders were studied extensively during the 1970's, among which a Lysholm screw expander in a twin screw machine proposed by Sprankle and further studied by Steudel, et al. [35] was said to have adiabatic efficiencies of the order of 50%. However, studies conducted by Smith, et al. show that it is possible to design and construct twin screw expenders for trilateral flash cycle applications with predicted adiabatic efficiencies of the order of 80% or more [35]. They reported the design, and test results of screw machines showing two-phase fluid expansion with adiabatic efficiencies of more than 70% [36].

All of the aforesaid trilateral flash cycles used pure components as the working fluids. The most recent study done by Zamfirescu and Dincer used an ammonia-water mixture as the working fluid [37]. They thermodynamically assessed the performance of a trilateral flash cycle using ammonia-water as the working fluid, which they described as a "novel ammonia–water trilateral Rankine cycle". They compared the cycle with a Rankine cycle using pure R141b, R123, R245ca, and R21 as the working fluids, and a Kalina cycle under the same heat source temperature of 150 ºC, and found the exergy efficiency of the trilateral Rankine cycle to be roughly 7% higher than the other cycles. The authors mentioned that a number of positive

displacement expanders, such as reciprocation, centrifugal, rotating vane, and screw or scroll type could be applied in this cycle for power generation, but no further experiments have been conducted so far.

There is no trilateral flash cycle power plant reportedly in operation. However, some pilot demonstrations have been conducted by Smith, Stosic and Kovacevic [38]. The following Figure 2.1 shows the setup of the expander and its components.

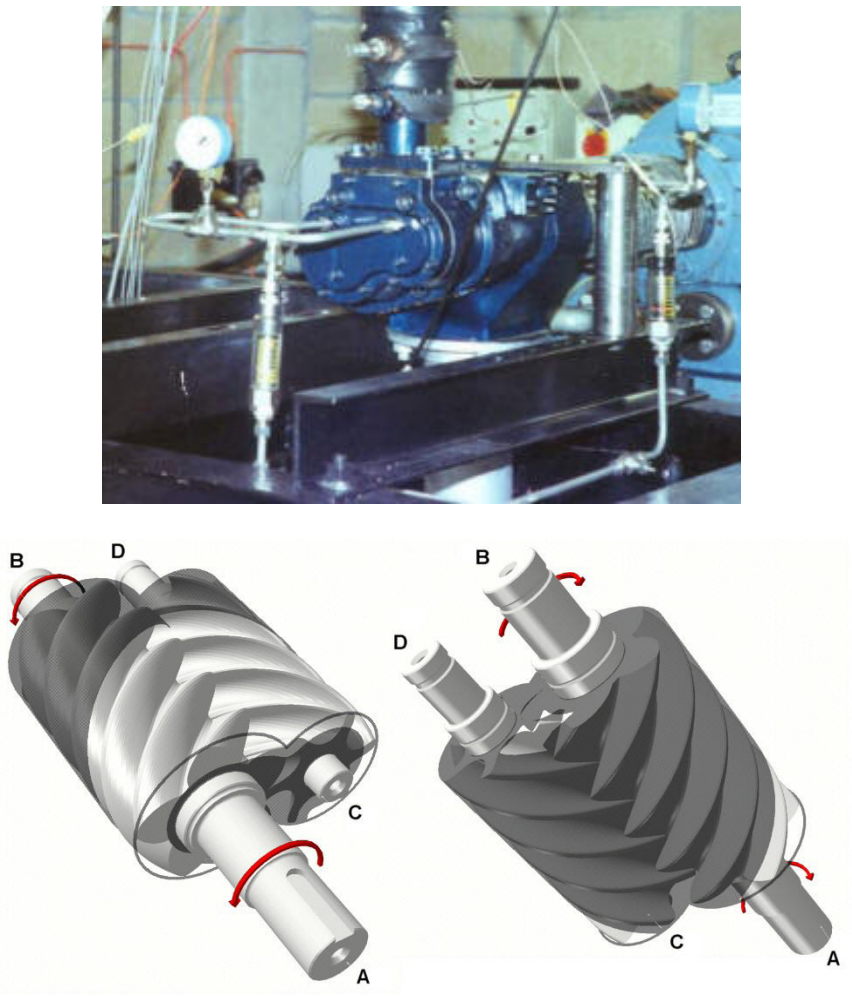

Figure 2.11 A trilateral flash cycle and its expander [38]

2.2.4 Organic Rankine Cycles (ORCs)

The organic Rankine cycle (ORC) is a Rankine cycle that uses organic working fluids with low boiling points, instead of steam, to recover heat from a lower temperature heat source. Figure 2.12 shows a schematic of an ORC and its process plotted in a T-s diagram. The cycle consists of an expansion turbine, a condenser, a pump, a boiler and a superheater (provided that superheat is needed).

Pure working fluids such as HCFC123 (CHCl2CF3) [39-41], [1], PF5050 ($CF_3(CF_2)_3CF_3$) [40], HFC-245fa ($CH_3CH_2CHF_2$) [42], [43], HFC-245ca (CF_3CHFCH_2F) [1], isobutene ($(CH_3)_2C=CH_2$) [1], n-pentane [44], [45] and aromatic hydrocarbons [46], have been studied for organic Rankine cycles. Fluid mixtures were also proposed for organic Rankine cycles [47-54]. The organic working fluids have many different characteristics than water [55]. The slope of the saturation curve of a working fluid in a T-S diagram can be positive (e.g. isopentane), negative (e.g. R22) or vertical (e.g. R11), and the fluids are accordingly called “dry”, “wet” or “isentropic”, respectively. Wet fluids, like water, usually need to be superheated, while many organic fluids, which may be dry or isentropic, do not need superheating. Another advantage of organic working fluids is that a turbine built for ORCs typically requires only a single-stage expander, resulting in a simpler, more economical system in terms of capital costs and maintenance [56].

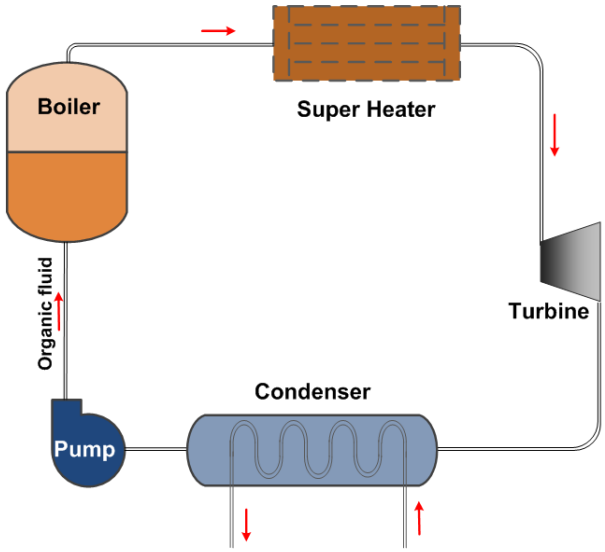

(a) The configuration

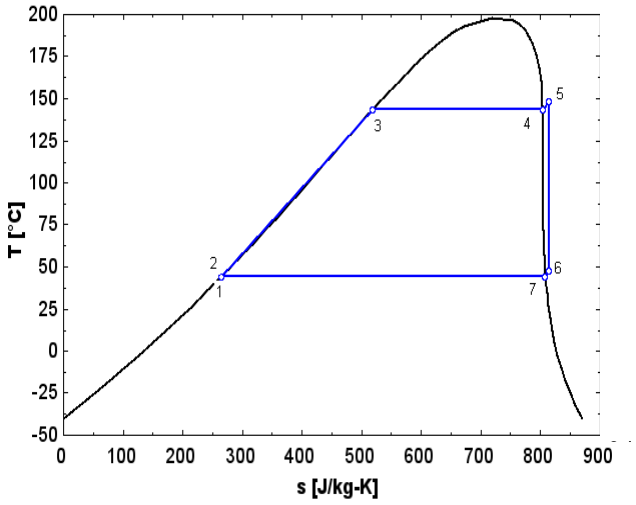

(b)The process

Figure 2.12 Demonstration of an organic Rankine cycle

Different forms of combined systems with an organic Rankine cycle as the bottoming cycle were studied [57-59], as well as organic Rankine cycles used in different industrial fields, such as in power plants [2],[57], [60-62], [2] desalination [63-66], cement industry [67], and the furniture manufacturing industry [68], [69].

Technical and economical analyses of the organic Rankine cycles have also been carried out [70-73]. The results show that despite the fact the organic Rankine cycle is linked with low efficiencies, its coupling with waste heat recovery from biogas digestion plants or micro-CHP systems provide very promising solutions for low cost, decentralized applications. Gerotor and scroll expanders were experimentally tested for performance in organic Rankine cycle, and got isentropic efficiencies of 0.85 and 0.83, respectively [74], which indicates that both types of expanders are good candidates to be used in an organic Rankine cycle. The advantage of ORC over steam Rankine cycle can be obvious in terms of the cycle efficiency for low-grade heat sources when appropriate working fluids and operating conditions are selected [39].

Among all of the thermodynamic cycles for low-grade heat-to-power conversion, organic Rankine cycle is so far the most commercially developed one. Both M-watts and k-watts scales can be found in operation. The Arizona Public Service Company (APS) completed construction of a solar trough organic Rankine cycle power plant in the United States in 2007 [75], which is the first new organic Rankine cycle power plant built in the past two decades, and the first power plant that combines solar trough technology with an organic Rankine cycle power block.

Figure 2.13 Organic Rankine cycle power plant in Saguaro, Arizona [75]

The organic Rankine cycles are favored for their simplicity in configuration, as it can be seen from in Figure 2.12. However, the bad thermal match of the working fluid with the heat source during the heating process causes irreversibility and low energy conversion efficiency.

2.2.5 Supercritical Rankine Cycle

Working fluids with relatively low critical temperature and pressure can be compressed directly to their supercritical pressures and heated to their supercritical state before expansion so as to obtain a better thermal match with the heat source. Figure 2.14 shows the configuration and process of a CO_2 supercritical Rankine cycle shown in a T-s diagram.

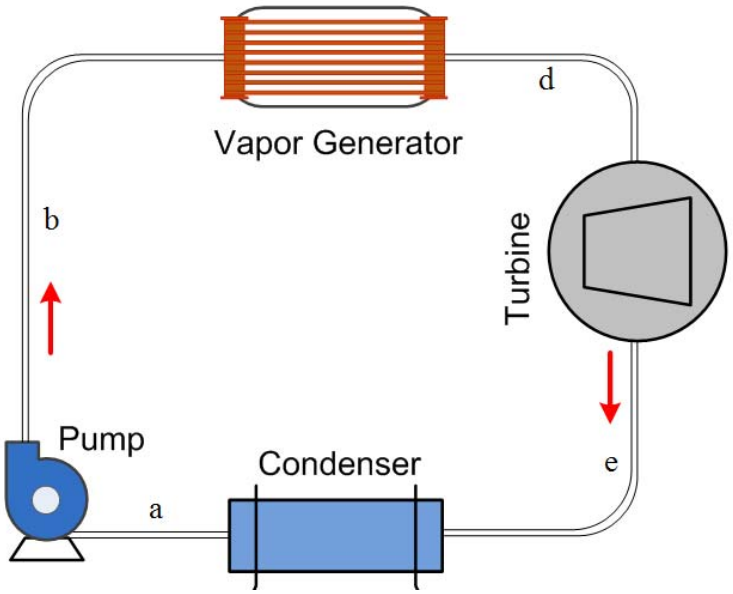

(a) The configuration

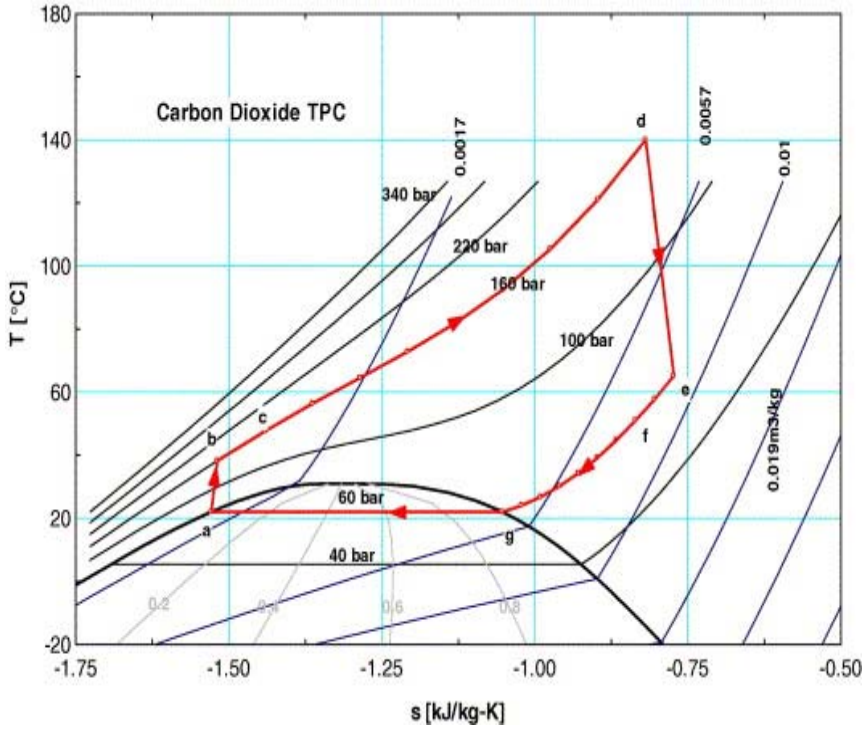

(b) The process in a T-s diagram (a→b→c→d→e→f→g) [76]

Figure 2.14 Configuration and process of a CO_2 supercritical Rankine cycle

The heating process of a supercritical Rankine cycle does not pass through a distinct two-phase region like a conventional organic Rankine cycle, resulting in a better thermal match in the boiler with less irreversibility. Figure shows the different thermal matches for R152a in a conventional organic Rankine cycle and R143a in a supercritical Rankine cycle for the same maximum temperature and pinch limitation [77], [78], [76].

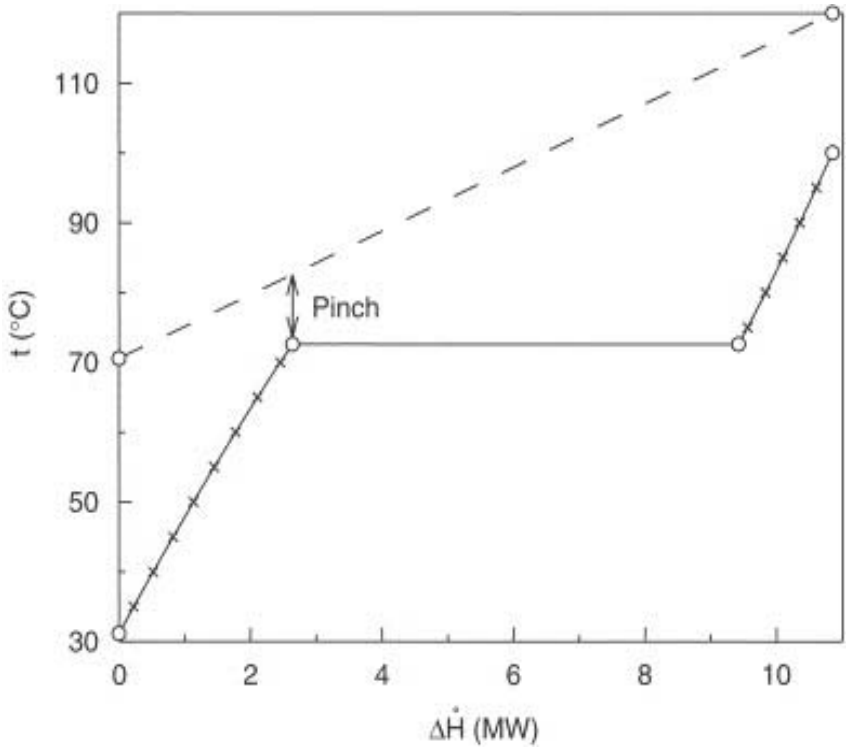

(a) Heating R152a in an organic Rankine cycle at 20bar from 31.16°C to 100°C

Figure 2.15 T-ΔḢ diagram demonstrating thermal match in an organic Rankine cycle and a supercritical Rankine cycle [79]

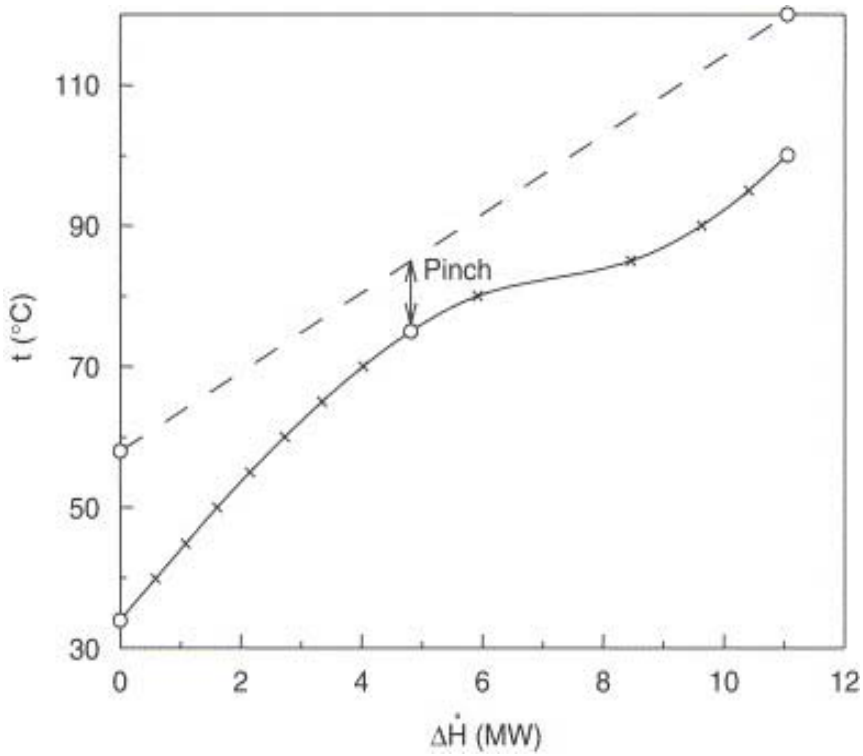

(b) Heating R143a in a supercritical Rankine cycle at 40bar from 33.93 °C to 100 °C

Figure 2.15 (Continued)

Chen et al. [77], [78], [76] did a comparative study of the carbon dioxide supercritical power cycle and compared it with an organic Rankine cycle using R123 as the working fluid in a waste heat recovery application. It shows that a CO_2 supercritical power cycle has higher system efficiency than an ORC when taking into account the heat transfer behavior between the heat source and the working fluid. The CO_2 cycle shows no pinch limitation in the heat exchanger. Zhang et al. [80-87] also conducted research on the supercritical CO_2 power cycle. Their experiments revealed that the power generation efficiency was 8.78% to 9.45% [80] and the COP for the

overall outputs from the cycle was 0.548 and 0.406, respectively, on a typical summer and winter day in Japan [81]. COP is defined as the total energy efficiency, including the power generation efficiency and the heat recovery efficiency [81]. Organic fluids like isobutene, propane, propylene, difluoromethane and R-245fa [60], [88] have also been suggested for supercritical Rankine cycles. It was found that supercritical fluids can maximize the efficiency of the system [60]. However, detailed studies on the use of organic working fluids in supercritical Rankine cycles have not been widely published.

As a working fluid for supercritical Rankine cycle, carbon dioxide has desirable qualities such as low critical point, stability, little environmental impact and low cost. However, the low critical temperature of carbon dioxide, 31.1°C, might be a disadvantage for the condensation process. As we can see in Figure 2.14, carbon dioxide has to be cooled below the critical point (31.1°C), preferably to around 20°C in order to condense, which is quite a challenge for the design of a cooling system. Meanwhile, an operating condition of 60-160bar is a safety concern. Therefore, new working fluids need to be considered to realize the supercritical Rankine cycle.

It has to be mentioned that although the supercritical Rankine cycle can obtain better thermal match than the organic Rankine cycle, it normally needs higher operating pressures, which may lead to difficulties in operation and a safety concern

to the power generation system. That makes it more critical to find proper working fluids for supercritical Rankine cycles.

CHAPTER 3 WORKING FLUIDS FOR LOW-GRADE HEAT CONVERSION

The properties of the working fluids play a key role in a thermodynamic cycle for low-grade heat conversion. The fluid selection affects the system efficiency, operating conditions, environmental impact and economical decisions. This chapter discusses the selection criteria of potential working fluids for organic Rankine cycles and supercritical Rankine cycles, screens 35 working fluids candidates based on the selection criteria, and analyzes the influence of the fluid properties on cycle performance.

3.1 Thermodynamic and Physical Properties

In this section, selection criteria are set out to locate the potential working fluid candidates for organic Rankine cycles and supercritical Rankine cycles at various conditions. Types of working fluids and their properties, such as, fluid density, specific heat, latent heat, critical point, thermal conductivity, specific volume at saturation (condensing) conditions, as well as saturation volumes are analyzed and discussed. The desired properties are then discussed for the screening of potential working fluids.

3.1.1 Type of Working Fluids

A working fluid can be classified as a dry, isotropic, or wet fluid depending on the slope of the saturated vapor curve on a T-s diagram (dT/ds). If we define $\xi = ds/dT$, the type of working fluid can be classified by the value of ξ, i.e. $\xi > 0$ would mean a dry fluid (e.g. pentane), $\xi \approx 0$: an isentropic fluid (e.g. R11), and $\xi < 0$: a wet fluid (e.g. water). Figure 3.1 shows the three types of fluids in a T-s diagram.

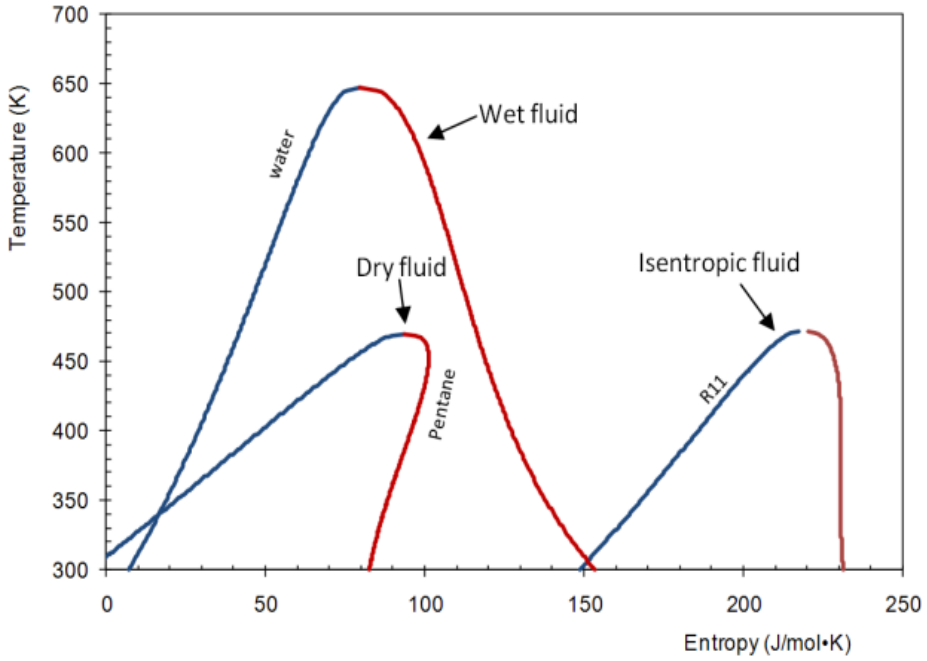

Figure 3.1 Three types of working fluids: dry, isentropic, and wet

Liu et al. derived an expression to compute ξ, which is [4]:

$$\xi = \frac{C_p}{T_H} - \frac{\frac{n \cdot T_{rH}}{1 - T_{rH}} + 1}{T_H^2} \Delta H_H \tag{3.1}$$

where ξ (ds/dT) denotes the inverse of the slope of the saturated vapor curve on T-s diagram, n is suggested to be 0.375 or 0.38 [89], T_{rH} ($= T_H/T_C$) denotes the reduced evaporation temperature, and ΔH_H is the enthalpy of vaporization.

It needs to be mentioned that equation (3.1) is developed through simplifications. The reliability of the equation was verified at the fluids' normal boiling points by Liu et al. [4]. However, our calculations based on the definition of the slope (ds/dT) show that large deviations can occur when using equation (1) at off-normal boiling points. Therefore, it is recommended to use the entropy and temperature data directly to calculate ξ if their values are available.

Isentropic or dry fluids were suggested for the organic Rankine cycle to avoid liquid droplet impingent in the turbine blades during the expansion. However, if the fluid is "too dry," the expanded vapor will leave the turbine with substantial "superheat", which is a waste and adds to the cooling load in the condenser. The cycle efficiency can be increased by using this superheat to preheat the liquid after it leaves the feed pump and before it enters the boiler.

Figure 3.2 shows a dry fluid, propyne, and a wet fluid pentane used in supercritical Rankine cycles. If the expansion is carried out such that the expansion does not go into the two-phase region (the dashed lines in Figure 3.2), dry fluids may leave the turbine with substantial amount of superheat, which adds to the burden for the condensation process unless a recovery system is used. Wet fluids, on the other

hand, will need a higher turbine inlet temperatures to avoid the two phase region, but, in this case, there is less concern about desuperheating after expansion. If the expansion process is allowed to pass through the two phase region (the solid lines in Figure 3.2), the dry fluid can leave the turbine in a superheated state; however, the wet fluid stays in the two phase region. For dry fluids, Goswami et al. [90] and Demuth [91], [92] found that only extremely fine droplets (fog) were formed in the two phase region and no liquid was actually formed to damage the turbine before it started drying during the expansion. Demuth [91] hypothesized that the turbine performance should not degrade as a result of the two phase expansion if the fluid is dry or superheated at the exit. The study conducted by Goswami et al. confirmed this hypothesis [90]. Demuth concluded that two – phase expansion of a drying fluid can result in potential gains in the net fluid effectiveness on the order of 8% [91]. To this end, dry fluids may serve better than wet fluids in a supercritical Rankine cycle if the turbine expansion involves a two-phase region.

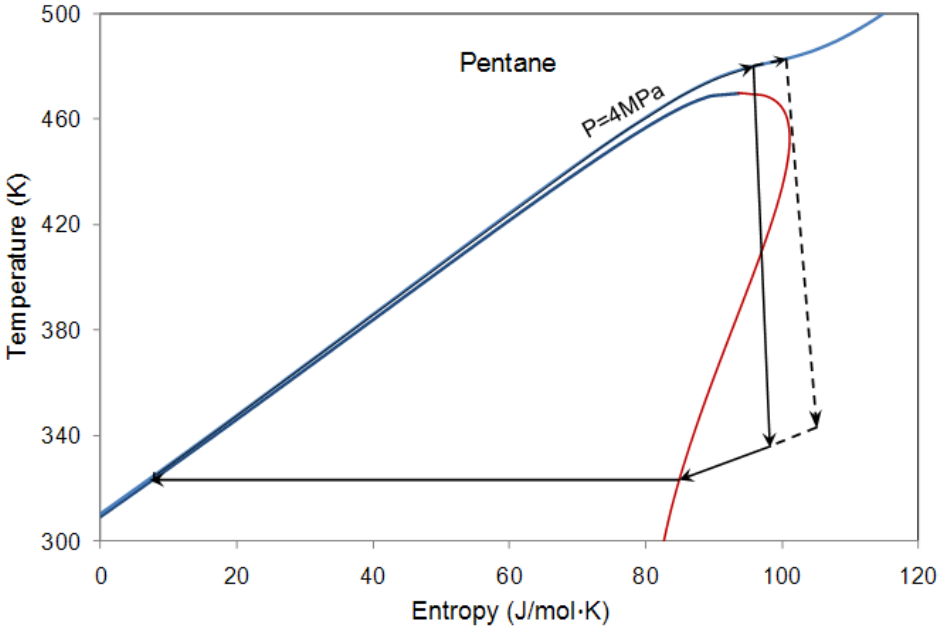

(a) Pentane as a dry working fluid

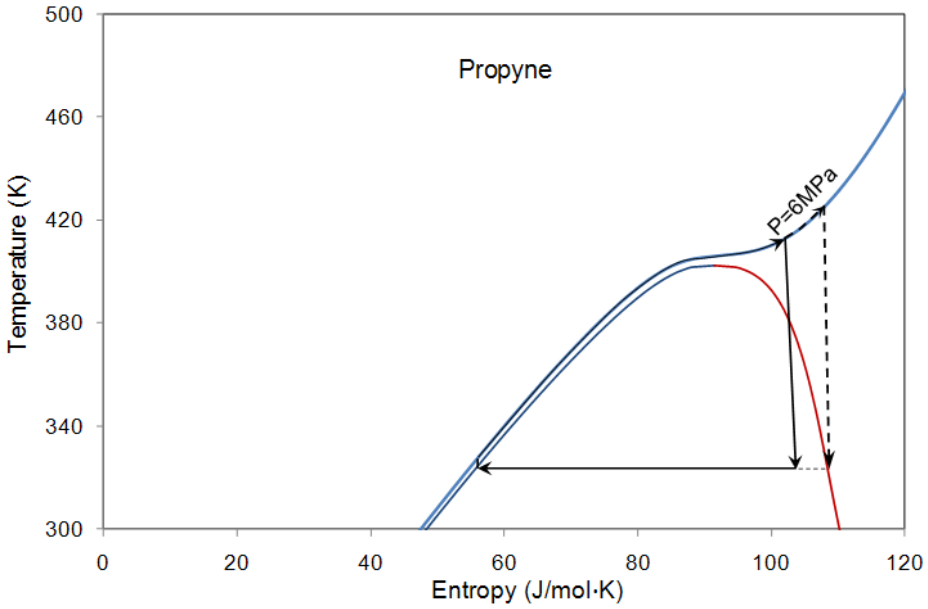

(b) Propyne as the wet working fluid

Figure 3.2 T-s diagram showing a dry fluid and a wet fluid used in supercritical Rankine cycles

3.1.2 Critical Points of the Working Fluid

Condensation is a necessary process in any Rankine cycle. The designed condensation temperature is normally above 300K in order to reject heat to the ambient; therefore, fluids like methane with critical temperature far below 300K are out of consideration because of the difficulty in condensing. On the other hand, the critical point of a fluid considered as the working fluid of a supercritical Rankine cycle should not be too high to achieve for the heat source.

Another important thermodynamic property is the freezing point of the fluid, which must be below the lowest operating temperature in the cycle. The fluid must also work in an acceptable pressure range. Very high pressure or high vacuum have a tendency to impact the reliability of the cycle or increase the cost.

3.1.3 Influence of Latent Heat, Density and Specific Heat

Maizza and Maizza [47] suggested that high latent heat, high density and low liquid specific heat are preferable, as a fluid with a high latent heat and density absorbs more energy from the source in the evaporator and thus reduces the required flow rate, the size of the facility, and the pump consumption. However, Yamamoto et al. [39] suggested that low latent heat is better because the saturated vapor at the turbine inlet would provide the best operating condition. The authors conducted a theoretical analysis by deriving the expression of the enthalpy change through the turbine expansion, in order to verify their conclusion.

The phase transition between two phases of matter can be characterized by Clausius-Clapayron relation, which is:

$$\frac{dP}{dT} = \frac{L}{T\Delta V} \tag{3.2}$$

where *dP/dT* denotes the slope of the coexistence curve on a P-T diagram, L is the latent heat, T is the temperature, and ΔV is the volume change of the phase transition. When the transition is to a gas phase, the specific volume can be many times higher that the initial specific volume, so $\Delta V = V_{gas}$ can be approximated, which is also applied in the current situation.

Here it is assumed that the vapor follows the ideal gas law for the sake of simplification. Since high pressure vapor cannot be considered as an ideal gas, this analysis is only for a qualitative investigation and not meant for accurate calculations. The ideal gas law is:

$$V_{gas} = \frac{RT}{P} \tag{3.3}$$

Combining Equation (3.2) and Equation (3.3) and after integration, the pressure ratio of any two points on the coexistence line of a phase diagram is obtained as:

$$\ln \frac{P_2}{P_2} = \frac{L}{R}\left(\frac{1}{T_1} - \frac{1}{T_2}\right) \tag{3.4}$$

From Equation (3.4) one can notice that the pressure ratio of a working fluid is decided by its latent heat when the saturation temperatures are defined.

The unit isentropic enthalpy drop (i.e. the work output) through a turbine is calculated from: [93]

$$\Delta h_{isentropic} = c_p T'_{in}\left[1-\left(\frac{P_{dis}}{P_{in}}\right)^{(\gamma-1)/\gamma}\right] \tag{3.5}$$

where $\gamma = \frac{c_p}{c_v}$, and T'_{in} is the turbine inlet temperature. The above expression for the enthalpy drop was widely accepted for discussion although it is derived under the assumption of ideal gas with constant specific heats [94], [93].

Combining Equation (3.4) and Equation (3.5) one obtains:

$$\Delta h_{isentropic} = c_p T'_{in}\left[1-e^{\frac{L}{c_P}\left(\frac{1}{T_1}-\frac{1}{T_2}\right)}\right] \tag{3.6}$$

where T_1 and T_2 are the saturation temperatures of two points on the coexistence line and $T_1 > T_2$, T'_{in} is the turbine inlet temperature, and the other notations remain the same. This can be explained by an organic Rankine cycle with superheat in a T-s diagram in Figure 3.3.

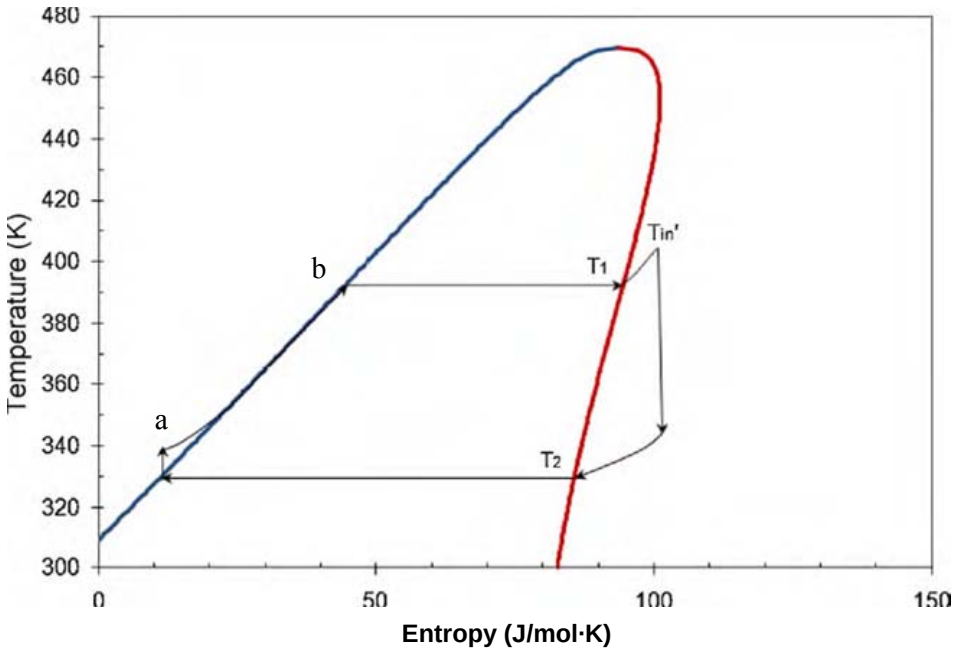

Figure 3.3 T-s diagram of an organic Rankine cycle with superheat

Equation (3.6) shows that fluids with higher latent heat give higher unit work output when the temperatures and other parameters are defined. The influence of the latent heat can also be explained by observing the T-s diagram in Figure 3.3. Under defined temperatures, the length of the horizontal line segment is proportional to the latent heat. Long line segment (i.e. latent heat) is expected to obtain large work output because the area formed by the process of the cycle is the work output from the turbine. This result agrees with the conclusion from Equation (3.6).

By comparing the process of an organic Rankine cycle in Figure 3.3 with a Carnot cycle in a T-s diagram, it can be easily concluded that the bigger the slope of the liquid heating curve (a to b in Figure 3.3), the closer the organic Rankine cycle to a Carnot cycle.

By definition, the heat capacity of a fluid gives:

$$C = \frac{\delta Q}{dT} = T\frac{ds}{dT} \tag{3.7}$$

Rearranging it yields,

$$\frac{\delta T}{ds} = \frac{T}{C} \tag{3.8}$$

where $\frac{\delta T}{ds}$ is the slope of the temperature profile.

Therefore, under a defined temperature, a fluid with low liquid heat capacity (liquid specific heat) is expected. Meanwhile, as it has been mentioned, Equation (3.6) is the unit mass work output from the turbine, it can be inferred that fluids with higher density need smaller equipment for the same power production. In brief, working fluids with high density, low liquid specific heat and high latent heat are expected to give high turbine work output.

3.1.4 Effectiveness of Superheating

A large amount of superheat is used in a traditional steam Rankine cycle to improve thermal efficiency. However, superheat does not always lead to a higher efficiency for all working fluids. It is the rate at which the constant pressure lines diverge in a h-s diagram or a T-s diagram that determines the impact of superheating. For a given incremental increase in the degree of superheat from some reference point, incremental efficiency $\Delta\eta'$ can be defined as the ratio of incremental work and heat, shown in Equation (3.7) and Figure 3.4.

$$\Delta\eta' = \frac{\Delta w}{\Delta q} = \frac{\Delta h_1 - \Delta h_2}{\Delta h_1} \tag{3.9}$$

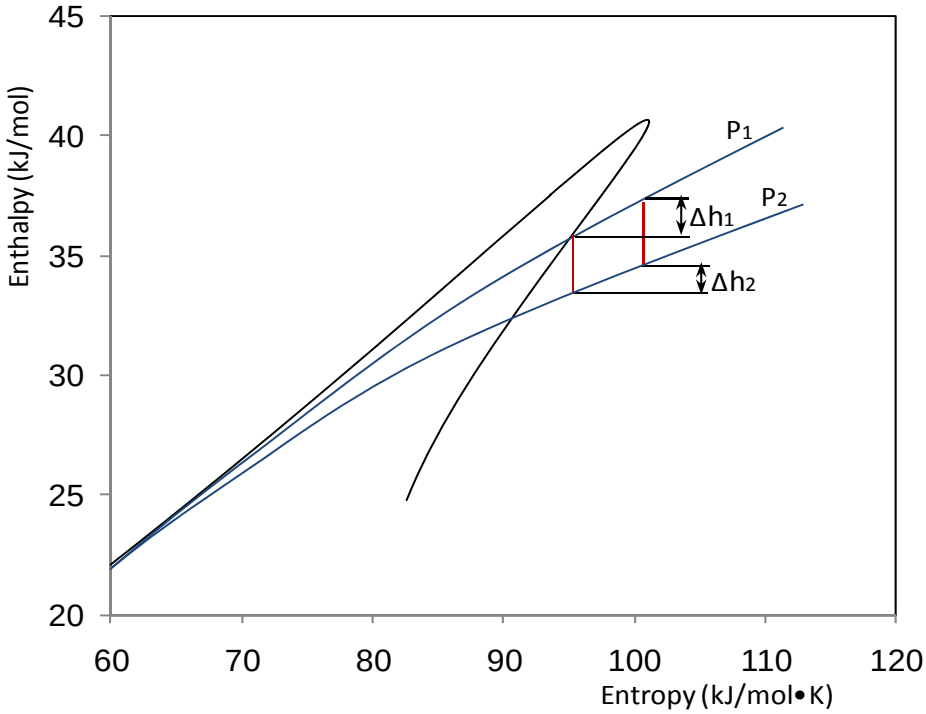

Figure 3.4 Enthalpy-entropy diagram of dry fluid pentane demonstrating the effect of superheat

In order for the cycle efficiency to increase with the degree of superheat, the incremental efficiency must be greater than the efficiency at the reference state (here it is the saturated vapor state). For the operation between two isobaric curves, the system efficiency increases for wet fluids while it decreases for dry fluids. The isentropic fluid achieves an approximately constant value for high turbine inlet temperatures [3]. Based on that, superheat contributes negatively to the cycle efficiency for dry fluids, and is not recommended. For wet fluids, superheat is mostly necessary to avoid turbine blades erosion and improve the cycle efficiency.

3.1.5 Stability of the Fluid and Compatibility with Materials in Contact

Unlike water, organic fluids usually suffer chemical transformation and decomposition at high temperatures [41]. The maximum operating temperature is thus limited by the chemical stability of the working fluid. Additionally, the working fluid should be non-corrosive and compatible with engine materials and lubricating oil. Calderazzi and Paliano [95] studied the thermal stability of R-134a, R-141b,R-13I1, R-7146 and R-125 associated with stainless steel as the container material. Andersen and Bruno [56] presented a method to assess the chemical stability of the potential working fluids by ampule testing techniques. The method allows the determination of the decomposition reaction rate constant of simple fluids at the temperature and pressure of interest.

3.1.6 Environmental Aspects

As to the environmental aspects, the main concerns include the ozone depletion potential (ODP), global warming potential (GWP) and the atmospheric lifetime (ALT). The ODP and GWP represent a substance's potential to contribute ozone degradation and globe warming. Due to the environmental concerns, some working fluids have been phased out, such as R-11, R-12, R-113, R-114, and R-115, while some others are being phased out in 2020 or 2030 (such as R-21, R-22, R-123, R-124, R-141b and R-142b). Those substances are not included in the following discussions for potential working fluids.

Alternative fluids are being found and applied. The alternatives are expected to retain the attractive properties and avoid their adverse environmental impact [96]. The most promising candidates are still found among fluids containing fluorine and carbon atoms. The inclusion of one or more hydrogen atoms in the molecule, results in it being largely destroyed in the lower atmosphere by naturally occurring hydroxyl radicals, ensuring that little of the fluid survives to enter the stratosphere [96].

3.1.7 Availability and Cost

The availability and cost of the working fluids are among the considerations when selecting working fluids. Traditional refrigerants used in organic Rankine cycles are expensive. This cost could be reduced by a greater mass production of those refrigerants, or by the use of low cost hydrocarbons.

3.2 Fluid Candidates and Their Properties

Based on the author's analysis and discussion, working fluids can be evaluated by thermodynamic and physical properties, stability and compatibility, environmental impacts, safety, and availability and cost. More than 50 working fluids have been suggested in the literature, among which some have been phased out due to environmental concerns, and some, such as methane, are not practical for this application due to their properties.

Totally 35 potential working fluid candidates for organic Rankine cycles and supercritical Rankine cycles have been screened, as shown in Table 3.1, among which

water is listed for comparison. Although aspects other than the thermodynamic properties, such as stability, compatibility, environment impact, availability and cost, were pointed out in the former sections, they are better off being discussed in engineering design. Important thermodynamic properties of the fluids were calculated and listed, such as molecular weight, critical temperature, critical pressure, critical density, vapor specific heat capacity, latent heat, and *ds/dT* (See Table 3.1). It needs to be mentioned that the vapor specific heat capacity Cp, the latent heat L, and the ratio *ds/dT* are functions of temperature, and the values given in the table are based on 320K, for those whose critical temperatures are above 320K, because 320K is the approximate design temperature for condensation. For those fluids whose critical temperatures are below 320K, it is assumed that the condensation is designed to be at 290K, and the calculation is based on that.

Multi-component fluids are not included in this study, because the mixing rule is rather complicated and there are numerous combinations. Investigators can still make their own multi-component fluids based on the properties of the pure fluids.

Table 3.1 Properties of the screened working fluids

SHRAE Number	*Name*	*Molecular weight*	*Tc (K)*	*Pc (MPa)*	*Vapor Cp (J/kg.K)*	*Latent heat L (kJ/kg)*	*ξ (J/kg•K2)*
R-21	Dichlorofluoromethane	102.92	451.48	5.18	339.85	216.17	-0.78
R-22	Chlorodifluoromethane	86.47	369.30	4.99	1069.13	158.46	-1.33
*R-23**	Trifluoromethane	70.01	299.29	4.83	3884.02	89.69	-6.49
R-32	Difluoromethane	52.02	351.26	5.78	2301.61	218.59	-4.33
*R-41**	Fluoromethane	34.03	317.28	5.90	3384.66	270.04	-7.20
*R-116**	Hexafluoroethane	138.01	293.03	3.05	4877.91	30.69	-5.54
R-123	2,2-Dichloro-1,1,1-trifluoroethane	152.93	456.83	3.66	738.51	161.82	0.26
R-124	2-Chloro-1,1,1,2-tetrafluoroethane	136.48	395.43	3.62	908.70	132.97	0.26
R-125	Pentafluoroethane	120.02	339.17	3.62	1643.89	81.49	-1.08
R-134a	1,1,1,2-Tetrafluoroethane	102.03	374.21	4.06	1211.51	155.42	-0.39
R-141b	1,1-Dichloro-1-fluoroethane	116.95	477.50	4.21	848.37	215.13	0.00
R-142b	1-Chloro-1,1-difluoroethane	100.50	410.26	4.06	1036.52	185.69	0.00
R-143a	1,1,1-Trifluoroethane	84.04	345.86	3.76	1913.97	124.81	-1.49
R-152a	1,1-Difluoroethane	66.05	386.41	4.52	1456.02	249.67	-1.14
*R-170**	Ethane	30.07	305.33	4.87	5264.72	223.43	-8.28
R-218	Octafluoropropane	188.02	345.02	2.64	1244.87	58.29	0.45
R-227ea	1,1,1,2,3,3,3-Heptafluoropropane	170.03	375.95	3.00	1013.00	97.14	0.76
R-236ea	1,1,1,2,3,3-Hexafluoropropane	152.04	412.44	3.50	973.69	142.98	0.76
R-245ca	1,1,2,2,3-Pentafluoropropane	134.05	447.57	3.93	1011.26	188.64	0.60
R-245fa	1,1,1,3,3-Pentafluoropropane	134.05	427.20	3.64	980.90	177.08	0.19
HC-270	Cyclopropane	42.08	398.30	5.58	1911.81	366.18	-1.54
R-290	Propane	44.10	369.83	4.25	2395.46	292.13	-0.79

Table 3.1 (Continued)

SHRAE Number	*Name*	*Molecular weight*	*Tc (K)*	*Pc (MPa)*	*Vapor Cp (J/kg.K)*	*Latent heat L (kJ/kg)*	*ξ (J/kg•K2)*
R-C318	Octafluorocyclobutane	200.03	388.38	2.78	896.82	93.95	1.05
R-3-1-10	Decafluorobutane	238.03	386.33	2.32	928.83	77.95	1.32
FC-4-1-12	Dodecafluoropentane	288.03	420.56	2.05	884.25	86.11	1.56
R-600	Butane	58.12	425.13	3.80	1965.59	336.82	1.03
R-600a	Isobutane	58.12	407.81	3.63	1981.42	303.44	1.03
R-601	Pentane	72.15	469.70	3.37	1824.12	349.00	1.51
R-717	Ammonia	17.03	405.40	11.33	3730.71	1064.38	-10.48
R-718	Water	18.00	647.10	22.06	1943.17	2391.79	-17.78
*R-744**	Carbon dioxide	44.01	304.13	7.38	3643.72	167.53	-8.27
R-1270	Propene	42.08	365.57	4.66	2387.36	284.34	-1.77
	Propyne	40.06	402.38	5.63	2100.54	431.61	-1.87
	Benzene	78.11	562.05	4.89	1146.72	418.22	-0.70
	Toluene	92.14	591.75	4.13	1223.90	399.52	-0.21

*The critical temperature of the fluid is below 320K, and the data is given based on 290K.

Table 3.1 is very useful as it suggests how well the substance can serve as a working fluid in an organic Rankine cycle or a supercritical Rankine cycle. The molecular weight suggests the density of the fluid. The critical point suggests the possible operating temperature and pressure range. The turbine work output can be estimated from Equation (3.6) with the value of vapor specific heat capacity (Cp) and the latent heat (L). Parameter ξ, calculated directly from the definition, describes the fluid type and suggests the effectiveness of superheating.

3.3 Fluid Candidate Discussion

There is no best fluid that meets all the criteria discussed in Section 3.1 for heat sources with different temperatures. Compromise must be made when selecting the fluids. Among all the criteria and concerns, the authors find that the critical temperature and the ξ value are important parameters that suggest which type of cycle a fluid may serve and the applicable operating temperature of the fluid. Thereby, T– ξ charts are introduced in this work. The screened 35 fluids were distributed in the charts with their critical temperature and ξ value. Figure 3.5 is the distribution of the 35 working fluids in a T– ξ (ds/dT) chart, from which the critical temperature and the type of each working fluid is shown. Water, toluene, benzene and ammonia are labeled in Figure 3.5; the remaining fluids are shown in an expanded view in Figure 3.6. The fluids are divided into 5 groups based on their locations in the T– ξ chart and discussed in the following.

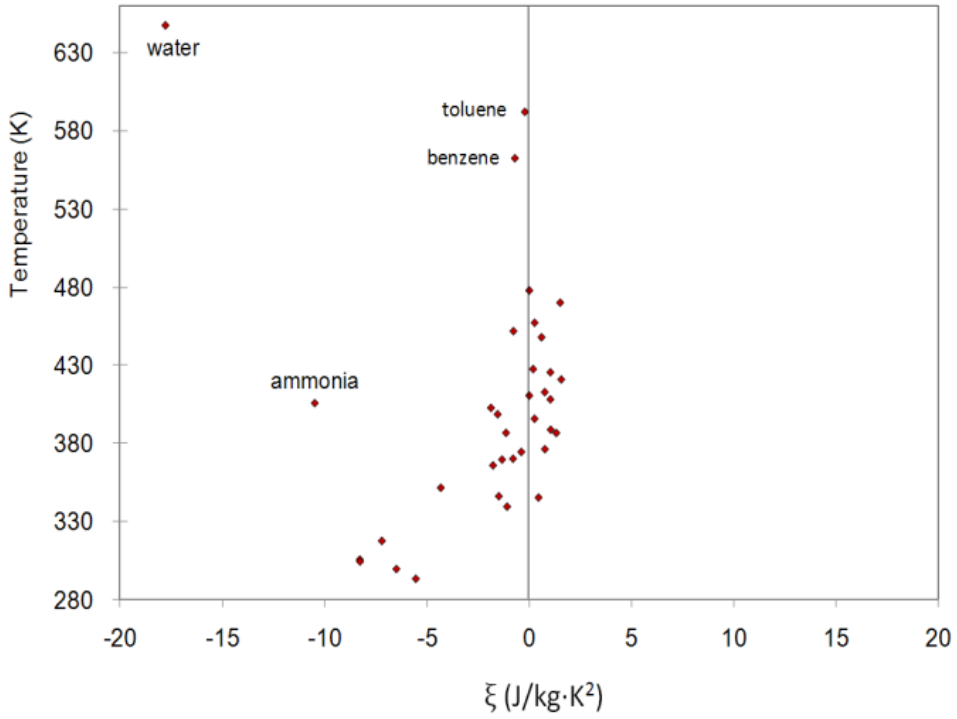

Figure 3.5 Distribution of the screened 35 working fluids in T- ξ chart

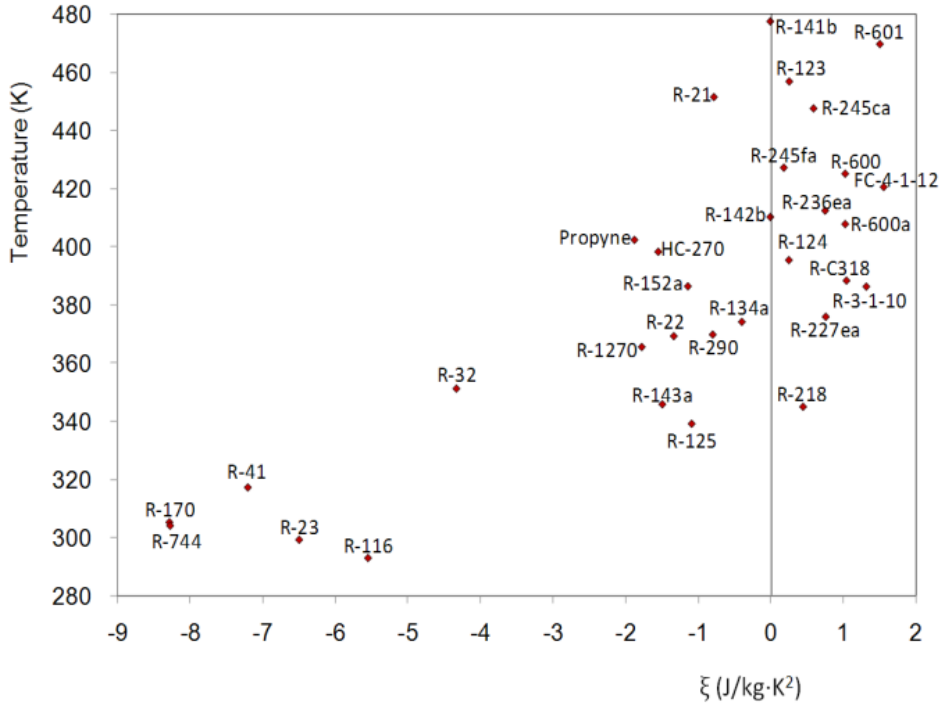

Figure 3.6 Expanded view of the distribution of the remaining 31 fluids in T- **ξ** chart

3.3.1 Fluids Ammonia, Benzene and Toluene

It can be observed from Figure 3.5 that water is located in the upper left of the chart, which indicates it is the wettest fluid and has the highest critical temperature among all the fluids plotted. These characteristics make it unsuitable for low temperature heat conversion. Ammonia as a deep wet fluid with a ξ value of -10.48 J/kg·K^2, needs superheating when used in an organic Rankine cycle (here we still call it ORC, although ammonia is not organic). Ammonia is not recommended in supercritical Rankine cycles, since the critical pressure (11.33 MPa) is relatively high. Meanwhile, ammonia is highly hydrophilic, and the ammonia-water solution is corrosive, limiting the materials that may be used.

Benzene and toluene are considered as isentropic fluids with relatively high critical temperatures, which are desirable characteristics for organic Rankine cycles. Benzene and toluene are chemically stable in these potential operating conditions [56].

3.3.2 Fluids R-170, R-744, R-41, R-23, R-116, R-32, R-125 and R-143a

From Figure 3.6 it can be observed that fluids R-170, R-744, R-41, R-23, R-116, R-32, R-125 and R-143a are wet fluids with low critical temperatures and reasonable critical pressures (from Table 3.1), which are desirable characteristics for supercritical Rankine cycles. Carbon dioxide (R-744) and R134a have been studied in supercritical Rankine cycles in the literature as reviewed in Chapter 2. Among these

fluids, R-170, R-744, R-41, R-23 and R-116 have critical temperatures below 320K, which might be hard for the condensing process in many circumstances. The critical temperature of R-32, R-125 and R-143a is above 320K, so condensation is not a big concern. Provided other aspects are satisfied, R-32, R-125 and R-143a could be promising working fluids for supercritical Rankine cycle.

3.3.3 Fluids Propyne, HC-270, R-152a, R-22 and R-1270

Propyne, HC-270, R-152a, R-22 and R-1270 are wet fluids with relatively high critical temperatures (Figure 3.6). Superheat is usually needed for this group of fluids when applied in organic Rankine cycles. They might be applied in supercritical Rankine cycles if the temperature profile of the heat source meets the requirements. However, propyne, HC-270 (cyclopropane) and R-1270 (propene) are not normally seen in their supercritical state due to the stability concerns. Propyne, HC-270 and R-1270 have relatively low molecular weight (Table 3.1). Applying these fluids implies a larger system size compared to those fluids with higher molecular weight.

3.3.4 Fluids R-21, R-142b, R-134a, R-290, R-141b, R-123, R-245ca, R-245fa, R-236ea, R-124, R-227ea, R-218

This group of fluids can be considered isentropic fluids (Figure 3.6). They can be applied in an organic Rankine cycle or a supercritical Rankine cycle depending on the temperature profile of the heat source. Since the isentropic expansion will not cause wet fluid problems, superheat is not necessary in an organic Rankine cycle with

these fluids. Among these fluids, R-141b, R-123, R-21, R-245ca, R-245fa, R-236ea and R-142b have critical temperature above 400K, making them more likely to be used in an organic Rankine cycle than in a supercritical Rankine cycle, while the rest may be used in either cycle, depending on the heat source profile.

3.3.5 Fluids R-601, R-600, R-600a, FC-4-1-12, R-C318, R-3-1-10

Fluids R-601, R-600, R-600a, FC-4-1-12, R-C318, R-3-1-10 are dry fluids as it can be seen from Figure 3.6. Based on the analysis before, dry fluids may be used in supercritical Rankine cycles and organic Rankine cycles. Since superheat has a negative effect on the cycle efficiency when dry fluids are used in an organic Rankine cycle, superheating is not recommended. The decision on which fluids could be used may be based on how the operating temperature is tailored to cope with the heat source temperature profile.

3.4 Concluding Remarks

The properties of the working fluids play a vital role in the cycle performance. The thermodynamic and physical properties, stability, environmental impacts, safety and compatibility, and availability and cost are among the considerations when selecting a working fluid. Types of working fluids, influences of latent heat, density, specific heat, and the effectiveness of superheating were discussed in detail. Working fluids with high density and high latent heat provide high unit turbine work output. The study also showed that isentropic and dry fluids are preferred in organic Rankine

cycles. Superheating is necessary for wet fluids in the organic Rankine cycle. However, for dry fluids superheat could play a negative role in the cycle efficiency. Fluids with low critical temperatures and pressures are potential candidates for the supercritical Rankine cycle. Among all the fluids suggested, 35 fluids were screened out, and plotted in the newly introduced T- ξ charts. The fluids were discussed through grouping based on their distributions in the T- ξ chart.

CHAPTER 4 SUPERCRITICAL RANKINE CYCLE USING PURE WORKING FLUIDS

It has been stated that the organic Rankine cycle (ORC) is the most studied cycle for the purpose of low-grade heat conversion due to its simplicity and relative high efficiency. However, an important limitation of the ORC is isothermal evaporation, which creates a poor thermal match between the working fluid and the heat source, leading to a large irreversibility. Supercritical Rankine cycles, on the other hand, can reduce the irreversibility loss during the heating processes [87], [97].

The configurations of the ORC and supercritical Rankine cycle have been shown in CHAPTER 2 (Figure 2.12 and Figure 2.14, respectively). The major difference between a subcritical and a supercritical Rankine cycle lies in the heating process of the working fluid shown in Figure 4.1. In a supercritical Rankine cycle, the working fluid is heated directly from the liquid state into the supercritical state, bypassing the two phase region, which allows it to have a better thermal match with the heat source, resulting in less exergy loss. Furthermore, by avoiding the boiling process, the configuration of the heating system is potentially simplified.

Carbon dioxide (CO_2), being abundant, non-flammable, non-toxic and inexpensive, has been extensively studied as a supercritical working fluid by a

number of researchers. Zhang et al. [84], [85], [80], [86] indicates the thermal efficiency of a CO_2-based supercritical Rankine cycle to be 8.0-11.4% depending on the working condition. Chen et al. [77], [78] found that under the same thermodynamic mean heat rejection temperature, a CO_2-based supercritical power cycle gives a slightly higher power output than a R123-based ORC. Beside CO_2, hydrocarbons [98] and refrigerants [57], [60-62], [2] have also been studied as working fluids in supercritical Rankine cycles, and the results showed that the thermal efficiency could improve by 10-20% [57], [60-62], [2], compared to the same working fluids used in ORC.

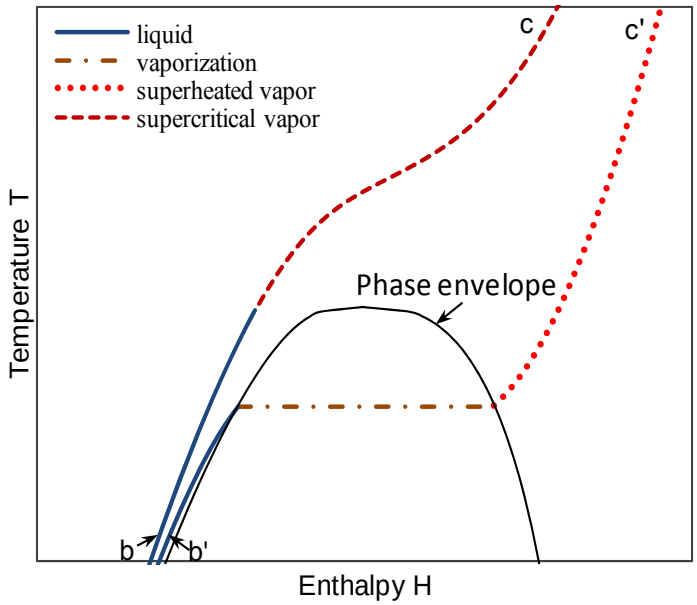

Figure 4.1 The heating process of a fluid under supercritical pressure and subcritical pressure

The review of the literature shows that the supercritical Rankine cycle can achieve higher efficiency than the ORC, and major attention has been paid to CO_2-based supercritical Rankine cycles. However, it raises the question of whether CO_2 still holds advantages when compared to organic fluids in supercritical Rankine cycles. In this context, the author conducts a rigorous comparative study between a CO_2-based and a R32-based supercritical Rankine cycle for the conversion of low-grade heat into mechanical power to find that the R32-based supercritical Rankine cycle has many advantages over the CO_2-based supercritical Rankine cycle.

4.1 Properties of the Working Fluids under Investigation

Peng-Robinson Equation of State, validated with NIST data adopted from [99] for CO_2 and [100] for R32 was used to predict the properties of the working fluid. An expression of the Peng-Robinson EOS is found as follows:

$$p = \frac{RT}{V_m - b} - \frac{a(T)}{V_m(V_m + b) + b(V_m - b)} \tag{4.1}$$

where

$$a(T) = 0.45724 \frac{R^2 T_c^2}{P_c} \text{alpha}(T)$$

$$b = 0.07780 \frac{RT_c}{P_c}$$

$$\text{alpha}(T) = [1 + k(1 - \text{squrt}\frac{T}{Tc})]^2$$

$$k = 0.37464 + 1.54226w - 0.26992w^2$$

where V_m is the mole volume, T_c denotes the critical temperature, P_c the critical pressure, ωthe acentric factor of the species, and R the universal gas constant.

Key properties of R32 and CO_2 are demonstrated for discussion. The phase envelopes of R32 and CO_2 with a couple of characteristic isobaric lines of each are shown in a temperature-entropy diagram in Figure 4.2 (b). It is seen that CO_2 has a much lower critical temperature (304.13K). Since condensation could only happen at temperatures below the fluid's critical temperature, the design of a condenser for CO_2 could be hard to achieve economically and effectively. On the other hand, R32 has a much higher critical temperature (351.26K), making it much easier to condense. The thermal conductivities of the working fluids are highly temperature dependent in the supercritical condition and affect the heat exchange processes of the system. Higher thermal conductivity improves the heat transfer performance. Figure 4.2 (b) shows the thermal conductivities of R32 and CO_2 from 297K to 397K at 1.1 times of their critical pressures. It is seen that for both fluids the thermal conductivity decreases with increase in the temperature. However, there is a rebound for both fluids during the phase transition. Compared with CO_2, R32 has higher thermal conductivity in both liquid and vapor phases, which may indicate a smaller heat exchange area needed for R32 under the same conditions.

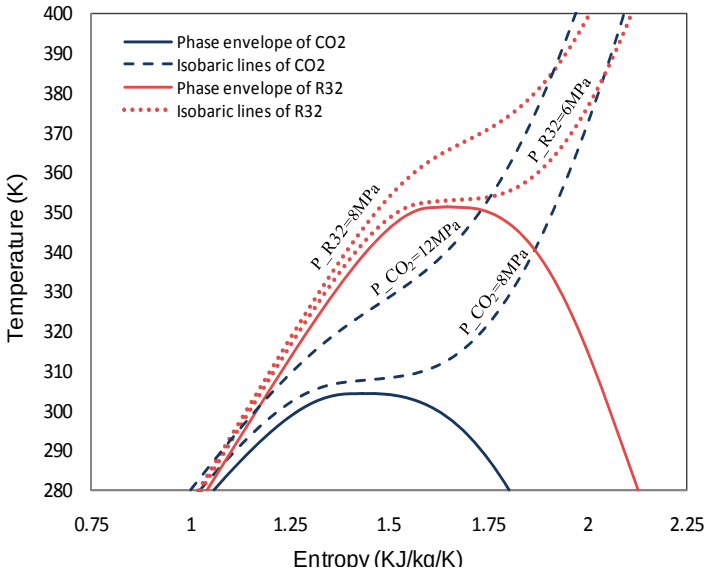

(a) Properties of R32 and CO_2 in a T-s diagram

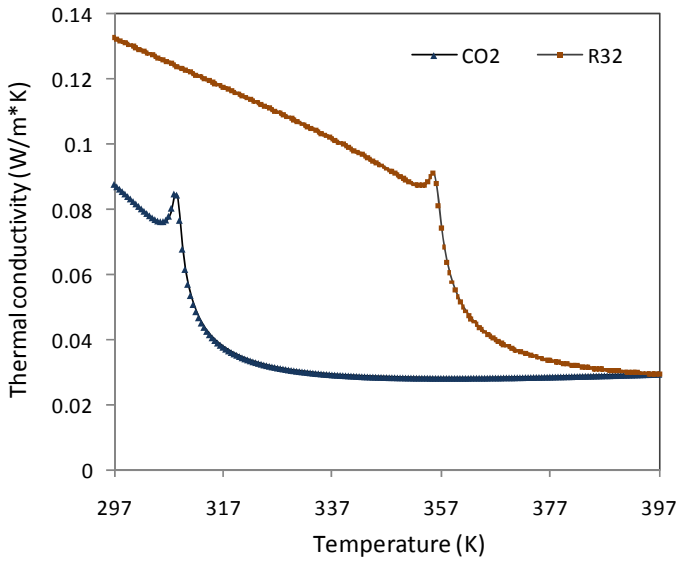

(b) Thermal efficiencies of CO_2- and R32- based supercritical Rankine cycles

Figure 4.2 Properties of CO_2 and R32 as the working fluids of supercritical Rankine cycles

In the following two sections, performance of CO_2 and R32 in a supercritical Rankine cycle for heat-to-power conversion are conducted through energetic and exergy analyses.

4.2 Energetic Analysis

The thermal efficiencies of the two cycles are simulated at different temperatures and pressures based on the First Law of Thermodynamics. The following assumptions are made for the calculation: 85% efficiency for both the pump and the turbine, and the working fluids are condensed at 297K.

Figure 4.3 shows the processes (a→b→c→d→a) of a CO_2- and a R32- based supercritical Rankine cycle in a P-H diagram. In both cycles, a stream of the working fluid is pumped above its critical pressure (a→b), and then heated isobarically from liquid directly to supercritical vapor (b→c); the supercritical vapor is expanded in the turbine to extract mechanical work (c→d); after expansion, the fluid is condensed in the condenser by dissipating heat to a heat sink (d→a); the condensed liquid is then pumped to the high pressure again, which completes the cycle. The energy equations are follows:

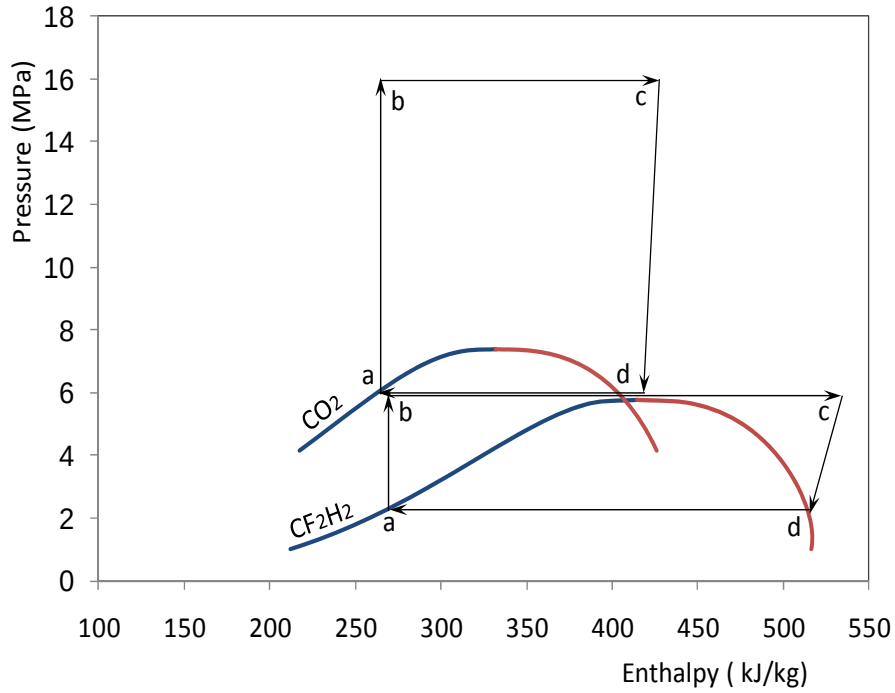

Figure 4.3 The two supercritical Rankine cycles shown in enthalpy-pressure diagram

For the pump:

$$\dot{w}_p = h_b - h_a \tag{4.2}$$

For the turbine:

$$\dot{w}_t = h_c - h_d \tag{4.3}$$

For the vapor generator:

$$\dot{q}_{in} = h_c - h_b \tag{4.4}$$

For the condenser:

$$\dot{q}_{out} = h_d - h_a \tag{4.5}$$

Then the specific net work output:

$$w_{net} = \dot{w}_t - \dot{w}_p \tag{4.6}$$

The thermal efficiency of the cycle:

$$\eta_{th} = \left(\dot{w}_t - \dot{w}_p\right) / \dot{q}_{in} \tag{4.7}$$

The CO_2- and R32- based supercritical Rankine cycles are simulated under the turbine inlet temperature of 373- 453K with an interval of 10K over a wide pressure range, i.e., from the fluids' critical pressure upward. The vapor quality of the turbine exhaust fluid was set to be no less than 0.95 in order to avoid droplet erosion, which constrained the turbine inlet pressure.

The thermal efficiencies of the supercritical Rankine cycle with R32 and CO_2 working fluids at various turbine inlet temperatures and pressures are shown respectively in Figure 4.4. It is seen that for CO_2 there is an optimum inlet pressure for each inlet temperature, while for R32 there is a maximum limiting pressure for each inlet temperature. It is also clear that R32 gives higher thermal efficiency for the same inlet temperature, while it operates at much lower pressure. Take the turbine inlet temperature of 453K for example, the CO_2-based supercritical Rankine cycle obtains thermal efficiencies of 0.04-0.15 with turbine inlet pressures of 7.88-34.38MPa; while the R32-based supercritical Rankine cycle achieves 0.14-0.17 efficiency at 6.04-15.29MPa.

At low pressures, the thermal efficiencies of the CO_2-based Rankine cycle are extremely low (0.02) at all the temperatures investigated, while those of the R32-based cycle are above 0.1. It is seen that for CO_2 there is an optimum inlet pressure

for each inlet temperature, while for R32 there is a maximum limiting pressure for each inlet temperature. It is also clear that R32 gives higher thermal efficiency for the same inlet temperature, while it operates at much lower pressure. No efficiency was obtained for R32 at 373K because of the limitation of the vapor content after turbine expansion.

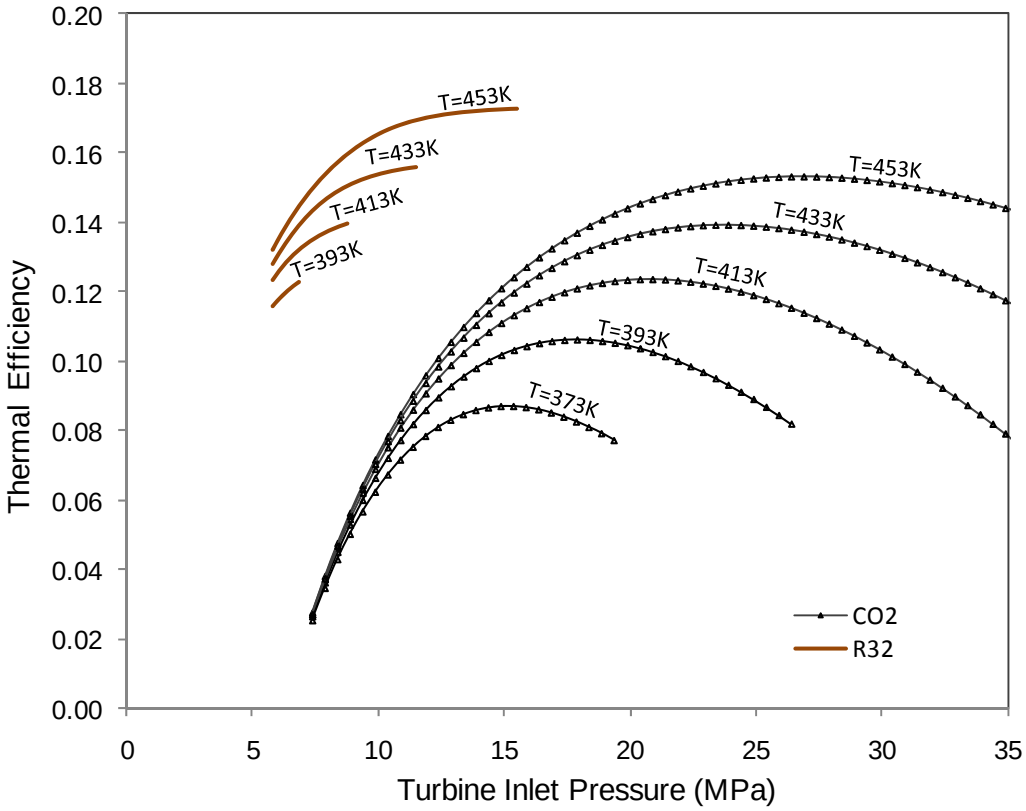

Figure 4.4 The thermal efficiencies of CO_2- and R32- based supercritical Rankine cycles

By analogy with the Carnot cycle, a reversible triangular cycle corresponding to a sensible heat source is found in a T-s diagram in Figure 4.5. For the triangular reversible cycle, the total heat input and net work output yield:

$$q_{in} = \frac{1}{2}\Delta s(T_h - T_l) + \Delta s T_l \tag{4.8}$$

$$w_{net} = \frac{1}{2}\Delta s(T_h - T_l) \tag{4.9}$$

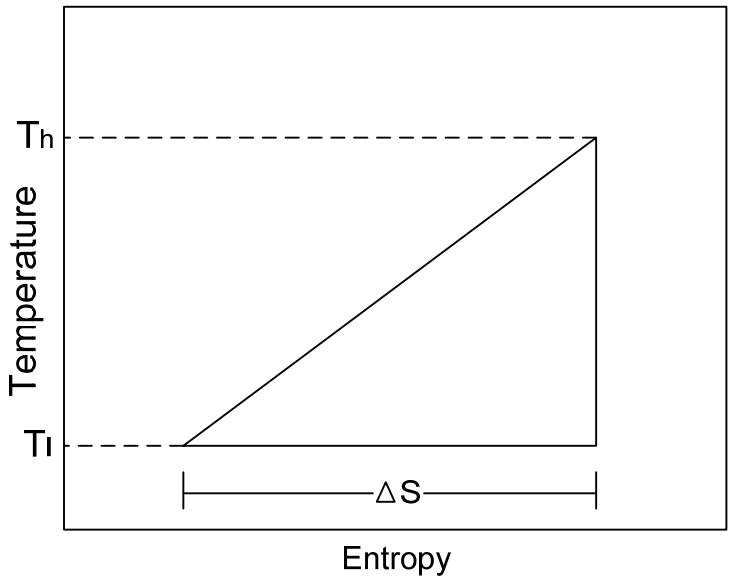

Figure 4.5 A reversible thermodynamic cycle for sensible heat source

The thermal efficiency of the reversible cycle, i.e. the maximum allowable thermal efficiency under the defined heat source and heat sink can be expressed as:

$$\eta_{reversible} = \frac{W_{net}}{Q_{in}} = \frac{\frac{1}{2}\Delta s(T_h - T_l)}{\frac{1}{2}\Delta s(T_h - T_l) + \Delta s T_l} \tag{4.10}$$

Rearranging it gives:

$$\eta_{reversible} = 1 - \frac{2T_l}{T_h + T_l} \tag{4.11}$$

where $\eta_{reversible}$ is the maximum allowable thermal efficiency, T_h and T_l denote the cycle high and low temperatures.

The maximum thermal efficiencies of the two cycles obtained at the turbine temperature of 373-453K are shown in Figure 4.6 along with the theoretical maximum efficiencies from the reversible cycle for comparison. It is found that the R32-based supercritical Rankine cycle achieves efficiencies of 12.6% to 17.3 %, which is a 12.6%-18.6% improvement as compared to 10.6% to 15.3 for the CO_2-based supercritical Rankine cycle for the cycle high temperature of 393K to 453K. However, by comparing with the theoretical maximum efficiencies in Figure 4.6, both the CO_2- and R32- based supercritical Rankine cycles have considerable room for improvement.

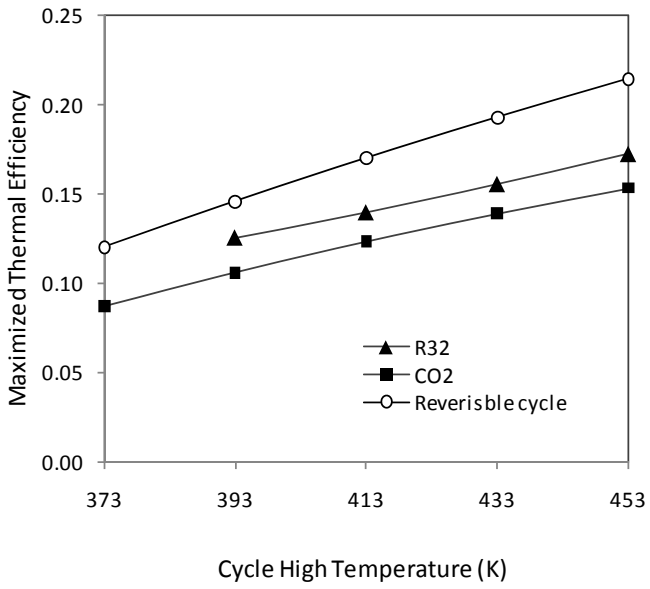

Figure 4.6 Maximized thermal efficiency of the R32- and CO_2- based supercritical Rankine cycles

4.3 Exergetic Analysis

Irreversibility is the cause of inefficiency and exergy loss/destruction. An exergetic analysis is necessary to know the extent of irreversibilities in each process, identify where irreversibility happens, and therefore the potential of improvements. The irreversibility of a process, I, is the sum of all of the increases and decreases in exergy occurring and its rate can be shown to be equal to:

$$\dot{I} = T_0 \sum \dot{m}_n \Delta s_n \tag{4.12}$$

where T_0 is the dead state temperature; $\dot{m}_n$, the mass flow rate of the nth stream, and Δs_n the change in entropy for the *n*th stream.

In a supercritical Rankine cycle, the irreversibly i.e., the exergy destruction within the system and exergy loss to the environment of each element of the system can be expressed as [101]:

For the pump:

$$I_{Pump} = N_p - \left(E_p^{out} - E_p^{in}\right) = N_p - \left[\left(H_p^{out} - H_p^{in}\right) - T_0\left(S_p^{out} - S_p^{in}\right)\right] \tag{4.13}$$

where N_p denotes the power of the pump, E_p^{in} and E_p^{out} are the exergy inlet and outlet of the pump, respectively, and H the enthalpy. T_0 is the dead state temperature, taken as 273K.

For the turbine:

$$I_{Turbine} = \left(E_t^{in} - E_t^{out}\right) - N_t = \left[\left(H_t^{in} - H_t^{out}\right) - T_0\left(S_t^{in} - S_t^{out}\right)\right] - N_t \tag{4.14}$$

For the condensation:

$$I_{condensation} = E_c^{in} - E_c^{out} = \left(H_c^{in} - H_c^{out}\right) - T_0\left(S_c^{in} - S_c^{out}\right) \quad (4.15)$$

The exergy balance of a supercritical Rankine cycle can be written as:

$$E_h + E_p = E_{out} + I_{pump} + I_{turbine} + I_{condensation} \quad (4.16)$$

where E_h is the exergy of the working fluid obtained by absorbing heat from the heat source, E_p is the exergy input by the pump. The exergy of a stream in steady flow yields:

$$\dot{E} = \dot{m}[(h - h_o) - T_o(s - s_0)] \quad (4.17)$$

Therefore, the exergy efficiency of a supercritical Rankine cycle can be defined as:

$$\eta_{Exergy} = \frac{W_{net}}{E_h + E_p} = \frac{E_{out} - E_p}{E_h + E_p} \quad (4.18)$$

Exergetic analyses of the two systems are conducted at the turbine inlet temperature of 433K over a wide pressure range. Figure 4.7 and Figure 4.8 indicate the changes in exergy distributions and the exergy efficiencies with turbine inlet pressure in the two cycles.

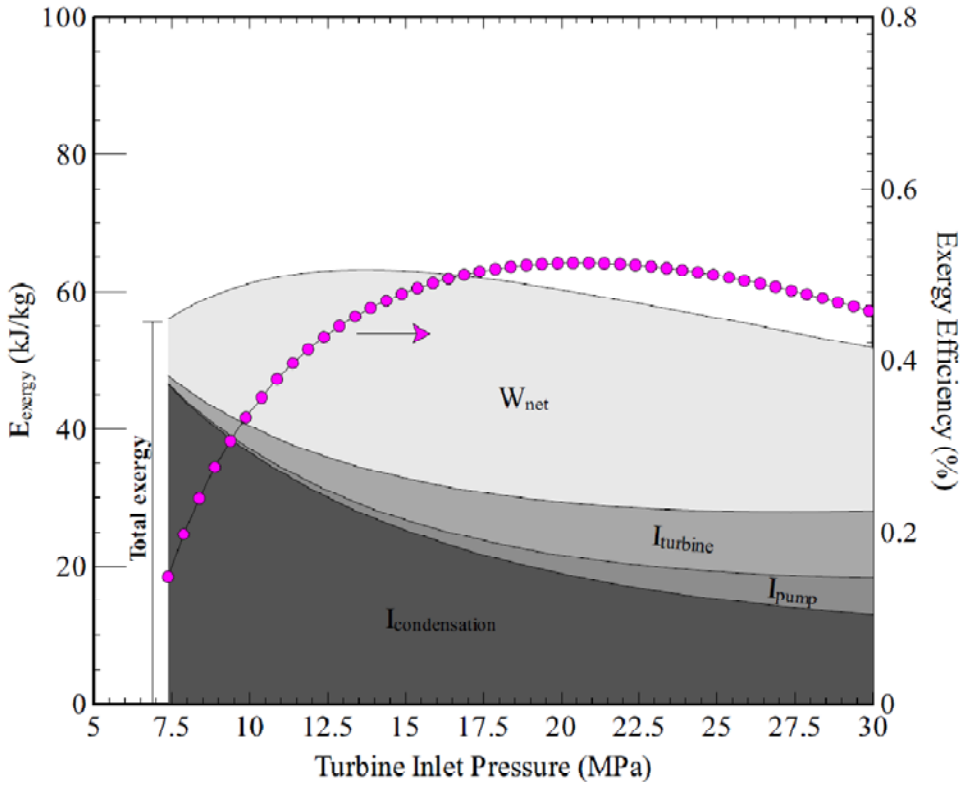

Figure 4.7 The exergy distribution in a CO_2-based supercritical Rankine cycle

The summation of net work output (W_{net}), turbine exergy destruction ($I_{turbine}$), pump exergy destruction (I_{pump}), and condensation exergy ($I_{condensation}$) is the total exergy brought into the system by unit mass of the working fluid at a temperature of 433K. First of all, the total exergy brought by unit mass of CO_2 is in the order of 60kJ/, while R32 is in the order of 90kJ/kg, which indicates that at the same temperature R32 has higher "exergy density" than CO_2, therefore, less mass flow is needed for R32 for the same amount of work output. Secondly, in the CO_2-based supercritical Rankine cycle, the exergy destructions by the turbine and the pump become evident when the turbine inlet pressure gets higher. While in the R32-

based supercritical Rankine cycle, the exergy destruction by the pump is insignificant owning to the relatively lower operating pressure. The assumption of 85% efficiency for the turbines and pumps are reasonably practical, and significantly reducing the exergy destructions by improving their efficiencies is technologically challenging. Thirdly, a large portion of the total exergy is lost in the condensation process in both cycles by dissipating heat to the environment. It is seen for the CO_2-based supercritical Rankine cycle, the exergy loss of the condensation is dominating the panel at lower turbine inlet pressures, which is partly caused by desuperheating the turbine exhaust. This indicates that a recuperater is recommended when the CO_2-based supercritical Rankine cycle operates at lower turbine inlet pressures. For the R32-based supercritical Rankine cycle (Fig.9), not much desuperheating is needed for the whole pressure range investigated, therefore, the exergy loss during the condensation is relatively stable.

It is worth to point out that if the heat exchange processes of the condensations were included in the system, a mismatch between the isothermal condensations and the sensible heat sinks would show large exergy destruction during the heat exchange process. Applying zeotropic mixtures that can create appropriate thermal glides during the condensation will allow the reduction of the exergy destruction of the heat exchange process. Finally, the exergy efficiencies of the CO_2-and R32- based

supercritical Rankine cycle are in the ranges of 0.15-0.51 and 0.56-0.61, respectively, indicating that the R32-based cycle conserves significantly more exergy.

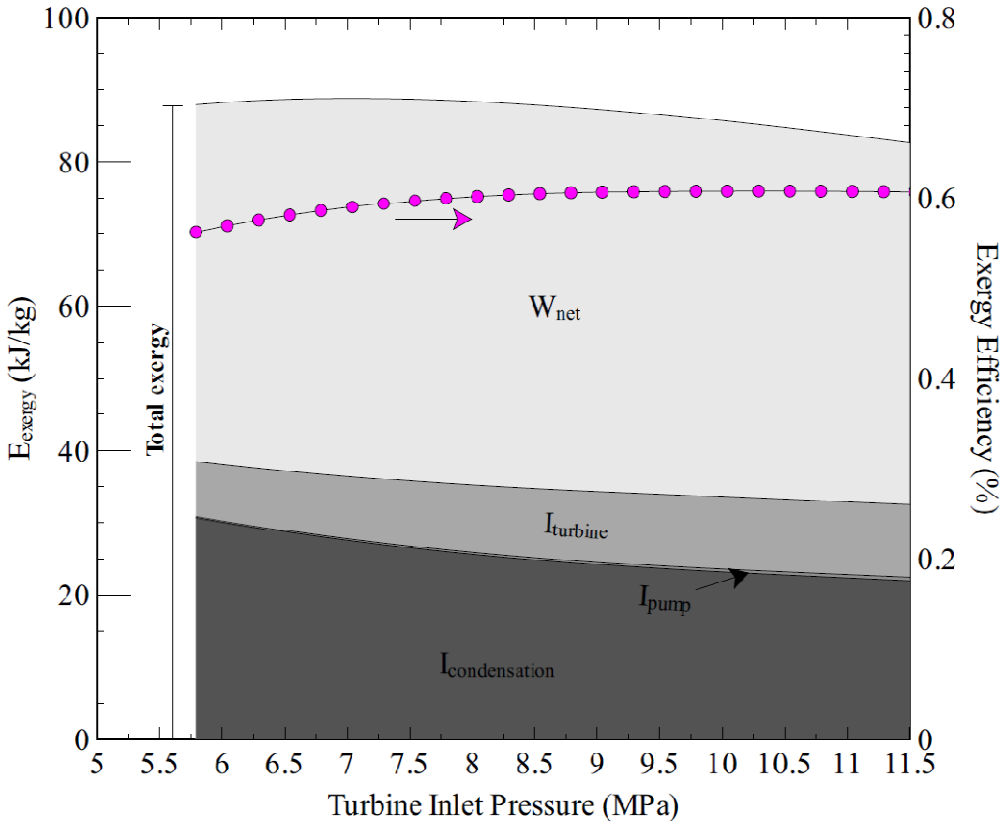

Figure 4.8 The exergy distribution in a R32-based supercritical Rankine cycle

4.4 Ideal Supercritical Rankine Cycle

Based on the exergetic analysis, a large amount of the exergy is lost during the heat exchange processes. For a heat exchange process between the working fluid of a supercritical Rankine cycle and a heat source or heat sink, the irreversibility can be shown to be equal to:

$$d\dot{I} = -T_0(\dot{m}_1 ds_1 + \dot{m}_2 ds_2) \tag{4.19}$$

Combining the above equation and $ds = \frac{\delta \dot{q}}{T}$, and integrating one can get:

$$\dot{I} = \int_0^Q T_0 \left(\frac{\dot{m}_1}{T_1} - \frac{\dot{m}_2}{T_2}\right) \delta \dot{q} = T_0 \int_0^Q \left(\frac{T_2 \dot{m}_1 - T_1 \dot{m}_2}{T_1 T_2}\right) \delta \dot{q} \tag{4.20}$$

According to the above equation, in order to minimize the irreversibility, $\frac{\dot{m}_1}{T_1}$ should approach $\frac{\dot{m}_2}{T_2}$ as much as it can, in the heat exchange process without violating the pinch limitation. Besides that, an important observation is that if T_1 and T_2 are significantly greater than T_0, the irreversibility per unit heat transfer at fixed $(T_2 \dot{m}_1 - T_1 \dot{m}_2)$ is significantly lower and vice versa. This implies that optimizing the thermal match is even more advantageous in the condensation process than in the heating process.

An "ideal" working fluid for the supercritical Rankine cycle is conceived to minimize the exergy destruction during the heat exchange processes, with the concept demonstrated in a temperature-enthalpy diagram in Figure 4.9. In order to have a perfect thermal match during the heating process, the heat capacity of the "ideal" working fluid is directly proportional to that of the heat source during the whole heating process, resulting in two parallel lines (or curves) in the temperature-enthalpy diagram. In the same way, the "ideal" working fluid may be condensed isobarically yet with a thermal glide, in order to match with the coolant perfectly. A perfect temperature profile match with the heat source and the coolant minimizes irreversibility.

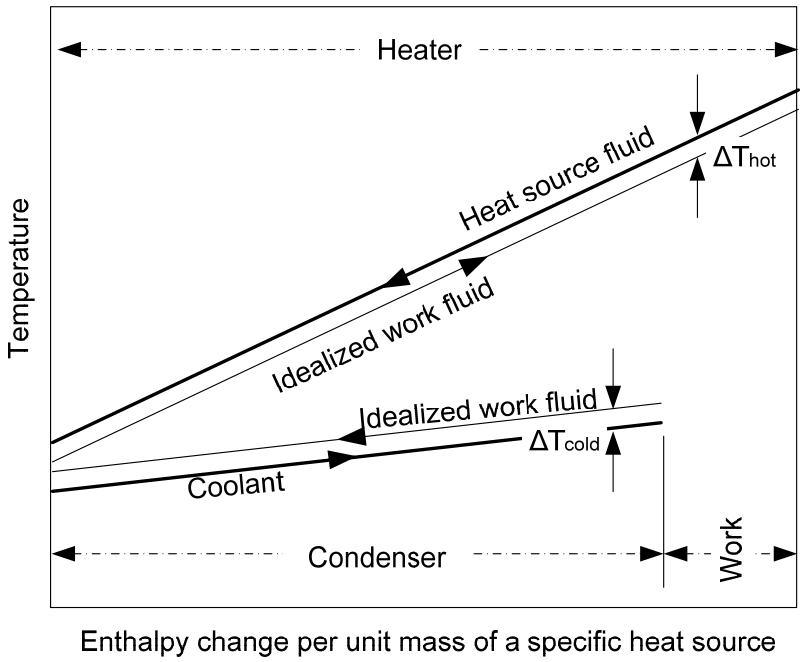

Figure 4.9 A supercritical Rankine cycle with an "ideal" working fluid

The "ideal" working fluid may never be found, but there are ways to approach it. Provided that the sensible heat source has a constant heat capacity, the temperature profile of the heat source would be a straight line during the heating process. Therefore, a "straighter" isobaric line indicates the potential for a better thermal match. As we can see from Figure 4.2 (a), the isobaric lines far beyond the critical pressure are much "straighter" than the ones close to it. However, it must be kept in mind that pumping the working fluid to a very high pressure causes additional exergy destruction, as seen in the CO_2-based supercritical Rankine cycle. In addition, very high pressures introduce safety concerns.

Looking at the condensation process, zeotropic mixtures may be considered in order to condense the working fluid isobarically with a thermal glide. Zeotropic mixtures have been applied in the refrigeration system for better performance, are mixtures of fluids that have different condensation and vaporization points. A proper choice of zeotropic mixture will create a preferable thermal glide during the condensation. The properties of a zeotrpoic mixture of 0.3R32/0.7R134a mass fraction are shown in a T-s diagram in Figure 4.10. It was observed that thermal glides of about 6K are created along the isobaric lines. With this thermal glide, the condensation process can happen with less irreversibility and exergy loss.

In addition, a working fluid could be selected such that after expansion, the turbine exhaust is a saturated vapor or slightly wet to avoid the problem of droplet erosion, while also not requiring desuperheating of the turbine exhaust.

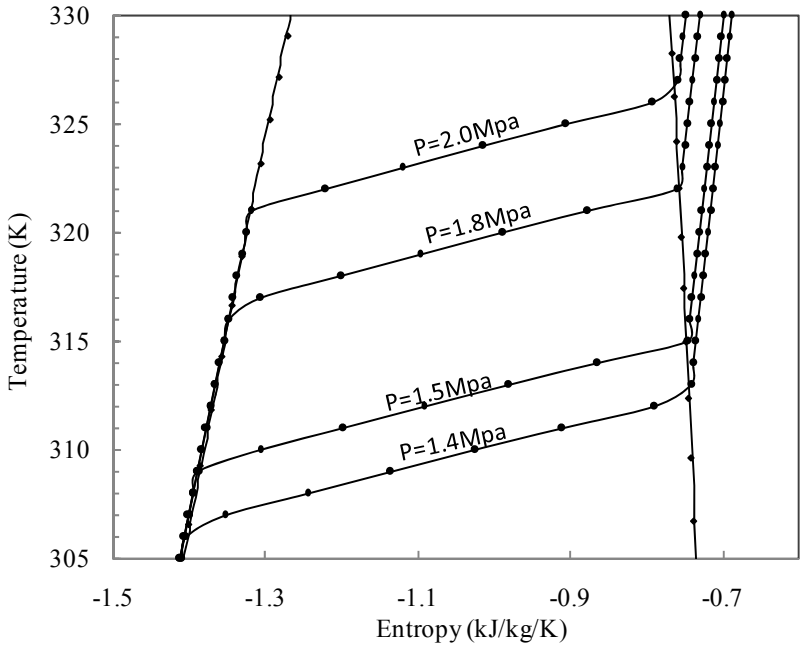

Figure 4.10 A zeotropic mixture of 0.3R32/0.7R134a with non-isothermal isobaric lines

To sum up, developing zeotropic mixtures that can approach the qualities of the "ideal" working fluid could lead to a significant improvement in the efficiency of conversion of low-grade heat into power. The potential of using a zeotropic mixture in a supercritical Rankine cycle is studied in the next chapter.

4.5 Concluding Remarks

Supercritical Rankine cycles using CO_2 and R32 as the working fluids for the conversion of low-grade heat to power are investigated. Although CO_2 has the merits of being abundant, non-flammable, non-toxic and inexpensive, its thermodynamic

performance and operating pressures are inferior to R32. Besides, the low critical temperature of CO_2 introduces difficulties for condensation.

Energetic and exergetic analyses of supercritical Rankine cycles for low-grade heat conversion were conducted using CO_2 and R32 as the working fluids. The analysis shows that:

(1) The thermal efficiency of the R32-based supercritical Rankine cycle is 12.6% to 17.3%, which is a 12.6-18.6% improvement as compared to 10.6% to 15.3% for the CO_2- based cycle for the cycle high temperature of 393K to 453K, and R32 works at much lower pressures.

(2) Since R32 has higher exergy density, less mass flow is needed for R32 than CO_2 for same amount of work output.

(3) For the cycle high temperature of 433K, the exergy efficiency of the CO_2- and R32 based supercritical Rankine cycles range from 0.15-0.51 and 0.56-0.61, respectively, over a wide range of the cycle high pressure.

In addition, an “ideal” working fluid for the supercritical Rankine cycle is conceived. Developing zeotropic mixtures that can approach the quality of the “ideal” working fluid will be a significant improvement for the supercritical Rankine cycle study.

CHAPTER 5 SUPERCRITICAL RANKINE CYCLE USING A ZEOTROPIC MIXTURE WORKING FLUID

It has been revealed in CHAPTER 4 that a supercritical Rankine cycle using a pure fluid as the working fluid does overcome the pinch point limitations of ORCs during the heating process, the condensation process is still isothermal. The novel concept of using zeotropic mixtures as the working fluids in a supercritical Rankine cycle was proposed at the end of last chapter. By applying a proper zeotropic mixture in a supercritical Rankine cycle, the proposed cycle cannot only overcome the pinch point limitations of an organic Rankine cycle during the heating process, but also allow an optimized condensation process since the condensation process is not isothermal anymore.

This chapter compares the performance of a conventional organic Rankine cycle with a zeotropic mixture-based supercritical Rankine cycle under the same temperature limits, which shows the advantages of the zeotropic mixture-based supercritical Rankine cycle.

5.1 Cycle Configuration and the Processes

The basic configuration and the thermodynamic processes of a supercritical Rankine cycle using a zeotropic mixture working fluid are shown in Figure . Like

other supercritical Rankine cycles, the cycle consists of a pump, a vapor generator, an expansion turbine and a condenser. However, the supercritical Rankine cycle using zeotropic mixture as the working fluid has an important feature: in the condensation process, the working fluid is condensed isobarically but non-isothermally as it is seen for process 4→1 in Figure (b). This feature results in a temperature glide which allows us to reduce irreversibilities of the heat transfer process during condensation.

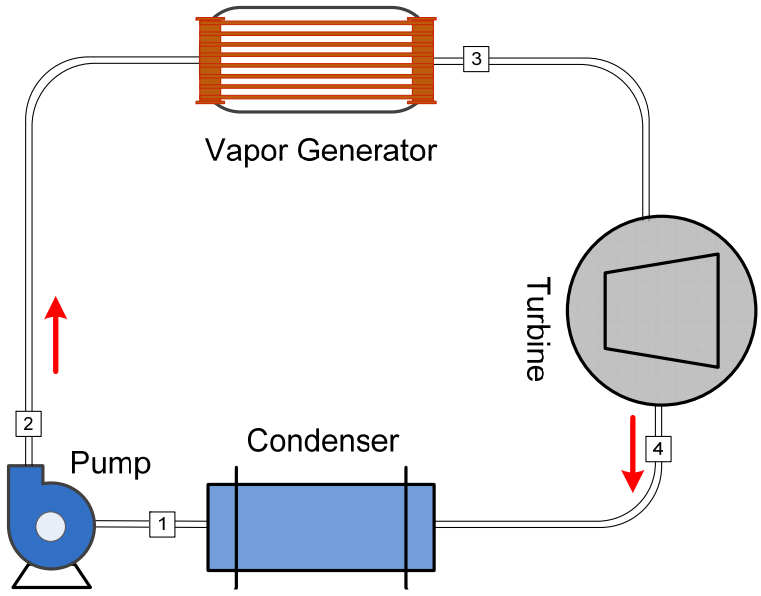

(a) Configuration of the supercritical Rankine cycle

Figure 5.1 Configuration and process of a zeotropic mixture supercritical Rankine cycle

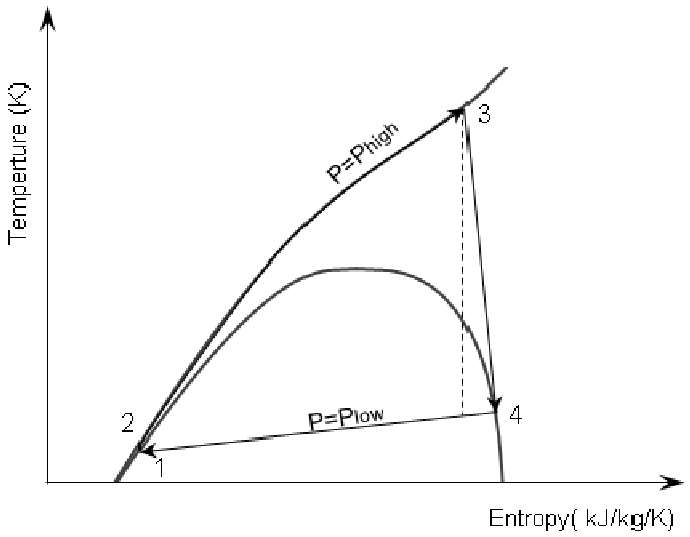

(b) Process of the cycle in a T-s plane

Figure 5.1 (Continued)

5.2 Zeotropic Mixtures as the Working Fluids

Regarding the zeotropic mixture working fluids for supercritical Rankine cycles, mixtures of refrigerants are the potential candidates for the proposed supercritical Rankine cycle due to their thermophysical properties and stability. The properties of the pure refrigerants have been studied in CHAPTER 3. R32 and R134a are selected to compose the zeotropic mixture of current study. The properties of the zeotropic mixture of 0.7R134a/0.3R32 (mass fraction) are demonstrated in Figure 5.2. The zeotropic mixture, considered safe and environmentally friendly, has been used in refrigeration systems [102], and pure R134a is often used as the working fluid of ORCs [3], [103], [73] and refrigeration cycles. If the fluid were condensed isobarically, the condensation process will follow one of the isobaric lines like

P=1.4Mpa or P=2Mpa, depending on the condensation design. The slopes of the isobaric lines enclosed in the phase envelope are the thermal glide of the condensation process. It is noticed that a thermal glide of about 5K is created by the 0.7R134a/0.3R32 zeotropic mixture.

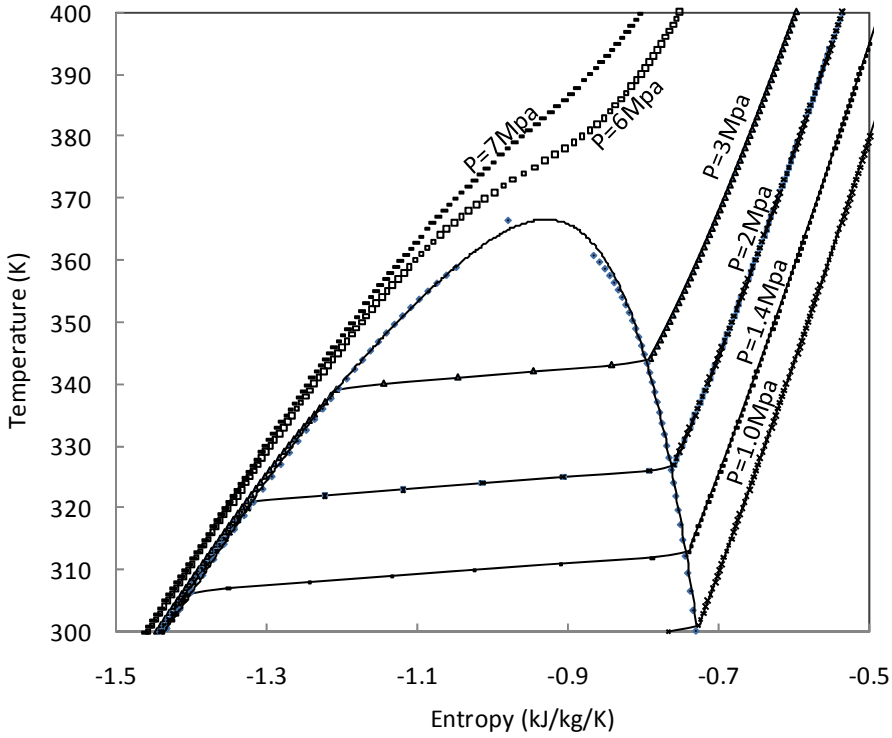

Figure 5.2 Properties of zeotropic mixture 0.7 R134a/0.3R32 mass fraction

5.3 Comparative Study of the Supercritical Rankine Cycle and an Organic Rankine Cycle

In order to investigate the performance of the proposed supercritical Rankine cycle using zeotropic mixtures as the working fluids, a 0.3R34/R134a-based supercritical Rankine cycle is comparatively studied with an R134a-based organic Rankine cycle over the same temperature range. The process of the R134a-based

organic Rankine cycle is shown in a T-s diagram in Figure 5.3 , while that of the zeotropic mixture-based supercritical Rankine cycle is shown in Figure 5.4.

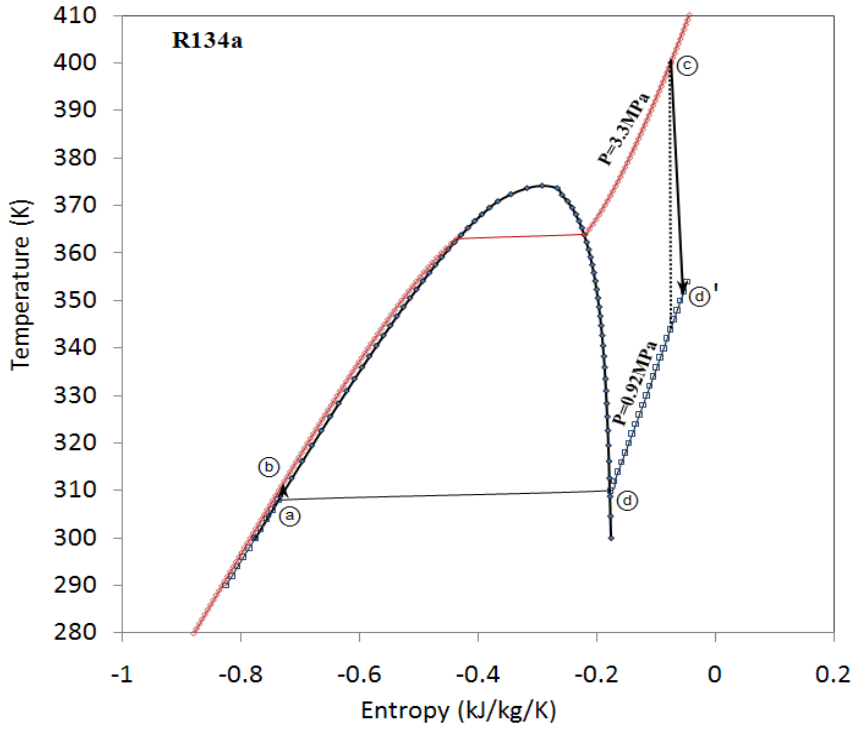

Figure 5.3 Process of an organic Rankine cycle using R134a as the working fluid (ⓐ →ⓑ→ⓒ→ⓓ'→ⓓ)

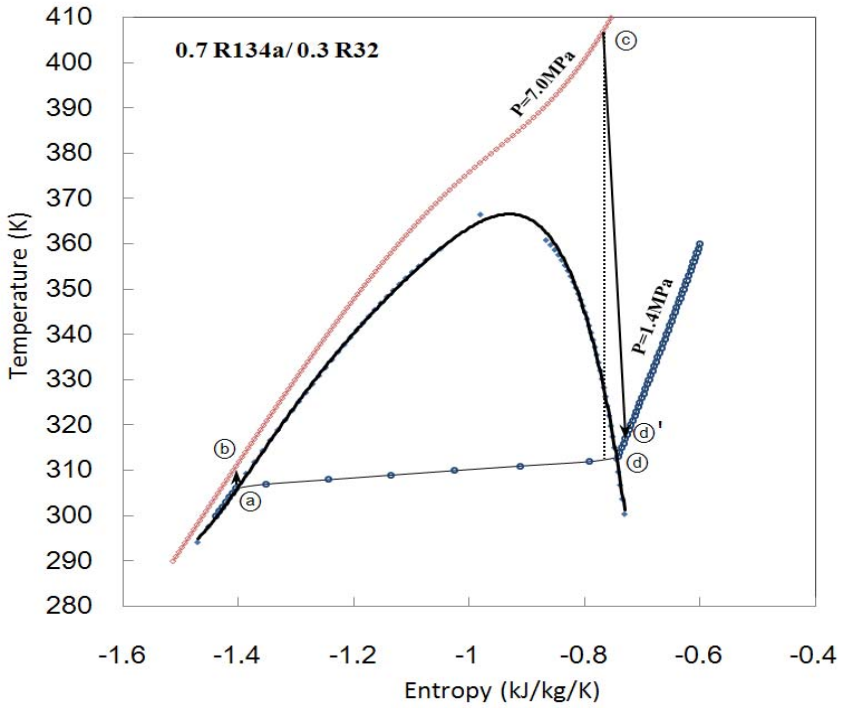

Figure 5.4 Process of a supercritical Rankine cycle using 0.7R134a/0.3R32 as the working fluid (ⓐ→ⓑ→ⓒ→ⓓ'→ⓓ)

5.3.1 Thermal Efficiencies and Net Work Outputs of the Cycles

The thermal efficiencies and the net work outputs of the two cycles are investigated with the following working conditions:

- Cycle high temperature: 393K-473K;
- Average condensing temperature: 309.5K;
- Pump efficiency: 85%;
- Turbine efficiency: 85%.

It is understood that the cycle high pressure of the organic Rankine cycle is below the working fluid's critical pressure, and that of the supercritical Rankine cycle

is above it (refer to Figure 5.3 and Figure 5.4). The cycle high pressure of the 134a-based organic Rankine cycle is set to be 3.3MPa (critical pressure 4.06MPa), and the high pressure of the zeotropic mixture-based organic Rankine cycle is 7MPa (critical pressure 5.13MPa) in the simulation. The low pressures of the cycles are decided based on the average condensation temperature (309.5K).

The computed thermal efficiencies of the organic Rankine cycle and the supercritical Rankine cycle are shown in Figure 5.5 (a). Over the investigated cycle high temperature range (393K-473K), the thermal efficiency of the organic Rankine cycle using pure R134a is 9.70-10.13%, while that of the supercritical Rankine cycle using the zeotropic mixture is 10.77-13.35% showing 10-30% increase over the R134a-based organic Rankine cycle. Figure 5.5 (a) also shows that the thermal efficiency of the R134a-based organic Rankine cycle shows no significant increase as the cycle high temperature is increased from 393K to 473K.

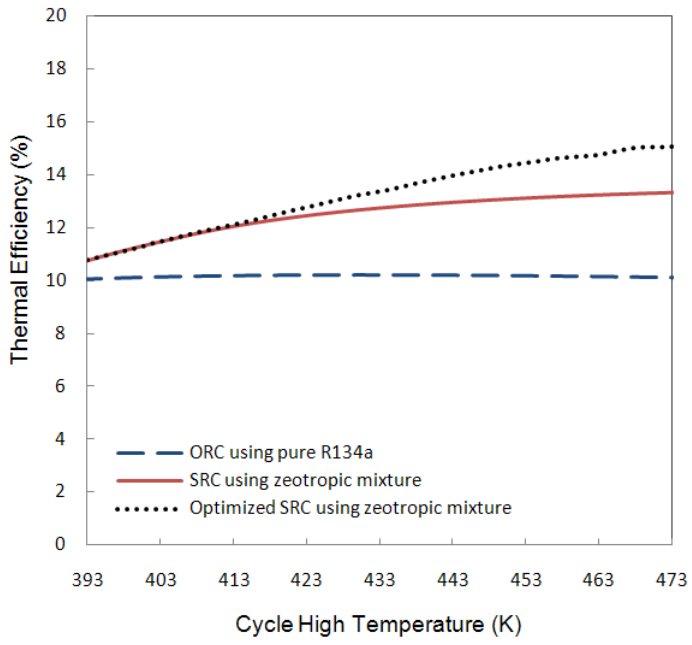

(a) Thermal efficiencies

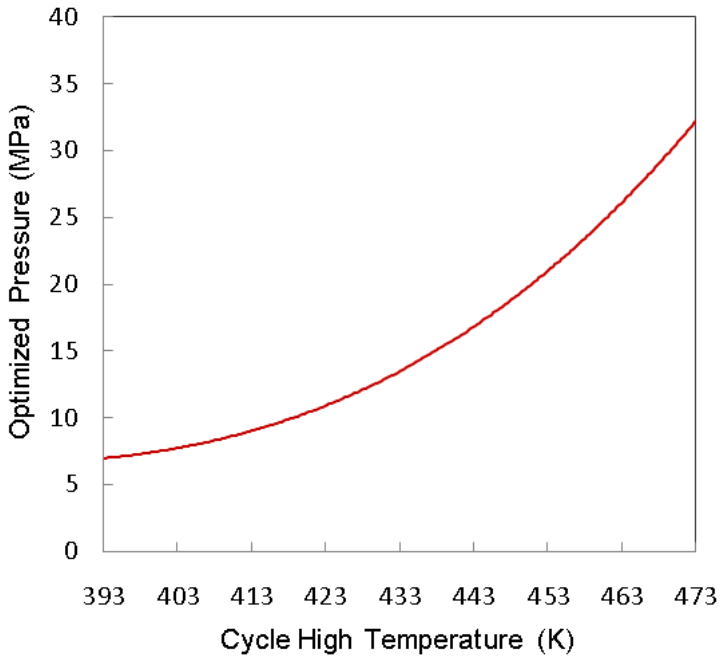

(b) Cycle high pressure needed for optimized thermal efficiency

Figure 5.5 Thermal efficiencies of the R134a-based organic Rankine cycle (ORC) and the zeotropic mixture-based supercritical Rankine cycle (SRC)

The above simulations were based on constant cycle high pressures. Computations were also made with changing cycle high pressures in order to optimize the cycle thermal efficiencies. Assuming the minimum vapor quality at the turbine exit is 90%, the optimized thermal efficiency of the supercritical Rankine cycle is shown with a dotted line in Figure 5.5 (a). Comparing it with the efficiency of the supercritical Rankine cycle working at 7MPa (continuous line in Figure 5.5 (a)), it is seen that there is a significant improvement at higher cycle temperatures. Figure 5.5 (b) shows the cycle high pressure of the supercritical Rankine cycle for optimized thermal efficiency. It is observed that in order to get the optimized thermal efficiency of 15.08% at 473K, the pressure of the cycle is as high as 33MPa. The analysis of optimized thermal efficiency is only to show that there is a potential for improvement of the supercritical Rankine cycle. A high pressure like that could be a concern in real practice. The analysis of optimized thermal efficiency is carried out in order to show that there is a potential for improvement of the supercritical Rankine cycle. However, the following analysis of the supercritical Rankine cycle is still based on a constant cycle high pressure of 7MPa.

The net work outputs of the two cycles are shown in Figure 5.6. It is seen that the net work output of the supercritical Rankine cycle is higher than that of the organic Rankine cycle and the difference between them increases along the increase

of the cycle high temperature. At 473K, the supercritical Rankine cycle outputs 38.9% more net work than the organic Rankine cycle.

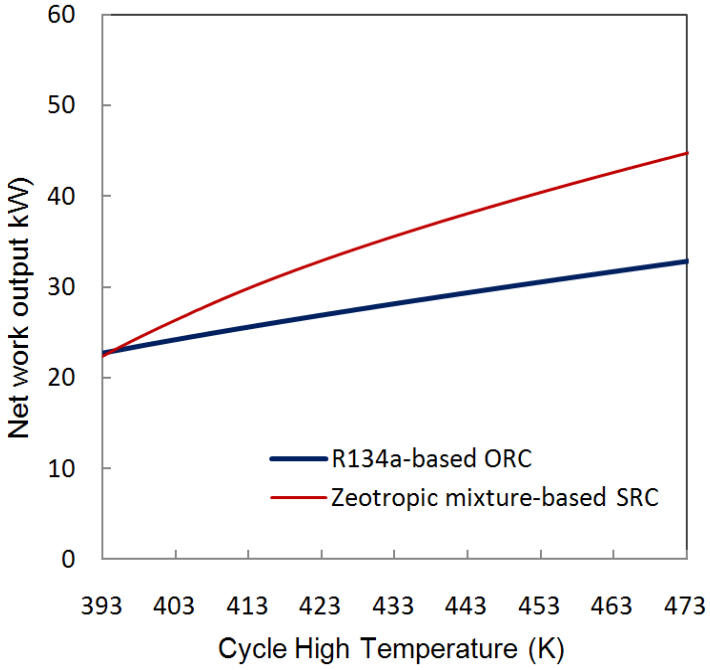

Figure 5.6 Net work outputs of the R134a-based organic Rankine cycle (ORC) and the zeotropic mixture-based supercritical Rankine cycle (SRC)

5.3.2 Exergy Efficiency of the Condensing Process

Exergy analyses of the condensing process in the two cycles are conducted in this section to study the condensation process of pure R134a in the organic Rankine cycle and the zeotropic mixture of 0.7R134a/0.3R32 in the supercritical Rankine cycle, which processes are shown in Figure 5.7 and Figure 5.8, respectively. The working fluids are condensed from saturated vapor at point ⓓ to saturated liquid at point ⓐ by dissipating the heat to the cooling fluid. The thermal matches between the

working fluids and the cooling fluids are shown at the top left corners of the figures. For the purpose of calculation, water is used as the cooling fluid in this study. The exergy analyses of the condensation processes in the two cycles are conducted under the following assumptions:

- Average condensation temperature: 309.5K;
- Working fluid mass flow rate: 1kg/s;
- Heat exchange pinch limitation: 8K;

Based on the average condensing temperature of 309.5K, the pure R134a is condensed isobarically at 0.92MPa and a constant temperature of 309.5K (Figure 5.7), while the zeotropic mixture is condensed isobarically at 1.4MPa with the condensation commencing at a temperature of 312.37K (point ⓓ in Figure 5.8 and ending at a temperature of 306.6 K (point ⓐ in Figure 5.8).

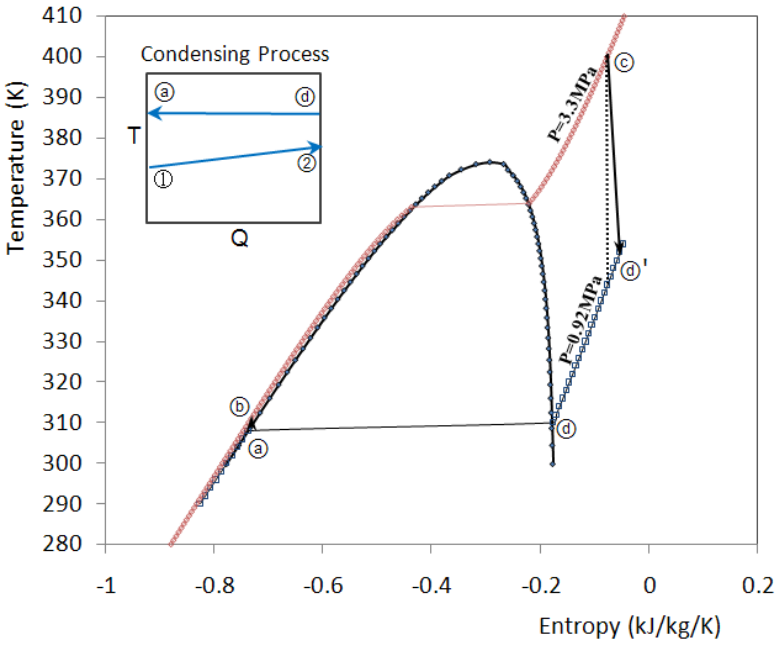

Figure 5.7 Condensing process of R134a and its thermal match with the cooling agent

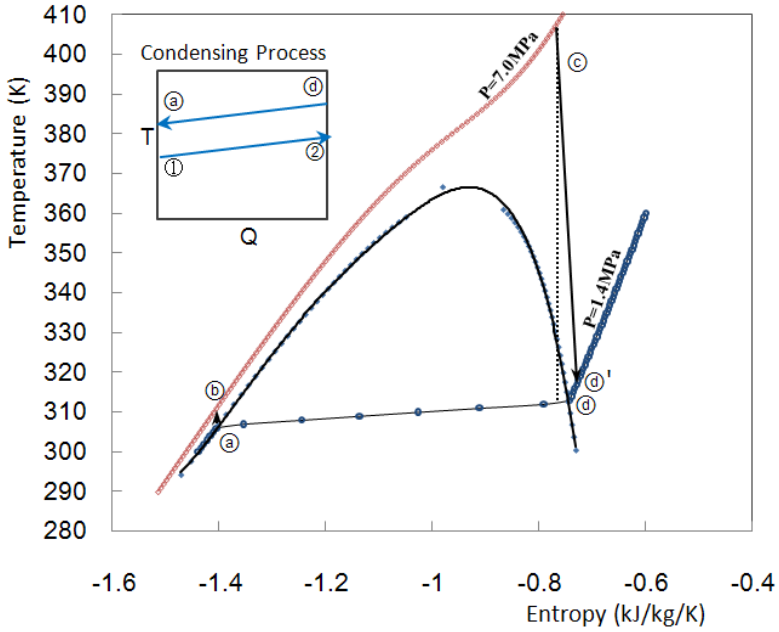

Figure 5.8 Condensing process of the zeotropic mixture of R134a and R32 and its thermal match with the cooling agent

Since the zeotropic mixture creates a thermal glide when condensed isobarically, the heat exchange process can be designed such that the temperature profile of the cooling water parallels that of the working fluid to obtain the best thermal match. Under this design, the mass flow rate of cooling water can be found from the energy balance of the condenser at steady state [104]:

$$\dot{m}_{water}(h_{①} - h_{②}) + \dot{m}_{zeo}\left(h_{ⓓ} - h_{ⓐ}\right) = 0 \tag{5.1}$$

where $\dot{m}_{water}$ is the mass flow rate of the cooling water, $h_{①}$ and $h_{②}$ denote the enthalpies of the cooling water at points ① and ②, respectively (See Figure 5.8). Similarly, $\dot{m}_{zeo}$ is the mass flow rate of the zeotropic mixture being condensed; $h_{ⓓ}$ and $h_{ⓐ}$ are the enthalpies of the zeotropic mixture at points ⓓ and ⓐ, respectively. The enthalpy values of all the four points can be obtained according to their temperature and fluid type. The flow rate of the cooling water is calculated to be 8.37 kg/s from equation (5.1).

The net change in the flow exergy rate from saturated vapor (point ⓓ in Figure 5.8 to saturated liquid (point ⓐ in Figure 5.8) for the zeotropic mixture is computed to be -383.05 kW using the following equation, neglecting the effects of motion and gravity [104]:

$$\Delta\dot{E}_{zeo} = \dot{m}_{zeo}\left(e_{ⓐ} - e_{ⓓ}\right) = \dot{m}_{zeo}\left[\left(h_{ⓐ} - h_{ⓓ}\right) - T_0\left(s_{ⓐ} - s_{ⓓ}\right)\right] \tag{5.2}$$

where T_0 is the dead-state temperature, 273K. The rest of the symbols remain the same.

Similarly, the change in the flow exergy rate from the inlet to the outlet for the cooling water is found to be 312.72kW by using the following equation (3):

$$\Delta\dot{E}_{water} = \dot{m}_{water}(e_{②} - e_{①}) = \dot{m}_{water}[(h_{②} - h_{①}) - T_0(s_{②} - s_{①})] \quad (5.3)$$

The exergetic efficiency of the heat exchanging process for condensing the zeotropic mixture can then be calculated from the following equation to be 81.64%:

$$\varepsilon = -\frac{\Delta\dot{E}_{water}}{\Delta\dot{E}_{zeo}} = \frac{\dot{m}_{water}(e_{①} - e_{②})}{\dot{m}_{zeo}(e_{ⓐ} - e_{ⓓ})} \quad (5.4)$$

With the same flow rate of cooling water and the aforesaid design and operating parameters, the enthalpy of the inlet cooling water ($h_{①}$) in the R134a-based organic Rankine cycle can be found by the following equation:

$$\dot{m}_{water}(h_{①} - h_{②}) + \dot{m}_{R134a}\left(h_{ⓓ} - h_{ⓐ}\right) = 0 \quad (5.5)$$

The net changes in the flow exergy rate of the pure R134a and its cooling water can be found through Equations (2) and (3), except that the working fluid is pure R134a. The exergetic efficiency of the heat exchange process for condensing pure R134a is calculated to be 66.55%.

Detailed results of the condensation processes in both cycles are listed in Table 5.1. It can be observed from Table 5.1 that the thermal glide of the zeotropic mixture is 312.4K-306.6K= 5.8K, while there is no thermal glide created by pure R134a. The cooling water temperature required by pure R134a is 293.7K, which is 4.8K lower than that of the zeotropic mixture. Exergy efficiency indicates the percentage of usable energy conserved during the condensation process. It is seen that

the 0.7R134a/0.3R32 condensation process is 22.67% higher than that of pure fluid R134a.

Table 5.2 Calculated results to compare the condensing process of the two working fluids in the cycles

Working Fluid		***R134a***	***Zeotropic mixture[b]***
Working fluid Temperature (K)	Point ⓓ [a]	309.5	312.4
	Point ⓐ[a]	309.5	306.6
Cooling Water Temperature (K)	Point ①[a]	293.7	298.6
	Point ②[a]	301.5	304.4
Exergy Efficiency (%)		**66.55**	**81.64**

Note: [a]Refer to Figure 5.7 and Figure 5.8 for point ⓓ, ⓐ, ②, and ①; [b]Zeotropic mixture of R32 and R134a (0.3/0.7, mass fraction).

5.3.3 Exergy Efficiency of the Heating Process

In this section, exergy analyses of the heating processes of the two cycles are carried out. Figure 5.9 and Figure 5.10 present the heating process of the two cycles with the thermal match shown on the top left corners. The working fluids are heated from state ⓑ to state ⓒ by a sensible heat source in counterflow heat exchangers in both cycles.

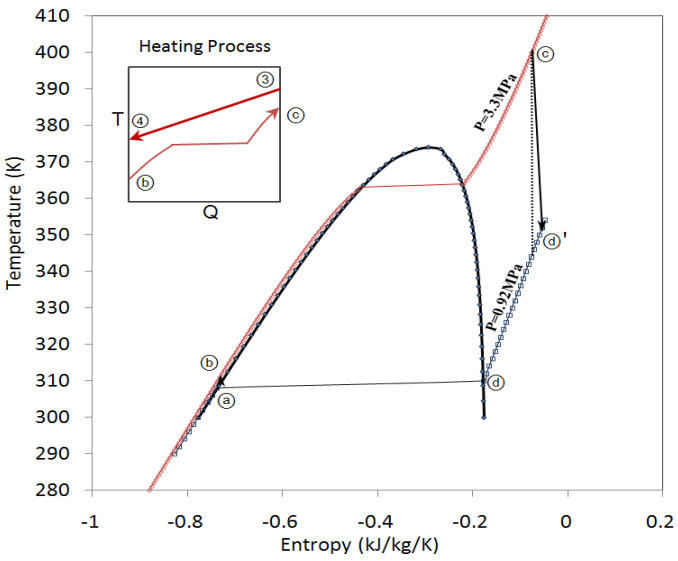

Figure 5.9 Heating process of the zeotropic mixture of R134a and R32 and its thermal match with the heat source

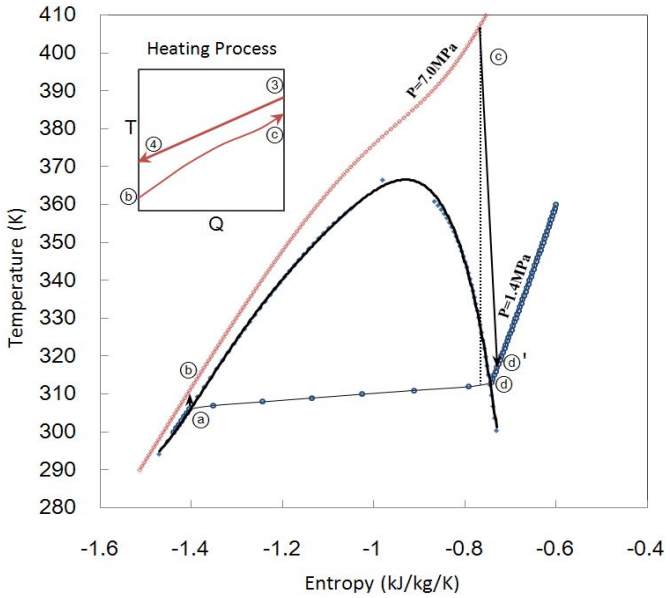

Figure 5.10 Heating process of the zeotropic mixture 0.7R134a/0.3 R32 and its thermal match with the heat source

Pressurized hot water (P=0.5MPa) at 410K is applied as the heat source for the sake of this simulation. The following assumptions are made for the calculation.

- Initial temperature of the heat source: 410K;
- Final temperature of the working fluids being heated: 400K;
- Mass flow rate of the working fluids: 1kg/s;
- Pinch limitation of the heat transfer: 10K;
- Energy loss during the heat transfer: 10%;

The mass flow rate of the heat source is just enough to heat the working fluids to 400K and meet the pinch limitation of 10K throughout the heat exchanging process.

In the organic Rankine cycle, the pinch limitation is reached at the saturated liquid point during the heating process (Figure 5.9). Since there is no obvious pinch point for the zeotropic mixture, multiple points are tested during the calculation. The heating processes of the pure R134a in the organic Rankine cycle and the zeotropic mixture of 0.7R134a/0.3R32 in the supercritical Rankine cycle are analyzed and the results are listed in Table 5.3.

It is seen from Table 5.3 that the discharge temperature of the heat source in the R134a-based organic Rankine cycle is 24K higher than that in the zeotropic mixture-based supercritical Rankine cycle (point ④ in Figure 5.9 and Figure 5.10), which indicates the effective utilization of the heat source is much less in the R134a-

based organic Rankine cycle than that of the 0.7R134a/0.3R32-based supercritical Rankine cycle. Such result is also obvious by comparing the exergy efficiencies of the heating process of the two cycles with supercritical Rankine cycle showing 7.30% higher exergy efficiency of the heating process than that of the pure R134a in the organic Rankine cycle.

Table 5.3 Calculated results to compare the heating process of the two working fluids

Working Fluid		**R134a**	**Zeotropic mixture[b]**
Heat Source Temperature (K)	Point ③[a]	410.0	410.0
	Point ④[a]	355.7	331.7
Working Fluid Temperature (K)	Point ⓑ[a]	309.5	306.6
	Point ⓒ[a]	400.0	400.0
Exergy Efficiency (%)		**82.64**	**88.67**

Note: [a]Refer to Figure 5.9 and Figure 5.10 for point ③, ④, ⓑ, and ⓒ; [b]Zeotropic mixture of R32 and R134a (0.3/0.7, mass fraction).

5.4 Results and Discussion

For a system composed of a heat source, a power cycle and a heat sink, a supercritical Rankine cycle *system* and an organic Rankine cycle *system* have been studied for their performance in the heat transfer from the heat source to the power cycle, the thermal efficiency of power cycle, and the heat dissipation from the power cycle to the heat sink. The 0.7R134a/0.3R32 zeotropic mixture-based supercritical Rankine cycle shows advantages over the pure R134a-based organic Rankine cycle in all of the aspects that have been analyzed, the results being summarized in Table 5.4.

Comparing the two cycles, the supercritical Rankine cycle improves the cycle thermal efficiency, exergy efficiency of the heating process and the exergy of the condensing process by 21.57%, 22.67%, and 7.30%, respectively, compared to the organic Rankine cycle using R134a.

The exergy efficiencies of the organic Rankine cycle *system* and the supercritical Rankine cycle system are also calculated by multiplying the exergy efficiencies of the heating process, the energy conversion cycle, and the condensation processes of the respective systems, which results are also listed in Table 5.4. It is noticed that the total exergy efficiency of the supercritical Rankine cycle system is 38.57%, which is a 60.02% improvement over that of the organic Rankine cycle (24.10%).

Table 5.4 Comparative study between the organic Rankine cycle and the supercritical Rankine cycle[a]

Working fluid & Thermodynamic cycle	**R134a, ORC**	**Zeotropic mixture[b], SRC**
Thermal efficiency (%)	9.92	12.06
Condensing process exergy Efficiency (%)	66.55	81.64
Heating process exergy Efficiency (%)	82.64	88.67
System total exergy efficiency (%)	24.10	38.57

Note: [a]Computation based on the cycle high temperature of 400K; [b]Zeotropic mixture of R32 and R134a (0.3/0.7, mass fraction).

The zeotropic mixture of 0.7R134a/0.3R32 considered as the working fluid of the supercritical Rankine cycle is not always the best choice. It can be observed from Figure 5.3 that there is little gain in thermal efficiency when the cycle high temperature is beyond 433K, which indicates that the zeotropic mixture of 0.7R134a/0.3R32 may be a good choice for heat sources with temperatures below 433K, while there may be other mixtures which could perform better above 433K. One should be able to compose other zeotropic mixtures from the screened fluids in Table 3.1 in CHAPTER 3 for different temperature applications. Beside the temperature considerations, it is recommended that a zeotropic mixture used as the working fluid of a supercritical Rankine cycle should have a thermal glide of at least 3K during the condensation process in order to take the advantage of non-isothermal condensation.

Beside the analysis presented in this work, pure R134a was also investigated as the working fluid of a supercritical Rankine cycle. The results show that the thermal efficiency of the pure R134a-based supercritical Rankine cycle could be 20% higher than that of the pure R134a-based organic Rankine cycle, which again indicates that supercritical Rankine cycle is more favorable in terms of the system efficiency. The proposed supercritical Rankine cycle using zeotropic mixture as the working fluid may further improve the system efficiency by conserving more exergy during the heat transfer of the condensing process.

5.5 Concluding Remarks

A supercritical Rankine cycle using zeotropic mixtures as the working fluids has been investigated in this chapter. The performance of the supercritical Rankine cycle is investigated through a comparative study of a supercritical Rankine cycle and an organic Rankine cycle working under the same thermal conditions. It was found that a supercritical Rankine cycle using a mixture of 0.7R134a/0.3R32 can achieve thermal efficiency of 10.77-13.35% with the cycle high temperature of 393-453K as compared to 9.70-10.13% for an ORC using pure R134a working fluid under the same thermal conditions. The supercritical Rankine cycle using the zeotropic mixture also improves the heat exchange processes: the exergy efficiencies of the heating and condensation processes for the zeotropic mixture are 88.67% and 81.64%, respectively, as compared to 82.65% and 66.55% for the pure R134a in organic Rankine cycle. Overall, the system exergy efficiency of the SRC using the zeotropic mixture of 0.7R134a/0.3R32 is 38.57%, while that of the ORC using pure R134a is 24.10%.

One should be able to compose zeotropic mixtures from the screened fluids in Table 3.1 in CHAPTER 3 for different temperature applications. However, it naturally raises the question of what is the optimal zeotropic mixture for a certain heat source, and how to minimize the irreversibility and maximize the conversion. This is problem of optimization, and intensive research and it is carried out in the following chapter.

CHAPTER 6 OPTIMIZING ENERGY CONVERSION USING SUPERCRITICAL RANKINE CYCLE AND ORGANIC RANKINE CYCLE

Zeotropic mixtures are innovatively applied as the working fluids of supercritical Rankine cycles in CHAPTER 5. The comparison study shows that there are significant advantages of using a zeotropic mixture than a pure fluid in supercritical Rankine cycles. Customized zeotropic mixtures should be designed for different heat source conditions. The optimization of organic Rankine cycles (ORCs) and supercritical Rankine cycles (SRCs) based on the heat source temperature level is of great significance for efficient utilization of low grade heat. However, no systematic analysis on the optimization of ORCs and SRCs has been offered in the literature.

In this chapter, a target function, i.e. system exergy efficiency, is used to optimize the energy conversion. The system under investigation is composed of a thermodynamic cycle for energy conversion, a heat exchanger to add heat into the thermodynamic cycle, and a condenser to dissipate heat to the heat sink. Rigorous analyses of 6 working fluids in 12 ORCs and SRCs are carried out.

6.1 The Ideal Cycles

In an ideal thermodynamic process for a given heat source, heat would be transferred from the source to the thermodynamic cycle at an infinitesimal temperature difference. The ideal thermodynamic processes are obviously impossible in reality, but they serve as benchmarks for all the thermodynamic processes working between the same heat source and sink conditions, and are important tools in the performance analysis, comparison and development of actual thermodynamic systems. In this section, three types of ideal thermodynamic cycles are analyzed.

6.1.1 The Carnot Cycle

Carnot cycle has been recognized as the most efficient thermodynamic cycle capable of converting thermal energy into work between two temperatures (see Figure 6.1).

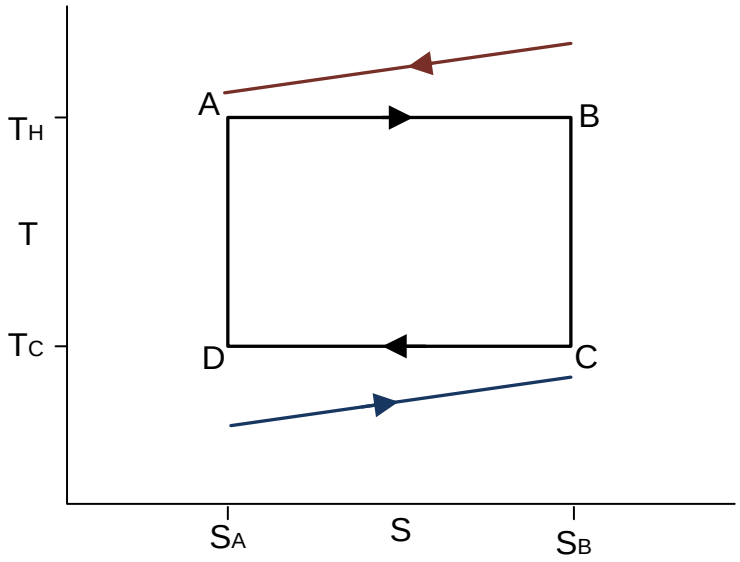

Figure 6.1 Carnot cycle with sensible heat source and sink

The total thermal energy transferred from the hot reservoir to the system is:

$$Q_H = T_H(S_B - S_A) \tag{6.1}$$

The amount of energy converted to work and the conversion efficiency of the Carnot cycle are:

$$W = \oint PdV = (T_H - T_c)(S_B - S_A) \tag{6.2}$$

$$\eta_{Carnot} = \frac{W}{Q_H} = 1 - \frac{T_C}{T_H} \tag{6.3}$$

In a Carnot cycle, the heat source has infinite heat capacity or size so that its temperature profile perfectly matches the isothermal vaporization and condensation processes of the working fluid. However, in reality, the heat sources and sinks have finite heat capacities and sizes, so that their temperatures change during the heat exchange process in the boiler and the condenser as depicted in Figure 6.1. The mismatch between the working fluid and the heat source temperature profiles leads to irreversibility, ergo exergy destruction.

6.1.2 The Lorenz Cycle

Lorenz cycle is an ideal cycle, conceptualized in 1894 by V. H. Lorenz [105] which improves the thermal matches between the working fluids and the heat source and sink temperatures as shown in Figure 6.2. If applied to working fluids that change phase during the heating and cooling processes of the Lorenz cycle, the working fluids would need to exhibit a temperature glide during vaporization and condensation.

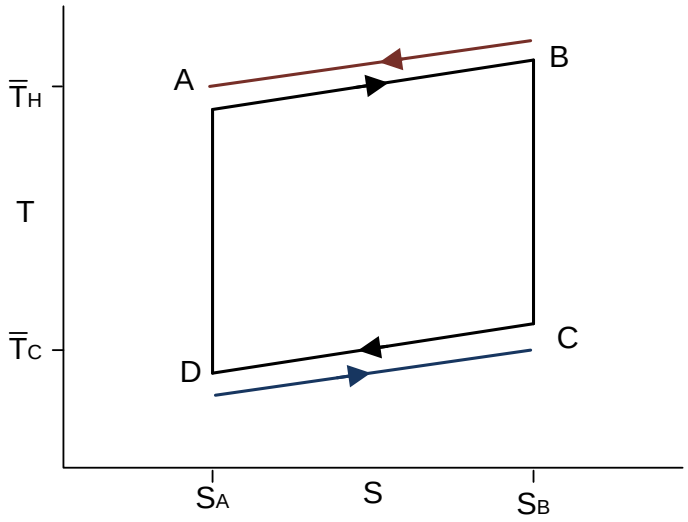

Figure 6.2 Lorenz cycle with sensible heat source and sink

The total thermal energy transferred from the hot reservoir to the system is given by:

$$Q_H = \int_{S_A}^{S_B} T\, dS = \overline{T}_H(S_B - S_A) \tag{6.4}$$

The amount of energy converted to work and the conversion efficiency of the Lorenz cycle are:

$$W = \oint P dV = (\overline{T}_H - \overline{T}_c)(S_B - S_A) \tag{6.5}$$

$$\eta_{Lorenz} = \frac{(\overline{T}_H - \overline{T}_c)(S_B - S_A)}{\overline{T}_H(S_B - S_A)} = 1 - \frac{\overline{T}_c}{\overline{T}_H} \tag{6.6}$$

where $\overline{T}_H$ and $\overline{T}_c$ are the log mean temperatures of the vaporization and condensation processes.

Pure working fluids cannot have a temperature glide during vaporization and condensation unless the pressure is varied continuously during these processes, which

is not practical. However, zeotropic mixtures of pure working fluids show a temperature glide which provides a practical approximation of the Lorenz cycle. Different mixtures have been studied for organic Rankine cycles [47-54] and refrigeration cycles [106], [107].

6.1.3 The Triangular Cycle

In both Carnot and Lorenz cycles, the heat addition and dissipation only happen at vaporization and condensation processes. If a working fluid is heated from the condensation temperature to the heat source temperature, a triangular cycle shown in Figure 6.3 (a) is the ideal cycle for the situation.

For a triangular cycle, the total heat input and net work output yield:

$$Q_{in} = \int_{S_A}^{S_B} TdS = \frac{1}{2}(S_B - S_A)(T_H - T_L) + (S_B - S_A)T_L \tag{6.7}$$

$$W_{net} = \oint PdV = \frac{1}{2}(S_B - S_A)(T_H - T_L) \tag{6.8}$$

The efficiency of the triangular cycle can be expressed as:

$$\eta_{triangular} = \frac{W_{net}}{Q_{in}} = \frac{\frac{1}{2}(S_B - S_A)(T_H - T_L)}{\frac{1}{2}(S_B - S_A)(T_H - T_L) + (S_B - S_A)T_L} = 1 - \frac{2T_L}{T_H + T_L} \tag{6.9}$$

A refrigeration cycle or a supercritical Rankine cycle is usually the practical approximation of a triangular cycle. The process of a supercritical cycle is shown in Figure 6.3 (b), in which the working fluid is pumped above its critical pressure, and then heated to supercritical state directly from liquid, bypassing the liquid-vapor two-phase region.

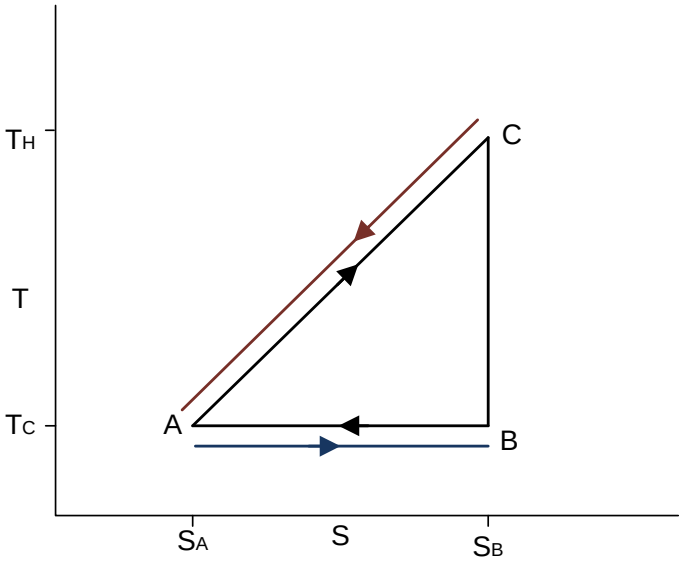

(a) A triangular cycle

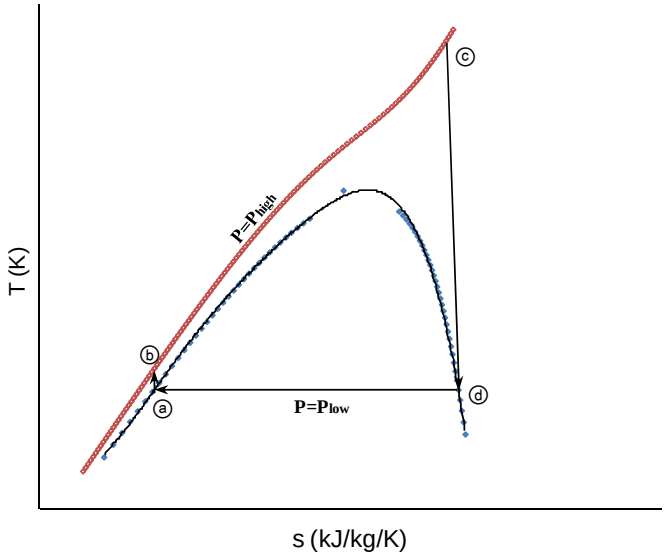

(b) A supercritical cycle

Figure 6.3 A triangular cycle and a supercritical Rankine cycle in T-s diagrams

6.2 The System and Target Function

The system under investigation is composed of a heat source, a power cycle and a heat sink (Figure 6.4). Therminol VP-1 (normally used as a heat transfer fluid in solar power plants) and cooling water are applied as the heat source and heat sink, respectively, for the sake of this simulation. The power cycles investigated are the practical approximations of the Carnot cycle, i.e., organic Rankine cycles with pure working fluids, the practical approximations of the Lorenz cycle, i.e., organic Rankine cycles with zeotropic mixture working fluids, and the practical approximation of the triangular cycle, i.e., supercritical Rankine cycles. A heat recuperator is used to recover the heat from the turbine exhaust when the turbine outlet temperature is more than 10K above the condensed fluid. The working fluids used for the power cycles are: R32, 0.5R32/0.5R134a, R134a, 0.5R134a/0.5R245fa, R245fa, and 0.5R32/0.5R245fa, among which 0.5R32/0.5R134a, 0.5R134a/0.5R245fa, and 0.5R32/0.5R245fa are zeotropic mixtures that can create temperature glides during the vaporization and condensation processes. The selection of these working fluids is meant to provide a wide range of fluid properties. R32 is a wet fluid with relatively low critical temperature (351.26K), R134a is an isentropic fluid with moderate critical temperature (374.21K), and R245fa can be considered as a dry fluid with relatively high critical temperature (427.20K). Detailed discussion on these working fluids is provided by Chen et al. [108].

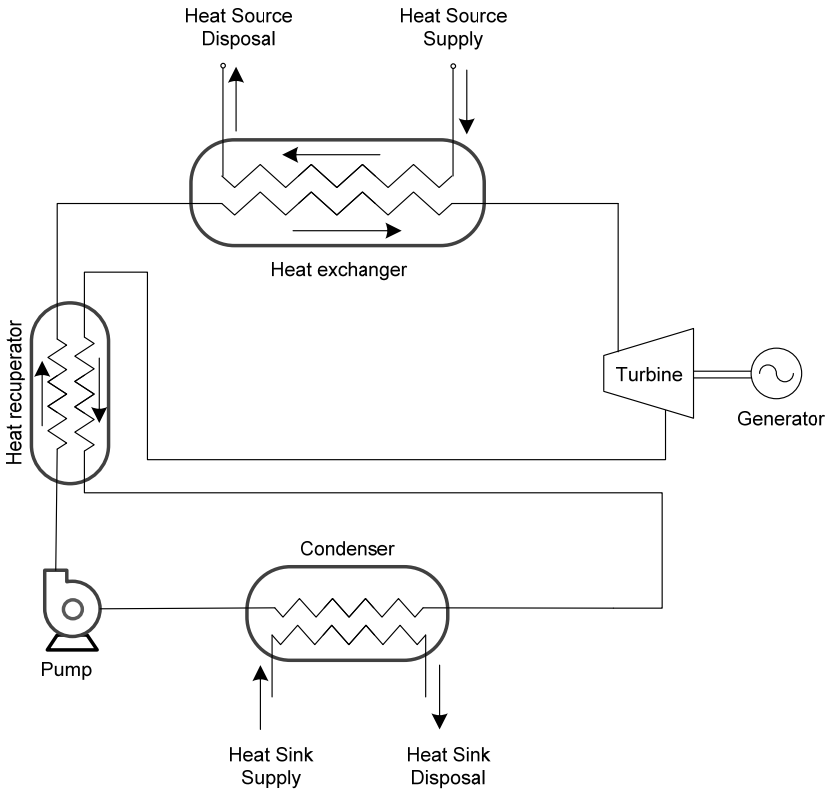

Figure 6.4 The system under investigation

A target function F is introduced to optimize the system. F is the exergy efficiency of the system, obtained from the exergy efficiencies of the heating process ($E_{h,ex}$), the power cycle ($E_{II,cov}$), and the condensation process ($E_{c,ex}$).

$$F = E_{h,ex}E_{\mathrm{II},cov}E_{c,ex} \tag{6.10}$$

6.3 System Analysis

6.3.1 Energetic and Exergetic Efficiencies of the Power Cycles

Thermal efficiency based on First Law of Thermodynamics is traditionally used to evaluate and compare different power cycles. In this analysis, isentropic efficiencies of the pump and the turbine are both set at 85%, and the condensation

temperature for the working fluids is set at 309K, which refers to an average condensation temperature for zeotropic mixtures. The efficiencies of the R32-based ORC and SRC, 0.5R32/0.5R134a-based ORC and SRC, R134a-based ORC and SRC, 0.5R134a/0.5R245fa-based ORC and SRC, R245fa-based ORC and SRC, and 0.5R32/0.5R245fa-based ORC and SRC are simulated under the turbine inlet temperatures of 365K-445K with the constraint that the vapor quality at the turbine exhaust is no less than 0.95 to avoid droplet erosion.

The thermal efficiencies of the power cycles with respect to the turbine inlet temperatures are shown in Figure 6.5. It is noticed that the thermal efficiency of the 0.5R134a/0.5R245fa-based supercritical Rankine cycle is significantly higher than the other cycles when the turbine inlet temperature is beyond 420K. At lower turbine inlet temperatures, 0.5R134a/0.5R245fa-based SRC and R134a-based ORC show the highest thermal efficiencies. When the same working fluids are used in different cycles, the SRCs obtain higher thermal efficiencies than the ORC at higher temperatures.

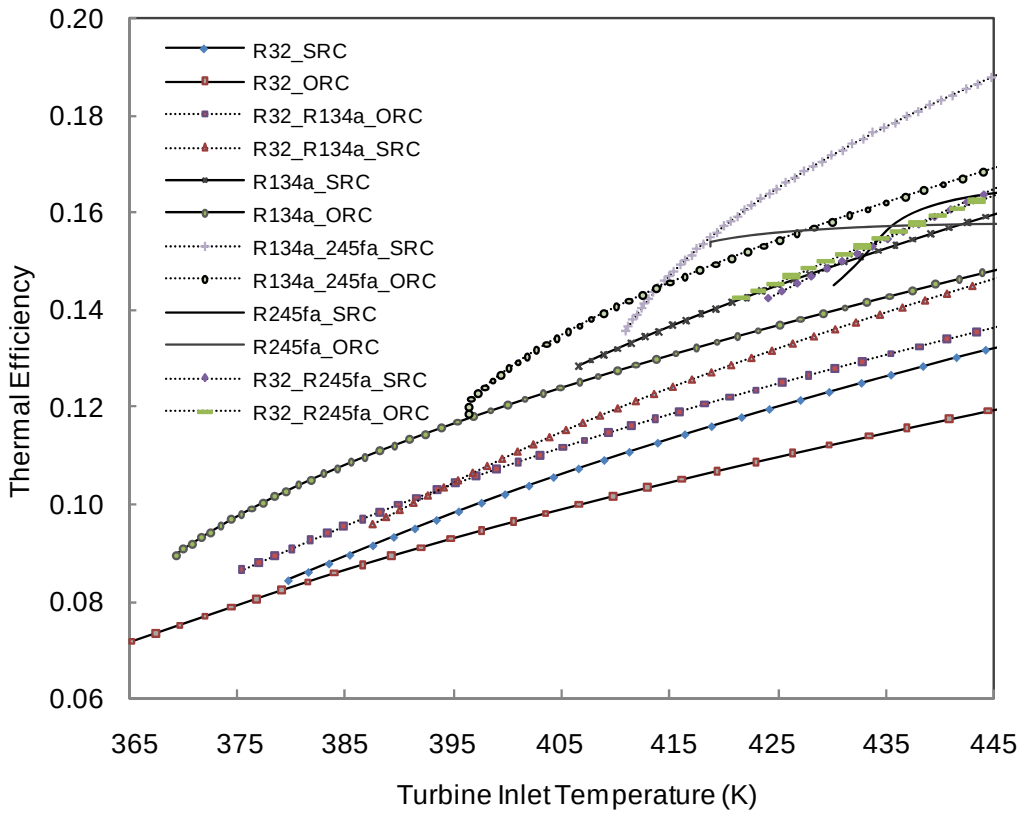

Figure 6.5 Thermal efficiencies of the cycles

For all these thermodynamic cycles, the net work is the exergy output, while the total exergy input is composed of the work input through the pump and the exergy brought in by the working fluids through extracting heat from the heat source. The exergy efficiency, $\eta_{\mathrm{II},cov}$ of a power cycle for energy conversion can be written as:

$$\eta_{\mathrm{II},cov} = \frac{W_{net}}{W_p + \Delta E_f} \tag{6.11}$$

where W_{net} is the net work output from the turbine, W_p is the power input to the pump, and ΔE_f is the exergy obtained by the working fluid through its heat exchange with the heat source, which can be expressed as:

$$\Delta E_f = m_f\left[\left(h_{f,in} - h_{f,out}\right) - T_0\left(s_{f,in} - s_{f,out}\right)\right] \quad (6.12)$$

where T_0 is the temperature of the ground state, set at 273K.

The exergy efficiencies of the power cycles are shown in Figure 6.6. Unlike the thermal efficiency curves, the exergy efficiencies do not necessarily increase with the turbine inlet temperature. Instead, the exergy efficiencies peak at certain temperature and then decline. The 0.5R134a/0.5R245fa-based SRC, 0.5R32/0.5R245fa-based ORC and SRC have the highest exergy efficiencies at temperatures above 410K. R32-based ORC has the lowest exergy efficiency.

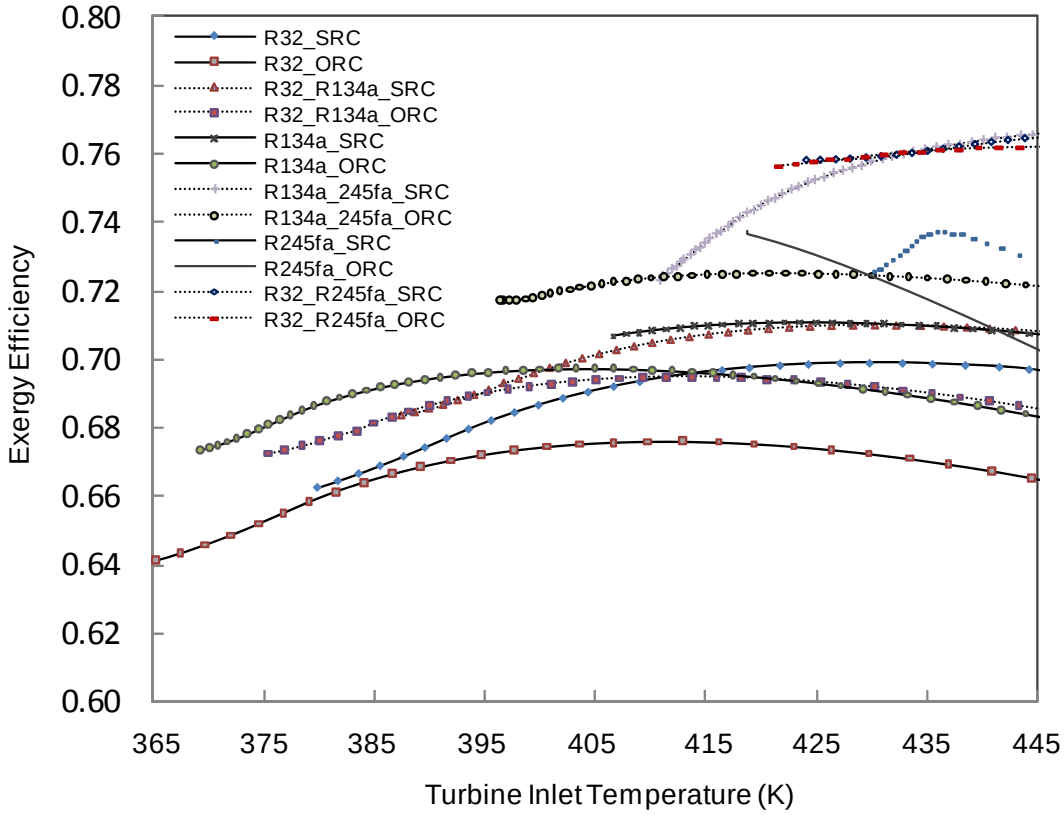

Figure 6.6 Exergy efficiency of the cycles

6.3.2 Exergy Efficiency of Heating and Condensation Processes

As heat is transferred from a high temperature fluid to a low temperature fluid irreversibly, exergy is destroyed. For a process transferring heat from a hot stream at T_h to a cold stream at T_c in steady flow, the exergy destruction is:

$$dE_d = -T_0(m_h ds_h + m_c ds_c) \tag{6.13}$$

Combining the above equation with $ds = \frac{\delta q}{T}$, and integrating one can get the exergy destruction of a heat transfer process to be:

$$E_d = T_0 \int_0^Q \left(\frac{T_h m_c - T_c m_h}{T_c T_h}\right) \delta q = T_0 \int_0^Q \left(\frac{m_c}{T_c} - \frac{m_h}{T_h}\right) \delta q \tag{6.14}$$

where q is the instantaneous heat transfer, and Q is the total heat transfer.

According to the above equation, in order to minimize the destruction, $\frac{m_c}{T_c}$ should approach $\frac{m_h}{T_h}$ as much as it can along the heat exchange process without violating the pinch limitation. Besides that, an important observation is that if T_c and T_h are significantly greater than T_0, the irreversibility per unit heat transfer at fixed $(T_h m_c - T_h m_c)$ is significantly lower. This implies that optimizing the thermal match is even more advantageous in the condensation process than in the heating process.

On the other hand, the exergy change of the hot stream during the heat exchange process is

$$\Delta E_h = m_h\left[\left(h_{h,in} - h_{h,out}\right) - T_0\left(s_{h,in} - s_{h,out}\right)\right] \tag{6.15}$$

Likewise, the exergy change of the cold stream during the heat exchange process is

$$\Delta E_c = m_c\left[\left(h_{c,out} - h_{c,in}\right) - T_0\left(s_{c,out} - s_{c,in}\right)\right] \quad (6.16)$$

With the above two equations, the exergy efficiency of the heat exchange processes can be expressed as:

$$\eta_{ex} = \frac{\Delta E_c}{\Delta E_h} = \frac{m_c\left[\left(h_{c,out} - h_{c,in}\right) - T_0\left(s_{c,out} - s_{c,in}\right)\right]}{m_h\left[\left(h_{h,in} - h_{h,out}\right) - T_0\left(s_{h,in} - s_{h,out}\right)\right]} \quad (6.17)$$

6.3.2.1 The Exergy Efficiency of the Heating Process

Figure (a), (b) and (c) show the heating processes of R245fa in ORC, 0.5R32/0.5R134a in ORC, and R32 in SRC from 300K to 400K. The exergy destructions due to the irreversible heat transfer processes can be calculated from Eq. (6.13). Alternatively, one can infer from the equation that the area between curves of the heat source and working fluids represents the exergy destruction. With the same pinch limitation, the heating process of the supercritical Rankine cycle has the least exergy destruction.

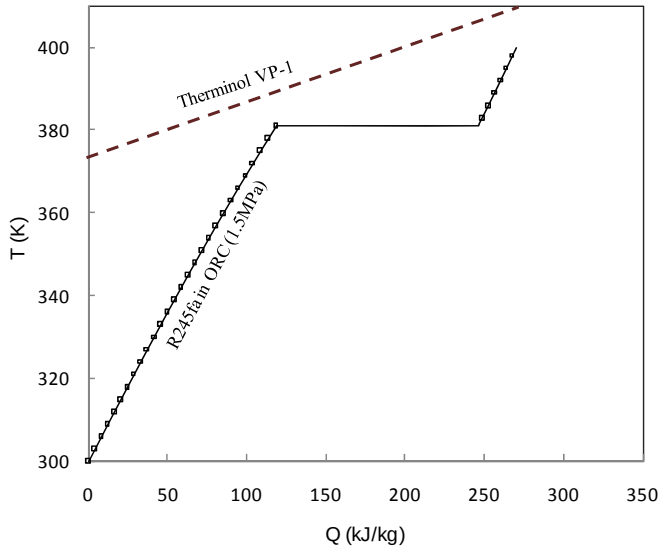

(a) Heating process of R245fa in ORC

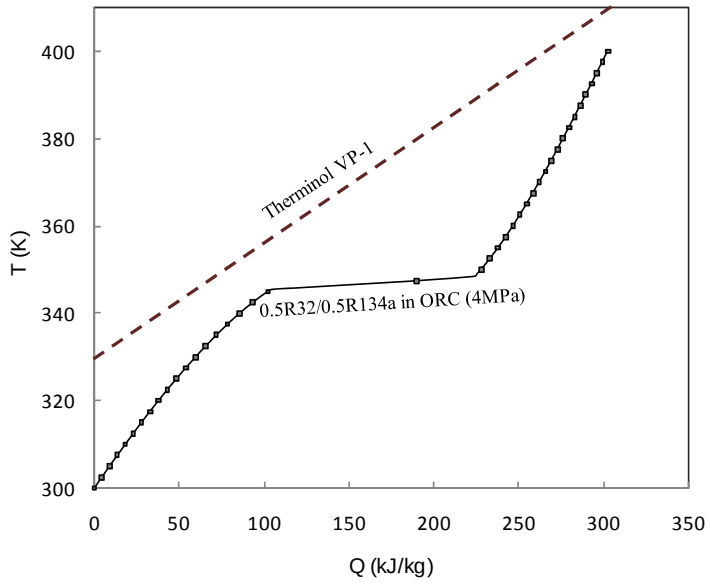

(b) Heating process of 0.5R32/0.5R134a in ORC

Figure 6.7 T-Δ$\dot{H}$ diagram demonstrating thermal matches of the heating processes

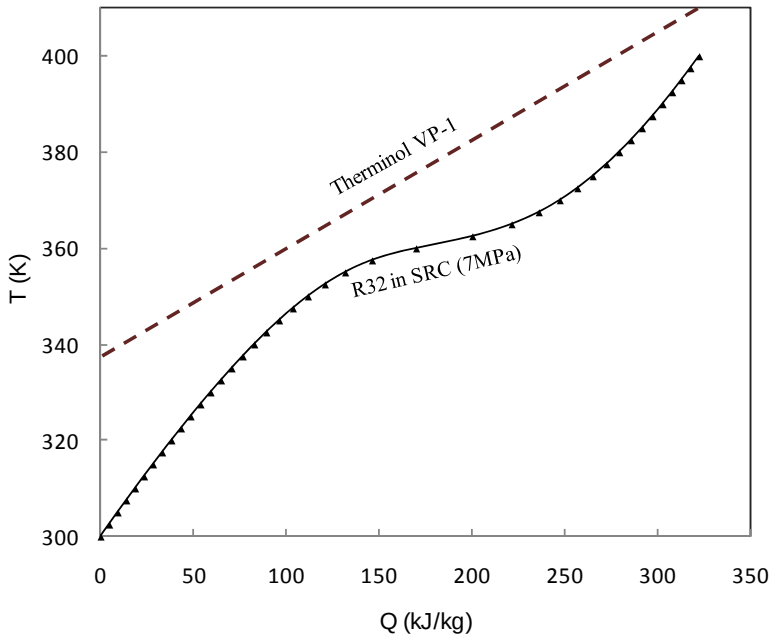

(c) Heat process of R32 in SRC

Figure 6.7 (Continued)

The exergy efficiencies of the working fluids' heating processes in ORCs and SRCs are shown in Figure . For the same working fluids, the exergy efficiencies of heating processes are higher in SRCs than ORCs, and the zeotropic mixture of 0.5R134a/0.5R245fa has the highest exergy efficiency in the heating process. It needs to be mentioned that the heating processes here refer to the primary heat exchange process between the heat source and the working fluid. Although recuperators are applied, they are internal heating as opposed to external heating.

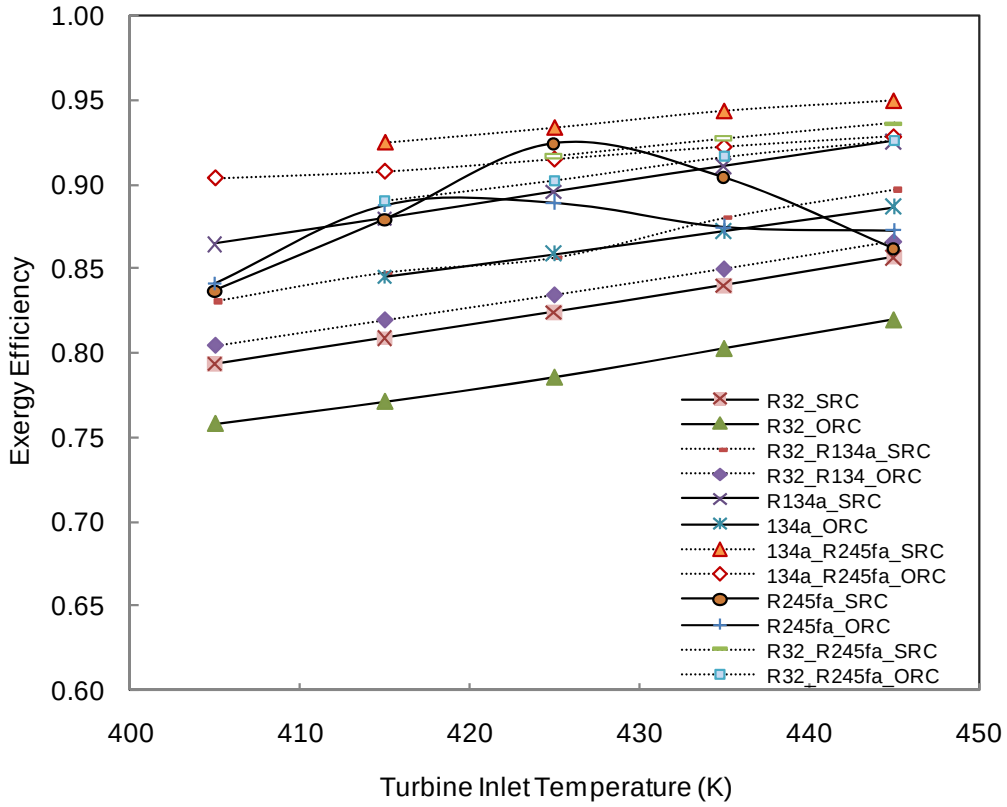

Figure 6.8 Exergy efficiencies of the heating processes

6.3.2.2 The Condensation Processes

For pure fluids, the condensation at constant pressure occurs isothermally. However, zeotropic mixtures condensate with temperature glides even at constant pressure. Because of these temperature glides, the condensation process can be designed such that the working fluids and the heat sinks obtain optimal thermal match, and therefore, minimal exergy destruction. The temperature glides created by 0.5R32/0.5R245fa, 0.5R134a/0.5R245fa, and 0.5R32/0.5R134a are shown in a T-s diagram in Figure 6.9, along with the pure fluid R134a. The zeotropic mixture of

0.5R32/0.5R245fa has the highest temperature glide, i.e., 29.5K. A larger temperature glide is not necessarily better, because it can be noticed that with a 29.5K temperature glide under a defined average condensation temperature (309K), the condensation of the zeotropic mixture of 0.5R32/0.5R245fa ends at 297.5K. A heat sink below 297.5K is required in order to condense it, which could be a challenge in practice.

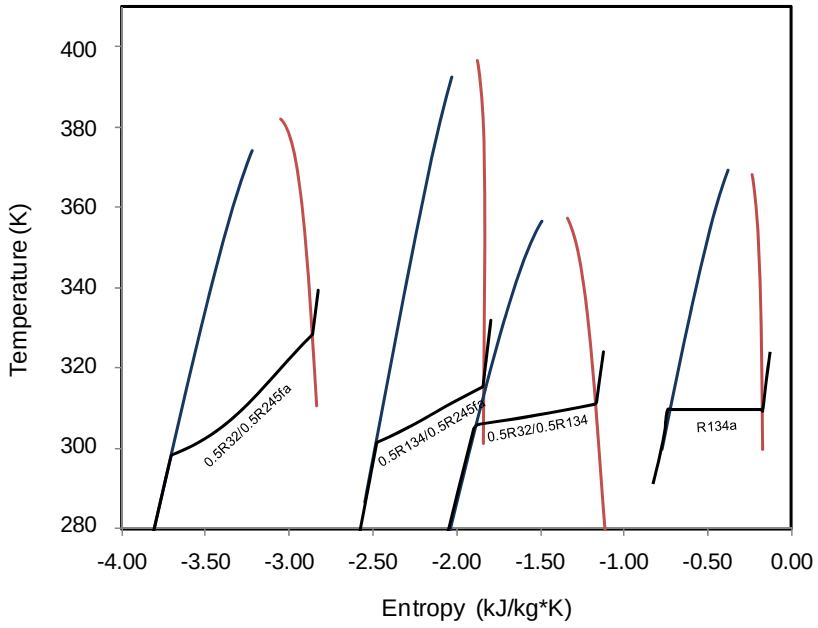

Figure 6.9 T-s diagram demonstrating the temperature glides of the condensation processes

Different from the heating processes, the condensation process has little to do with the type of the thermodynamic cycles or the turbine inlet temperature, because condensation of all of the working fluids is assumed to be at the same temperature (or average temperature for the zeotropic mixtures), and recuperators are applied if the turbine exhaust temperatures are high. For all of the condensation processes, the

thermal matches between the working fluid and the cooling water are optimized to get minimal exergy destruction. The exergy efficiencies of the condensation processes of the working fluids are shown in Figure 6.10 along with the mass flow rate of the cooling water and its temperature. It is seen that the zeotropic mixture of 0.5R32/0.5R134a has the highest condensation exergy efficiency, slightly higher that the zeotropic mixture of 0.5R134a/0.254fa. However, the zeotropic mixture of 0.5R134a/0.254fa needs a much smaller cooling water mass flow rate. What's interesting to note is that even with the largest thermal glide during the condensation, the zeotropic mixture of 0.5R32/0.254fa has the lowest exergy efficiency. This is caused by the non-linear condensation process of the fluid (see Figure 6.9). When the components have significantly different thermodynamic properties, their zeotropic mixtures would condense non-linearly, the zeotropic mixture of 0.5R32/0.254fa to be an example. In addition, the large temperature glide leads to the cooling water temperature to be as low as 288K.

Beside the exergy efficiency of the condensation process and the cooling water temperature, there are big differences in the demand of cooling water mass flow rates among the working fluids. For a unit mass flow of the working fluid, the 0.5R134a/0.5R245fa zeotropic mixture needs 3.43 kg/s cooling water for the condensation, which is less than 40% of the 9.21kg/s for R32, and 1/3 of the 11.8 kg/s for R134a and R245fa.

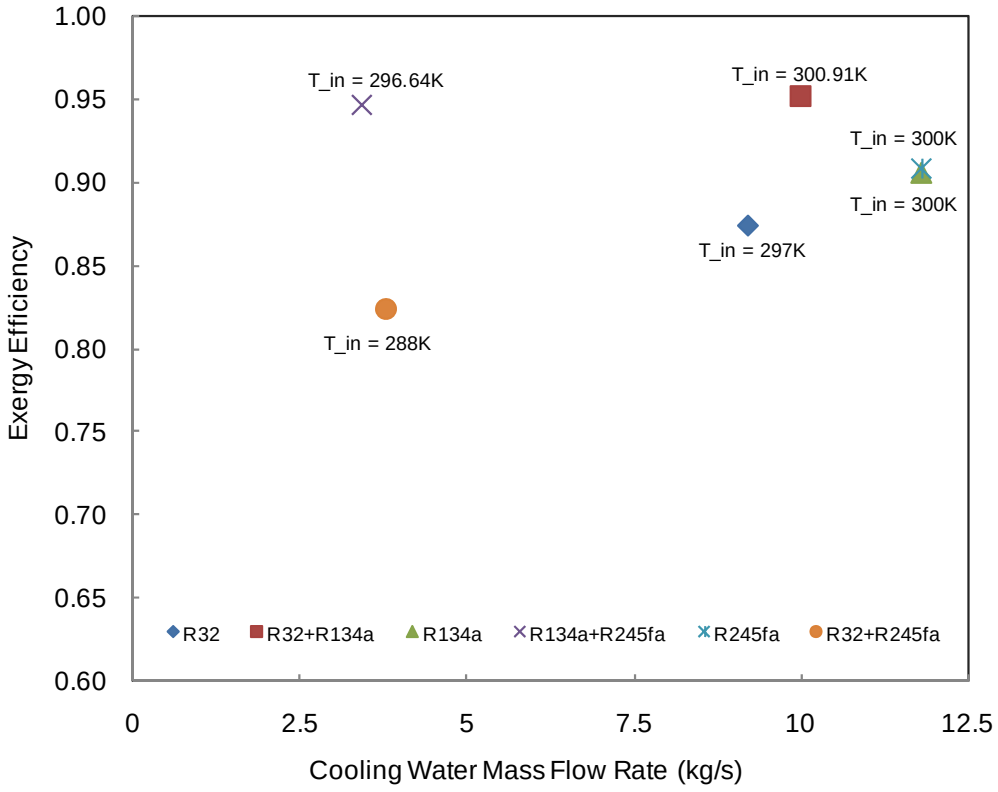

Figure 6.10 Exergy efficiency of the working fluids' condensation processes

6.4 Optimization of the System

Based on the analysis of the thermodynamic cycles, the heating and condensation processes, the exergy efficiency of the system, i.e., the target function of the optimization is calculated and shown in Figure 6.11. It is seen that the 0.5R134a/0.5R245fa-based SRC has the highest system exergy efficiency of 0.643-0.689. When compared with the R32-based ORC, which has exergy efficiency of 0.491-0.521, the efficiency of 0.5R134a/0.5R245fa is as much as 30% higher. This indicates that the choice of the working fluid and the thermodynamic cycle does make

a significant difference, and the system should be optimized to get the maximum exergy efficiency.

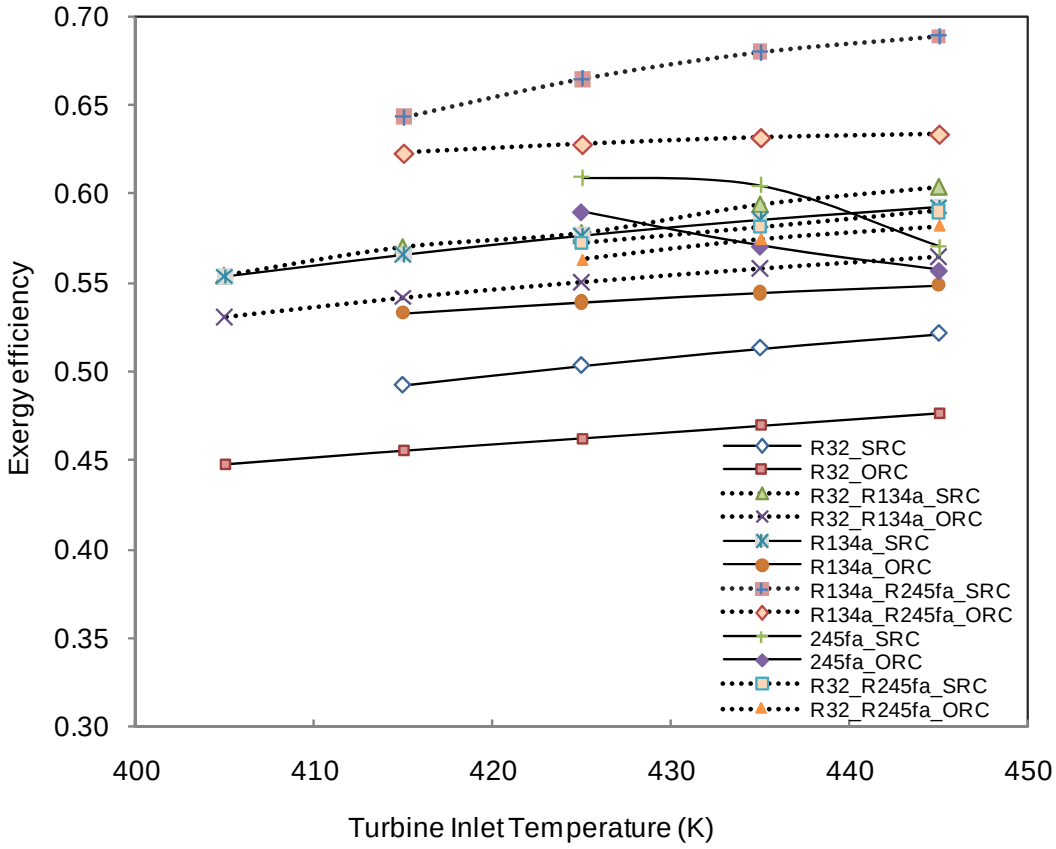

Figure 6.11 Exergy efficiency of the systems

6.5 Concluding Remarks

Choice of the working fluids for the ORCs and SRCs affects significantly the efficiency of the low-grade heat energy conversion system. Through energy and exergy analysis, optimization of the system is carried out for 6 working fluids in 12 thermodynamic cycles. The target function of the optimization is the system exergy efficiency, which is the combination of the exergy efficiency of the thermodynamic

cycle, the heating process and the condensation process. The optimal exergy efficiency of the system is dependent on the choice of the appropriate working fluid, the type of the thermodynamic cycle, and the working conditions. The maximum exergy efficiency is obtained for a supercritical Rankine cycle using 0.5R134a/0.5R245fa zeotropic mixture as the working fluid. The mixture shows advantages in the energy conversion, as well as its heat exchange with the heat source and the heat sink. The exergy efficiency of the 0.5R134a/0.5R245fa-based SRC system is 0.643-0.689 at the turbine inlet temperature of 415-445K, which is about 30% improvement as compared to 0.491-0.521 for the R32-based ORC. Furthermore, the 0.5R134a/0.5R245fa mixture saves more than 60% of the cooling water during the condensation process as compared to pure R32, R134a and R245fa.

CHAPTER 7 SUMMARY, CONCLUSIONS AND RECOMMENDATIONS

7.1 Summary

This work investigates the conversion of low-grade heat into work and electricity via supercritical Rankine cycles. The motivation for this research was to improve the efficiency of energy conversion.

The selection of working fluids for a supercritical Rankine cycle is of key importance. A rigorous investigation into the potential working fluids was carried out, and more than 30 substances were screened from all the available fluid candidates. Zeotropic mixtures are innovatively proposed to be used in supercritical Rankine cycles to improve the system efficiency.

Supercritical Rankine cycles and organic Rankine cycles with pure working fluids as well as zeotropic mixtures were studied to optimize the conversion of low-grade heat into power. The study shows that it is possible to extract and convert more energy using the supercritical cycle developed in this research than a conventional organic Rankine cycle. The working fluids can be optimized to match the heat source conditions to maximize conversion efficiency.

7.2 Conclusions

A review of the thermodynamic cycles for low-grade heat conversion is carried out in CHAPTER 2. The thermodynamic cycles includes: Kalina cycle, Goswami power and cooling cogeneration cycle, trilateral flash cycle, organic Rankine cycle, and supercritical Rankine cycle. The major obstacle with Kalina cycle is the corrosivity of ammonia. Impurities in liquid ammonia such as air or carbon dioxide can cause stress corrosion cracking of mild steel, in addition, ammonia is highly corrosive towards copper and zinc. The Goswami cycle is a novel thermodynamic cycle that outputs power and cooling simultaneously. The same obstacle applies to the Goswami cycle if ammonia-water is used as the working fluid, this cycle can use other binary working fluids, such as, CO_2-organic absorbents or, mixtures of hydrocarbons (refer to Appendix E). The trilateral flash cycle has been considered for over 30 years, but lack of a suitable two-phase expander with high adiabatic efficiency is the main obstacle for it to become reality. Among all of the thermodynamic cycles for low-grade conversion, the organic Rankine cycle is so far the most commercially developed due to its simplicity in configuration. However, the bad thermal match of the working fluid with the heat source during the heating process causes a large amount of irreversibility and exergy destruction. In a supercritical Rankine cycle, the heating process does not pass through a distinct two-phase region, resulting in a better thermal match in the boiler with less irreversibility.

The properties of the working fluids play a vital role in the cycle performance. The thermodynamic and physical properties, stability, environmental impacts, safety and compatibility, and availability and cost are among the considerations when selecting a working fluid. A detailed analysis on the selection criteria of working fluids for supercritical Rankine cycles and organic Rankine cycles is carried out in CHAPTER 3. Types of working fluids, influences of latent heat, density and specific heat, and the effectiveness of superheating are discussed in detail. Working fluids with high density and high latent heat provide high unit turbine work output. The study also shows that isentropic and dry fluids are preferred in organic Rankine cycles, and superheating is necessary for wet fluids in organic Rankine cycle. However, for dry fluids, superheat could play a negative role in the cycle efficiency. Fluids with low critical temperatures and pressures are the potential candidates for a supercritical Rankine cycle. Among all the fluids suggested, 35 fluids were screened out, and plotted in the newly introduced T- ξ charts. The fluids were discussed through grouping based on their distributions in the T- ξ chart.

Supercritical Rankine cycles using refrigerant R32 (CH_2F_2) and carbon dioxide (CO_2) as the working fluids were analyzed and compared for the conversion of low-grade heat into mechanical power in CHAPTER 4. Although CO_2 has merits as being abundant, non-flammable, non-toxic and inexpensive, its thermodynamic performance and operating pressures are inferior to R32. Compared to CO_2, R32 has

higher thermal conductivity and condenses easily. An energetic and exergetic analysis of the two fluids shows that for a turbine inlet temperature of 393K to 453K, a R32-based supercritical Rankine cycle can achieve thermal efficiencies of 12.6% to 17.3%, which is a 12.6-18.6% improvement over the 10.6% to 15.3% efficiency for a CO_2-based supercritical Rankine cycle. In addition, R32 works at much lower pressures, has higher exergy density, and less mass flow is needed for R32 than CO_2 for the same amount of work output. For a cycle high temperature of 433K, the exergy efficiency of the CO_2- and R32 based supercritical Rankine cycles ranges from 0.15-0.51 and 0.56-0.61, respectively, over a wide range of the cycle high pressure.

Based on the analyses of the CO_2- and R32 based supercritical Rankine cycles, an "ideal" working fluid for the supercritical Rankine cycle is conceived. The "ideal" working fluid is able to condense non-isothermally and vaporize linearly. The "ideal" working fluid not only has an optimal thermal match with the heat source, but also minimizes the irreversibility of the condensation.

Although an "ideal" working fluid may never be found, there are ways to approach it. Using proper zeotropic mixtures as the working fluids of supercritical Rankine cycles is one way to approximate the "ideal" working fluid. A supercritical Rankine cycle using a zeotropic mixture of 0.7R134a/0.3R32 for the conversion of low-grade heat into power is analyzed in CHAPTER 5. A comparative study between an organic Rankine cycle using pure R134a as the working fluid and supercritical

Rankine cycle using a zeotropic mixture of 0.7R134a/0.3R32 shows that the 0.7R134a/0.3R32 zeotropic mixture-based supercritical Rankine cycle can achieve thermal efficiencies of 10.8-13.4% with the cycle high temperature of 393K-473K as compared to 9.7-10.1% for the organic Rankine cycle, which is an improvement of 10-30%. When including the heating and condensation processes in the system, the system exergy efficiency is 38.6% for the proposed supercritical Rankine cycle as compared to 24.1% for the organic Rankine cycle.

The investigation of the 0.7R134a/0.3R32 zeotropic mixture-based supercritical Rankine cycle in CHAPTER 5 shows the advantages of zeotropic mixture working fluids in a supercritical Rankine cycle. But the zeotropic mixture of 0.7R134a/0.3R32 is not necessarily the optimal working fluid to use for the energy conversion of any heat source. Optimization of energy conversion is of great significance in the utilization of low-grade heat. CHAPTER 6 presents an analysis of 6 working fluids in 12 thermodynamic cycles to study the optimization of the energy conversion systems. The optimal exergy efficiency of the system is dependent on the choice of the working fluid, the type of thermodynamic cycle, and the working conditions. The zeotropic mixture of R134a and R245fa shows advantages in the energy conversion process, as well as its heat exchange with the heat source and heat sink. The exergy efficiency of a 0.5R134a/0.5R245fa-based supercritical Rankine cycle system is 0.643-0.689 at the turbine inlet temperature of 415-445K, which

shows about 30% improvement over the exergy efficiency of the R32-based organic Rankine cycle system working under the same temperature limits. Furthermore, the 0.5R134a/0.5R245fa mixture saves more than 60% of the cooling water during the condensation process than the pure working fluids.

7.3 Recommendations for Future Research

The results of this research demonstrate great potential for the application of the proposed supercritical Rankine cycle for low-grade heat conversion. This section offers recommendations to optimize the proposed supercritical Rankine cycle systems.

CHAPTER 3 conducts an overview of the potential working fluids for supercritical Rankine cycles and organic Rankine cycles, and screened 35 candidates from all the available working fluids. Although it is extensive, the future study should not be limited to these working fluids. Some of the fluids will be phased out in the future due to environmental concerns, and more organic and inorganic fluids could be explored for supercritical Rankine cycles and organic Rankine cycles.

The study conducted in CHAPTER 4 does not show directly the effect of factors, such as, the pressure of operation, the size of the unit, and the conductivity of the working fluids, on the efficiency of the cycle. However, these are very important factors in practice. A systematic analysis on these factors would be meaningful.

The optimization conducted in CHAPTER 6 is still preliminary. The optimization of the working fluids for different heat source conditions is a complex subject worthy of further research. The target function used in this work is the exergy efficiency of the energy conversion system. An "auxiliary function" could be added in the target function to reflect the influences of the operating pressure, the thermal conductivity, the exergy density, the environmental impact, and even the cost of the working fluid.

REFERENCES

[1] P. J. Mago, L. M. Chamra, K. Srinivasan, and C. Somayaji, "An examination of regenerative organic Rankine cycles using dry fluids," *Applied Thermal Engineering*, vol. 28, no. 8, pp. 998-1007, 2008.

[2] J. Larjola, "Electricity from industrial waste heat using high-speed organic Rankine cycle (ORC)," *International Journal of Production Economics*, vol. 41, no. 1, pp. 227-235, 1995.

[3] T. C. Hung, T. Y. Shai, and S. K. Wang, "A review of organic rankine cycles (ORCs) for the recovery of low-grade waste heat," *Energy*, vol. 22, no. 7, pp. 661-667, 1997.

[4] B. Liu, K. Chien, and C. Wang, "Effect of working fluids on organic Rankine cycle for waste heat recovery," *Energy*, vol. 29, no. 8, pp. 1207-1217, 2004.

[5] D. Y. Goswami, F. Kreith, and J. F. Kreider, *Principles of solar engineering*. Philadelphis, PA 19106: Taylor & Francis, 2000.

[6] National Energy Information Center, *International Energy Outlook 2010*. Washington,DC 20585: U.S. Energy Information Adminstration, 2010, pp. 1-338.

[7] H. Lu and A. H. Swift, "El Paso Solar Pond," *J. Sol. Energy Eng.*, vol. 123, no. 3, p. 1, 2001.

[8] C. Nielson, A. Akbarzedeh, J. Andrews, Humberto R Becerra L, and P. Golding, "The History of Solar Pond Science & Technology," in *Proceedings of the International Solar Energy Society*, 2005.

[9] "RMIT - Fresh water and salt on the table." [Online]. Available: http://www.rmit.biz/browse%3BID=a6mw5qwzkhwk. [Accessed: 19-Aug-2010].

[10] "Solar Thermal Generated Electricity - Future Dominating Technology? « The Green Technology Blog." [Online]. Available: http://www.thegreentechnologyblog.com/2009/solar-thermal-generated-electricity-future-dominating-technology/. [Accessed: 19-Aug-2010].

[11] H. N. Pollack, S. J. Hurter, and J. R. Johnson, “Heat flow from the Earth's interior: Analysis of the global data set,” *REVIEWS OF GEOPHYSICS*, vol. 31, no. 3, pp. 237-280, 1993.

[12] “Geothermal energy: An overview on resources and potential.” [Online].Available: http://pangea.stanford.edu/ERE/pdf/IGAstandard/ISS/2009Slovakia/I.1.Bertani.pdf

[13] “Geothermal Energy: International Market Update.” [Online].Available: http://www.geo-energy.org/pdf/reports/GEA_International_Market_Report_Final_May_2010.pdf

[14] “Geothermal Technologies Program: The Future of Geothermal Energy.” [Online].Available: http://www1.eere.energy.gov/geothermal/future_geothermal.html. [Accessed: 21-Aug-2010].

[15] K. Ferland and R. Papar, “Industrial Waste Heat Recovery.”[Online]. Available: http://texasiof.ces.utexas.edu/PDF/Presentations/RoundTable_0906.pdf.

[16] L. Shaoguang and D. Y. Goswami, “Optimization of a Novel Combined Power/Refrigeration Thermodynamic Cycle,” *Journal of Solar Energy Engineering*, vol. 125, no. 2, pp. 212-217, 2003.

[17] E. Rogdakis and K. Antonopoulos, “A high efficiency NH3/H2O absorption power cycle,” *Heat Recovery Systems and CHP*, vol. 11, no. 4, pp. 263-275, 1991.

[18] M. B. Ibrahim and R. M. Kovach, “A Kalina cycle application for power generation,” *Energy*, vol. 18, no. 9, pp. 961-969, Sep. 1993.

[19] P. Lolos and E. Rogdakis, “A Kalina power cycle driven by renewable energy sources,” *Energy*, vol. 34, no. 4, pp. 457-464, Apr. 2009.

[20] C. Dejfors, E. Thorin, and G. Svedberg, “Ammonia-water power cycles for direct-fired cogeneration applications,” *Energy Conversion and Management*, vol. 39, no. 16, pp. 1675-1681, 1998.

[21] P. K. Nag and A. V. S. S. K. S. Gupta, “Exergy analysis of the Kalina cycle,” *Applied Thermal Engineering*, vol. 18, no. 6, pp. 427-439, Jun. 1998.

[22] U. Desideri and G. Bidini, “Study of possible optimisation criteria for geothermal power plants,” *Energy Conversion and Management*, vol. 38, no. 15, pp. 1681-1691, 1997.

[23] H. Leibowitz and M. Mirolli, “First Kalina combined-cycle,” *Power Engineering*. [Online]. Available: http://pepei.pennnet.com/articles/article_display.cfm?article_id=44226. [Accessed: 10-Nov-2009].

[24] “Kalina cycle - Wikipedia, the free encyclopedia.” [Online]. Available: http://en.wikipedia.org/wiki/Kalina_cycle. [Accessed: 24-Aug-2010].

[25] “Wasabi Energy grants Kalina Cycle license for China | Think GeoEnergy News.” [Online]. Available: http://thinkgeoenergy.com/archives/1022. [Accessed: 10-Sep-2010].

[26] “Kalina Cycle Geothermal Power Plant Constructed by Mannvit Engineering.” [Online]. Available: http://www.azocleantech.com/details.asp?newsID=7969. [Accessed: 24-Aug-2010].

[27] “Geothermal Power Heats Up in Germany - BusinessWeek.” [Online]. Available: http://www.businessweek.com/globalbiz/content/jun2008/gb2008063_168366.htm. [Accessed: 24-Aug-2010].

[28] S. Vijayaraghavan and D. Y. Goswami, “A combined power and cooling cycle modified to improve resource utilization efficiency using a distillation stage,” *Energy*, vol. 31, no. 8, pp. 1177-1196, 2006.

[29] A. Vidal, R. Best, R. Rivero, and J. Cervantes, “Analysis of a combined power and refrigeration cycle by the exergy method,” *Energy*, vol. 31, no. 15, pp. 3401-3414, 2006.

[30] J. Wang, Y. Dai, and L. Gao, “Parametric analysis and optimization for a combined power and refrigeration cycle,” *Applied Energy*, vol. 85, no. 11, pp. 1071-1085, 2008.

[31] S. M. Sadrameli and D. Y. Goswami, “Optimum operating conditions for a combined power and cooling thermodynamic cycle,” *Applied Energy*, vol. 84, no. 3, pp. 254-265, 2007.

[32] V. Sanjay and D. Y. Goswami, “On Evaluating Efficiency of a Combined Power and Cooling Cycle,” *Journal of Energy Resources Technology*, vol. 125, no. 3, pp. 221-227, 2003.

[33] D. Y. G. Shaoguang Lu, "Theoretical analysis of ammonia-based conbined power/refrigeration cycle at low refrigeration temperatures," *Proceedings of solar 2002*, 2002.

[34] T. Gunnar and D. Y. Goswami, "Novel Combined Power and Cooling Thermodynamic Cycle for Low Temperature Heat Sources, Part II: Experimental Investigation," *Journal of Solar Energy Engineering*, vol. 125, no. 2, pp. 223-229, 2003.

[35] RF Stiedel, KA Brown, and DH Pankow, "The empirical modeling of a Lysholm screw expander," in *Proc., Intersoc. Energy Convers. Eng. Conf.; (United States)*, 1983.

[36] N. Stosic and A. Kovacevic, "Power Recovery from Low Cost Two-Phase Expanders," in *Expanders GRC Annual Meeting*, 2001.

[37] C. Zamfirescu and I. Dincer, "Thermodynamic analysis of a novel ammonia-water trilateral Rankine cycle," *Thermochimica Acta*, vol. 477, no. 1, pp. 7-15, Oct. 2008.

[38] "Screw Expanders Increase Output and Decrease the Cost of Geothermal Binary Power Plant Systems."

[39] T. Yamamoto, T. Furuhata, N. Arai, and K. Mori, "Design and testing of the Organic Rankine Cycle," *Energy*, vol. 26, no. 3, pp. 239-251, 2001.

[40] H. D. Madhawa Hettiarachchi, M. Golubovic, W. M. Worek, and Y. Ikegami, "Optimum design criteria for an Organic Rankine cycle using low-temperature geothermal heat sources," *Energy*, vol. 32, no. 9, pp. 1698-1706, 2007.

[41] S. Quoilin, "Experimental Study and modeling of a low temperature rankine cycle for samll scale cogeneration," Thesis, University of Liege, 2007.

[42] D. Wei, X. Lu, Z. Lu, and J. Gu, "Dynamic modeling and simulation of an Organic Rankine Cycle (ORC) system for waste heat recovery," *Applied Thermal Engineering*, vol. 28, no. 10, pp. 1216-1224, 2008.

[43] D. Wei, X. Lu, Z. Lu, and J. Gu, "Performance analysis and optimization of organic Rankine cycle (ORC) for waste heat recovery," *Energy Conversion and Management*, vol. 48, no. 4, pp. 1113-1119, 2007.

[44] I. Obernberger, P. Thonofer, and E. Reisenhofer, "Description and evaluation of the new 1,000kWel Organic Rankine cycle process integrated in the biomass CHP plant in Lienz, Austria," *Euorheat & Power*, vol. 10, pp. 1-17, 2002.

[45] V. M. Nguyen, P. S. Doherty, and S. B. Riffat, “Development of a prototype low-temperature Rankine cycle electricity generation system,” *Applied Thermal Engineering*, vol. 21, no. 2, pp. 169-181, 2001.

[46] U. Drescher and D. Bruggemann, “Fluid selection for the Organic Rankine Cycle (ORC) in biomass power and heat plants,” *Applied Thermal Engineering*, vol. 27, no. 1, pp. 223-228, 2007.

[47] V. Maizza and A. Maizza, “Working fluids in non-steady flows for waste energy recovery systems,” *Applied Thermal Engineering*, vol. 16, no. 7, pp. 579-590, 1996.

[48] K. Gawlik and V. Hassani, “Advanced binary cycles: optimum working fluids,” in *Energy Conversion Engineering Conference, 1997. IECEC-97., Proceedings of the 32nd Intersociety*, vol. 3, pp. 1809-1814 vol.3, 1997.

[49] V. Maizza and A. Maizza, “Unconventional working fluids in organic Rankine-cycles for waste energy recovery systems,” *Applied Thermal Engineering*, vol. 21, no. 3, pp. 381-390, 2001.

[50] G. Angelino and P. Colonna di Paliano, “Multicomponent Working Fluids For Organic Rankine Cycles (ORCs),” *Energy*, vol. 23, no. 6, pp. 449-463, 1998.

[51] C. J. Bliem and G. Mines, “Supercritical binary geothermal cycle experiments with mixed-hydrocarbon working fluids and a near-horizontal in-tube condenser,” *Report*, 1989.

[52] X. Wang and L. Zhao, “Analysis of zeotropic mixtures used in low-temperature solar Rankine cycles for power generation,” *Solar Energy*, vol. 83, no. 5, pp. 605-613, May. 2009.

[53] A. Borsukiewicz-Gozdur and W. Nowak, “Comparative analysis of natural and synthetic refrigerants in application to low temperature Clausius-Rankine cycle,” *Energy*, vol. 32, no. 4, pp. 344-352, Apr. 2007.

[54] R. Radermacher, “Thermodynamic and heat transfer implications of working fluid mixtures in Rankine cycles,” *International Journal of Heat and Fluid Flow*, vol. 10, no. 2, pp. 90-102, Jun. 1989.

[55] W. B. Stine and R. W. Harrigan, *Solar Energy Fundamentals and Design*. Wiley, 1985.

[56] W. C. Andersen and T. J. Bruno, “Rapid screening of fluids for chemical stability in organic rankine cycle applications,” *Ind. Eng. Chem. Res*, vol. 44, no. 15, pp. 5560-5566, 2005.

[57] R. Chacartegui, D. Sánchez, J. Muñoz, and T. Sánchez, "Alternative ORC bottoming cycles for combined cycle power plants," *Applied Energy*, vol. 86, no. 10, pp. 2162-2170, Oct. 2009.

[58] P. J. Mago and L. M. Chamra, "Exergy analysis of a combined engine-organic Rankine cycle configuration," *Proceedings of the Institution of Mechanical Engineers, Part A: Journal of Power and Energy*, vol. 222, no. 8, pp. 761-770, Dec. 2008.

[59] B. Sahin, "A study on performance of solid oxide fuel cell-organic Rankine cycle combined system," *International Journal of Energy Research*, vol. 33, no. 6, pp. 553-564, 2009.

[60] S. Karellas and A. Schuster, "Supercritical Fluid Parameters in Organic Rankine Cycle Applications," *Int. J. of Thermodynamics*, vol. 11, no. 3, pp. 101-108, 2008.

[61] A. McMahan, S. A. Klein, and D. T. Reindl, "A Finite-Time Thermodynamic Framework for Optimizing Solar-Thermal Power Plants," *Journal of Solar Energy Engineering*, vol. 129, no. 4, pp. 355-362, Nov. 2007.

[62] A. B. Etemoglu, "Thermodynamic Evaluation of Geothermal Power Generation Systems in Turkey," *Energy Sources, Part A: Recovery, Utilization, and Environmental Effects*, vol. 30, no. 10, p. 905, 2008.

[63] A. Schuster, J. Karl, and S. Karellas, "Simulation of an Innovative Stand-Alone Solar Desalination System Using an Organic Rankine Cycle," *International Journal of Thermodynamics*, vol. 10, no. 4, p. 155, 2007.

[64] A. M. Delgado-Torres and L. García-Rodríguez, "Double cascade organic Rankine cycle for solar-driven reverse osmosis desalination," *Desalination*, vol. 216, no. 1, pp. 306-313, Oct. 2007.

[65] J. C. Bruno, J. López-Villada, E. Letelier, S. Romera, and A. Coronas, "Modelling and optimisation of solar organic rankine cycle engines for reverse osmosis desalination," *Applied Thermal Engineering*, vol. 28, no. 17, pp. 2212-2226, Dec. 2008.

[66] D. Manolakos, G. Kosmadakis, S. Kyritsis, and G. Papadakis, "On site experimental evaluation of a low-temperature solar organic Rankine cycle system for RO desalination," *Solar Energy*, vol. 83, no. 5, pp. 646-656, May. 2009.

[67] J. Wang, Y. Dai, and L. Gao, "Exergy analyses and parametric optimizations for different cogeneration power plants in cement industry," *Applied Energy*, vol. 86, no. 6, pp. 941-948, Jun. 2009.

[68] R. Moro, P. Pinamonti, and M. Reini, "ORC technology for waste-wood to energy conversion in the furniture manufacturing industry," *Thermal Science*, vol. 12, no. 4, pp. 61-73, 2008.

[69] D. Chinese, A. Meneghetti, and G. Nardin, "Diffused introduction of Organic Rankine Cycle for biomass-based power generation in an industrial district: a systems analysis," *International Journal of Energy Research*, vol. 28, no. 11, pp. 1003-1021, 2004.

[70] A. Rentizelas, S. Karellas, E. Kakaras, and I. Tatsiopoulos, "Comparative techno-economic analysis of ORC and gasification for bioenergy applications," *Energy Conversion and Management*, vol. 50, no. 3, pp. 674-681, Mar. 2009.

[71] A. Schuster, S. Karellas, E. Kakaras, and H. Spliethoff, "Energetic and economic investigation of Organic Rankine Cycle applications," *Applied Thermal Engineering*, vol. 29, no. 8, pp. 1809-1817, Jun. 2009.

[72] D. Manolakos, E. S. Mohamed, I. Karagiannis, and G. Papadakis, "Technical and economic comparison between PV-RO system and RO-Solar Rankine system. Case study: Thirasia island," *Desalination*, vol. 221, no. 1, pp. 37-46, Mar. 2008.

[73] G. Kosmadakis, D. Manolakos, S. Kyritsis, and G. Papadakis, "Economic assessment of a two-stage solar organic Rankine cycle for reverse osmosis desalination," *Renewable Energy*, vol. 34, no. 6, pp. 1579-1586, 2009.

[74] J. A. Mathias, J. Johnston, J. Cao, D. K. Priedeman, and R. N. Christensen, "Experimental Testing of Gerotor and Scroll Expanders Used in, and Energetic and Exergetic Modeling of, an Organic Rankine Cycle," *Journal of Energy Resources Technology*, vol. 131, no. 1, pp. 012201-9, Mar. 2009.

[75] "Raising Arizona's renewable power: Back Issues, altenerG.com - enerG Alternative Sources Magazine - enerG, Archives." [Online]. Available: http://www.altenerg.com/back_issues/index.php?content_id=51. [Accessed: 24-Aug-2010].

[76] Y. Chen, P. Lundqvist, A. Johansson, and P. Platell, "A comparative study of the carbon dioxide transcritical power cycle compared with an organic rankine cycle with R123 as working fluid in waste heat recovery," *Applied Thermal Engineering*, vol. 26, no. 17, pp. 2142-2147, 2006.

[77] Y. Chen, “Novel cycles using carbon dioxide as working fluid: new ways to utilize energy from low-grade heat sources,” Thesis, KTH, 2006.

[78] Y. Chen, P. Lundqvist, and P. Platell, “Theoretical research of carbon dioxide power cycle application in automobile industry to reduce vehicle's fuel consumption,” *Applied Thermal Engineering*, vol. 25, no. 14, pp. 2041-2053, 2005.

[79] B. Saleh, G. Koglbauer, M. Wendland, and J. Fischer, “Working fluids for low-temperature organic Rankine cycles,” *Energy*, vol. 32, no. 7, pp. 1210-1221, 2007.

[80] X. Zhang, H. Yamaguchi, and D. Uneno, “Experimental study on the performance of solar Rankine system using supercritical CO2,” *Renewable Energy*, vol. 32, no. 15, pp. 2617-2628, 2007.

[81] X. Zhang, H. Yamaguchi, K. Fujima, M. Enomoto, and N. Sawada, “Study of solar energy powered transcritical cycle using supercritical carbon dioxide,” *International Journal of Energy Research*, vol. 30, no. 14, pp. 1117-1129, 2006.

[82] X. Zhang, H. Yamaguchi, and D. Uneno, “Thermodynamic analysis of the CO2-based Rankine cycle powered by solar energy,” *International Journal of Energy Research*, vol. 31, no. 14, pp. 1414-1424, 2007.

[83] H. Yamaguchi, X. R. Zhang, K. Fujima, M. Enomoto, and N. Sawada, “Solar energy powered Rankine cycle using supercritical CO2,” *Applied Thermal Engineering*, vol. 26, no. 17, pp. 2345-2354, 2006.

[84] X. R. Zhang, H. Yamaguchi, D. Uneno, K. Fujima, M. Enomoto, and N. Sawada, “Analysis of a novel solar energy-powered Rankine cycle for combined power and heat generation using supercritical carbon dioxide,” *Renewable Energy*, vol. 31, no. 12, pp. 1839-1854, 2006.

[85] X. R. Zhang, H. Yamaguchi, K. Fujima, M. Enomoto, and N. Sawada, “Experimental Performance Analysis of Supercritical CO[sub 2] Thermodynamic Cycle Powered by Solar Energy,” *AIP Conference Proceedings*, vol. 832, no. 1, pp. 419-424, 2006.

[86] X. R. Zhang, H. Yamaguchi, K. Fujima, M. Enomoto, and N. Sawada, “Theoretical analysis of a thermodynamic cycle for power and heat production using supercritical carbon dioxide,” *Energy*, vol. 32, no. 4, pp. 591-599, 2007.

[87] Xin-rong Zhang, H. Yamaguchi, and K. Fujima, “A feasibility study of CO2-based rankine cycle powered by solar energy,” *JSME Int J Ser B (Jpn Soc Mech Eng)*, pp. 8-540, 2005.

[88] H. B. Matthews and M. Boylston, “Geothermal energy conversion system,” U.S. Patent 41421081977.

[89] B. Poling, J. Prausnitz, and J. O. Connell, *The Properties of Gases and Liquids*, 5th ed. McGraw-Hill Professional, 2000.

[90] D. Y. Goswami, S. Hingorani, and G. Mines, “A Laser-Based Technique for Particle Sizing to Study Two-Phase Expansion in Turbines,” *Journal of Solar Energy Engineering*, vol. 113, no. 3, pp. 211-218, 1991.

[91] O. J. Demuth, *Analyses of mixed hydrocarbon binary thermodynamic cycles for moderate temperature geothermal resources*. Idaho: , 1981, pp. Medium: X; Size: Pages: 1316-1321.

[92] O. J. Demuth, *Preliminary assessment of condensation behavior for hydrocarbon-vapor expansions which cross the saturation line near the critical point*. Idaho: , 1983, p. Medium: ED; Size: Pages: 6.

[93] E. Logan, *Handbook of Turbomachinery*, 1st ed. CRC, 1994.

[94] E. Logan, *Turbomachinery*. CRC Press, 1993.

[95] L. Calderazzi and P. C. di Paliano, “Thermal stability of R-134a, R-141b, R-13I1, R-7146, R-125 associated with stainless steel as a containing material,” *International Journal of Refrigeration*, vol. 20, no. 6, pp. 381-389, 1997.

[96] A. W. Crook and I. O. E. Engineers, *Profiting from low-grade heat*. IET, 1994.

[97] G. Tsiklauri, R. Talbert, B. Schmitt, G. Filippov, R. Bogoyavlensky, and E. Grishanin, “Supercritical steam cycle for nuclear power plant,” *Nuclear Engineering and Design*, vol. 235, no. 15, pp. 1651-1664, Jul. 2005.

[98] T. L. Ochs and W. K. O'Connor, “Energy recovery during expansion of compressed gas suing power plant low-quality heat sources,” U.S. Patent US 7007474B1.

[99] R. Span and W. Wagner, “A New Equation of State for Carbon Dioxide Covering the Fluid Region from the Triple-Point Temperature to 1100 K at Pressures up to 800 MPa | Issue 6 - Journal of Physical and Chemical Reference Data,” *J. Phys. Chem. Ref. Data*, vol. 25, no. 6, pp. 1509-1596, 1996.

[100] R. Tillner-Roth and A. Yokozeki, “An International Standard Equation of State for Difluoromethane (R-32) for Temperatures from the Triple Point at 136.34 K to 435 K and Pressures up to 70 MPa | Browse - Journal of Physical and Chemical Reference Data,” *J. Phys. Chem. Ref. Data*, vol. 26, no. 6, pp. 1273-1328, 1997.

[101] V. Nikulshin, C. Wu, and V. Nikulshina, “Exergy efficiency calculation of energy intensive systems,” *Exergy, An International Journal*, vol. 2, no. 2, pp. 78-86, 2002.

[102] R. L. Powell, “CFC phase-out: have we met the challenge?,” *Journal of Fluorine Chemistry*, vol. 114, no. 2, pp. 237-250, 2002.

[103] D. Manolakos, G. Kosmadakis, S. Kyritsis, and G. Papadakis, “On site experimental evaluation of a low-temperature solar organic Rankine cycle system for RO desalination,” *Solar Energy*, 2008.

[104] M. J. Moran and H. N. Shapiro, *Fundamentals of Engineering Thermodynamics*, 6th ed. Wiley, 2007.

[105] Feng Xu, “Analysis of a novel combined thermal power and cooling cycle using ammonia-water mixture as a working fluid,” University of Florida, 1997.

[106] P. Domanski, “A simplified cycle simulation model for the performance rating of refrigerants and refrigerant mixtures,” *International Journal of Refrigeration*, vol. 15, no. 2, pp. 81-88, 1992.

[107] G. Venkatarathnam, “Effect of mixture composition on the formation of pinch points in condensers and evaporators for zeotropic refrigerant mixtures Influence des compositions de mélanges zéotropiques sur la formation de points de pincement dans les condenseurs et les évaporateurs utilisant ces mélanges,” *International Journal of Refrigeration*, vol. 22, no. 3, pp. 205-215, 1999.

[108] H. Chen, D. Y. Goswami, and E. K. Stefanakos, “A review of thermodynamic cycles and working fluids for the conversion of low-grade heat,” *Renewable and Sustainable Energy Reviews*, vol. 14, no. 9, pp. 3059-3067, Dec. 2010.

APPENDICES

Appendix A. The Equation of State

In thermodynamics, an equation of state is a relation between state variables. An equation of state is a thermodynamic equation describing the state of matter under a given set of physical conditions. It expresses a mathematical relationship between two or more state functions associated with the subject, such as its temperature, pressure, volume or internal energy. In this dissertation, equation of state is used to describe the properties of fluids and mixtures of fluids. The following is a

The ideal gas law is the equation of state to describe relationships among the thermodynamic properties of a hypothetical ideal gas. The ideal gas law was first stated by Émile Clapeyron in 1834 as a combination of Boyle's law and Charles's law. Although it has several limitations, especial for high pressure gas or big molecular gas, it is a good approximation to the behavior of many gases under many conditions.

The state of an amount of gas is determined by its pressure, volume, and temperature, which expression can be found as:

$$pV = nRT \tag{A1}$$

where p is the absolute pressure of the gas, in pascals; V is the volume in cubic metres; n is the amount of substance in moles; R is the gas constant with the value of 8.314472 $\mathrm{J{\cdot}K^{-1}{\cdot}mol^{-1}}$; and T is the absolute temperature in Kelvin.

The Van der Waals equation of state may be written as:

$$\left(p + \frac{a}{V_m^2}\right)(V_m - b) = RT \tag{A2}$$

where V_m is molar volume, and a and b are substance-specific constants. The values of a and b can be calculated from the critical pressure p_c, critical temperature T_c and critical molar volume V_c as:

$$a = 3p_c V_c^2$$

$$b = \frac{V_c}{3}$$

The values of a and b are also written as:

$$a = \frac{27(RT_c)^2}{64p_c}$$

$$b = \frac{RT_c}{8p_c}$$

The van der Waals equation of state was one of the first to describe the thermodynamic properties significantly better than the ideal gas law. In the equation, a is recognized as the attraction parameter and b the effective molecular volume. The van der Waals equation is superior to the ideal gas law and can predict the formation of a liquid phase due to two reasons:

(1) Molecules are considered as particles with volume, not material points. Thus V cannot be less than some constant, or it should be replaced by $(V - b)$.

(2) Instead of disregarding the interaction among the molecules, we consider molecules attracting others within a distance of several molecules' radii.

With consideration of the volume of the particles and their interaction among each other, another form of the van der Waals equation of state can be written as:

$$\left(P_r + \frac{3}{V_r^2}\right)(3V_r - 1) = 8T_r \tag{A3}$$

This equation is in a reduce format, where the reduced state variables are: $V_r=V_m/V_c$, $P_r=P/P_c$ and $T_r=T/T_c$.

Although the van der Waals equation of state is much more advanced, other modern equations of greater complexity developed based on different matters are much more accurate and used more often in modern days.

Developed in 1976, Peng-Robinson equation of state was developed to meet the following goals:

(1) The parameters should be able to be expressed in terms of the critical properties and the acentric factor.

(2) The model should predict the behavior of the matter near its critical point with reasonable accuracy, particularly for calculations of the compressibility factor and liquid density.

(3) The mixing rules should only employ a single binary interaction parameter, and it is independent of temperature and the composition.

(4) The equation of state should be applicable to all predictions of all fluids properties in natural gas processes.

An expression of the Peng-Robinson equation of state is:

$$p = \frac{RT}{V_m - b} - \frac{a\,\alpha}{V_m^2 + 2bV_m - b^2} \tag{A4}$$

$$a = \frac{0.45724\,R^2\,T_c^2}{p_c}$$

$$b = \frac{0.07780\,R\,T_c}{p_c}$$

$$\alpha = \left(1 + \left(0.37464 + 1.54226\,\omega - 0.26992\omega^2\right)\left(1 - T_r^{0.5}\right)\right)^2$$

$$T_r = \frac{T}{T_c}$$

In polynomial form:

$$A = \frac{a\alpha p}{R^2\,T^2}$$

$$B = \frac{bp}{RT}$$

$$Z^3 - (1 - B)\,Z^2 + (A - 2B - 3B^2)\,Z - (AB - B^2 - B^3) = 0$$

where, ω is the acentric factor of the species, R is the universal gas constant and Z=PV/(RT) is compressibility factor.

The thermodynamic properties of the working fluids appeared in this study are obtained based on Peng-Robinson equation of state, and validated using NIST database.

Appendix B. Error Analysis

Peng-Robinson Equation of State was used to get the properties of the working fluids and an expression of the equation is shown in Appendix A. For the completeness of this analysis, the Peng-Robinson equation of state is written again as:

$$P = \frac{RT}{V-b} - \frac{a(T)}{V(V+b)+b(V-b)} \tag{B1}$$

where

$$a(T) = 0.45724\frac{R^2T_c^2}{P_c}\text{alpha}(T)$$

$$b = 0.07780\frac{RT_c}{P_c}$$

$$\text{alpha}(T) = [1 + k(1 - \text{squrt}\frac{T}{Tc})]^2$$

$$k = 0.37464 + 1.54226w - 0.26992w^2$$

Substituting a(T), b, alpha(T),and k into the equation of state gives:

$$P = \frac{RT}{V-0.07780\frac{RT_c}{P_c}} - \frac{0.45724\frac{R^2T_c^2}{P_c}[1+(0.37464+1.54226w-0.26992w^2)(1-\text{squrt}\frac{T}{Tc})]^2}{V\left(V+0.07780\frac{RT_c}{P_c}\right)+(0.07780\frac{RT_c}{P_c})(V-0.07780\frac{RT_c}{P_c})} \tag{B2}$$

The acentric factor w is a constant, 0.7. Thus the equation of state of a fluid is a function of its critical temperature T_c, and critical pressure P_c.

In order to validate the property of the working fluids that used in the investigation, a comparison between the data from NIST and ChemCAD is carried out in the following.

The critical temperature and critical pressure data from the two data sources are tabulated below.

Appendix B. (Continued)

Table B.1 Error analysis

Working fluid / ***Data Source***	***R134a***		***R32***		***R245fa***		***CO_2***	
	Tc (K)	***Pc (MPa)***	***Tc (K)***	***Pc (MPa)***	***Tc (K)***	***Pc (MPa)***	***Tc (K)***	***Pc (MPa)***
NIST	374.21	4.0593	351.26	5.7820	427.20	3.6400	304.13	7.3773
Peng-Robinson Equation of state	374.23	4.0603	351.60	5.8302	427.20	3.6400	304.20	7.3815

The standard division of Tc is:

$$\sigma_{T_c} = \sqrt{\frac{\sum_k \left(T_{c_k} - \overline{T_c}\right)^2}{N}} = 0.34\text{K} \quad \text{(B3)}$$

The standard division of Pc is:

$$\sigma_{P_c} = \sqrt{\frac{\sum_k \left(P_{c_k} - \overline{P_c}\right)^2}{N}} = 0.0482\text{MPa} \quad \text{(B4)}$$

Appendix C. Selected Publication

Patent Pending:

D. Yogi Goswami, Huijuan Chen and Elias Stefanakos. Method and System for Generating Power from Low- and mid-Temperature Heat Sources, U.S. patent, filed February, 2010.

Journal Papers:

1. Huijuan Chen, D. Yogi Goswami, and Elias Stefanakos. A review of thermodynamic cycles and working fluids for the conversion of low-grade heat, Renewable and Sustainable Energy Reviews, 2010, 14(9), 3059-3067.
2. Huijuan Chen, D. Yogi Goswami, Muhammad M. Rahman, and Elias Stefanakos. A supercritical Rankine cycle using zeotropic mixture working fluids for the conversion of low-grade heat into power, Energy, in pressed.
3. Huijuan Chen, D. Yogi Goswami, Muhammad M. Rahman, and Elias Stefanakos. Energetic and Exergetic Analysis of CO2- and R32-based Supercritical Cycles for Low-grade Heat Conversion, Applied Energy, minor revision requested.
4. Huijuan Chen, D. Yogi Goswami, Muhammad M. Rahman, Elias Stefanakos, et al. Optimizing energy conversion using organic Rankine cycles and supercritical Rankine cycles, Energy, finished and to be submitted.

Appendix C. (Continued)

5. Huijuan Chen, Bin Chen, Zhi Zhuang, et al. Analytical study on the solar collecting performance of the Trombe wall in winter, Building Energy & Environment, 2006,25(2),1-6.

6. Bin Chen, Shirong Meng, Huijuan Chen, et al. The effect of Trombe wall on indoor humid climate, HV&AC, 2006, 36(3), 42-46.

7. Bin Chen, Huijuan Chen, Shirong Meng, et al. The effect of Trombe wall on indoor humid climate in Dalian, China, Renewable Energy, 2006, 31(3), 333-343.

8. Huijuan Chen and Bin Chen. Coupled heat and mass transfer research on porous building materials: A review, HV&AC, 2004, 34(11), 24-29.

Conference Proceedings:

1. Huijuan Chen, D. Yogi Goswami, Muhammad M. Rahman, and Elias Stefanakos. Supercritical thermodynamic cycle for power generation from low- and mid-temperature heat sources, Proceedings of ASME 2010 4th international conference on Energy Sustainability, Phoenix, AZ, May 17-22, 2010.

2. Huijuan Chen, D. Yogi Goswami, Muhammad M. Rahman, and Elias Stefanakos. The conversion of moderate temperature heat into power and refrigeration, Proceedings of the Annual Meeting of the American Institute of Chemical Engineers, Philadelphia, PA, November 16-21, 2008.

Appendix D. Patent Flyer

Below is the flyer of the patent filed based on my Ph. D. research.

Method and System for Generating Power from Low- and Mid-Temperature Heat Sources

Researchers at the University of South Florida have developed a technology that relates to power plants, and the ability to convert thermal energy into electricity. In particular, this technology converts low- to mid-temperature heat into work and electricity via a supercritical Rankine cycle using zeotropic fluids as the working fluids.

This invention was conceived in order to improve the efficiency of converting low to-mid-temperature (typically below 250°C) heat into electricity. Our system uses zeotropic fluid mixtures which, when heated at a high pressure, immediately flash into supercritical vapor. Once supercritical, the fluid powers a turbine. The supercritical vaporization improves the heat exchange efficiency in the boiler. Furthermore, our zeotropic fluid exhibits a temperature glide which improves the heat exchange efficiency in the condenser also.

The combined effect of both of these improvements is an increase in the efficiency of the system by 60%. The working fluid is claimed to be a mixture of various refrigerants or hydrocarbons. It is important to note that the fluids used in this zeotropic working fluid mixture are environmentally friendly.

Appendix D. (Continued)

The working fluid mixture used in this invention operates in the temperate range of 80°C-250°C, which is easily available from low- and mid- temperature solar collectors, geothermal wells, or waste thermal discharges in various industrial sectors. The major advantages are:

(1) Ability to convert low- to mid- temperature heat into electricity more efficiently.

(2) Requires a less complicated system setup.

Appendix E. Professional Activities

Organizer, E3 (Energy, Environment and Economy) Event in Tampa bay, 9/2010.

Presenter, ASME 2010 4th International Conference on Energy Sustainability, Phoenix, AZ, 5/1020.

Presenter, Earth Day event Tampa Bay edition, 4/2010

Participant, Solar Advisor Model (SAM) model online training by NREL, 1/2010

Organizer, American Solar Energy Society (ASES) Solar Tour Tampa Bay Edition, Tampa, FL, 10/2009

Delegate, Education Without Borders 2009, Dubai, UAE, 03-04/2009

Participant, UK Energy Research Center (UKERC) Energy Summer School, London, UK, 06/2008

Presenter, 2008 Poster Symposium & Competition: "Global Challenges for the 21st Century", Florida, USA, 11/2008

Presenter, Research One: College of Engineering Research Week Celebration, Florida, USA, 11/2008

Presenter, Showcase on "An Energy Forum to Discuss Energy Solutions", Florida, USA 10/2008

Presenter, Clean Energy Alternatives Series in Florida, St. Augustine, USA, 08/2008

Presenter, ASME conference in Jacksonville, Florida, USA, 08/2008

Presenter, AiChE conference in Philadelphia, Pennsylvania, USA 11/2008

Appendix E. (Continued)

Organizer, Focus the Nation symposium: Global Warming Solutions for America, Florida, USA, 01/2008

Presenter, Engineering Expos 2007, 2008 and 2009, Florida, USA

Participant, CFD modeling software training, Dalian, China. 07/2005

ABOUT THE AUTHOR

Huijuan Chen was born to her beloved parents Aiguo Chen and Darun Fu in Luoyang, China, a beautiful place and one of the cradles of Chinese civilization. After completing her Bachelor of Science at Daqing Petroleum Institute in 2003, she entered Dalian University of Technology to pursue a Master of Science degree, where she wrote a thesis on the design and modeling of a passive solar house.

In August 2006, she entered the Graduate School of the University of South Florida to conduct her Ph.D. study. During her Ph.D. study, she finished two projects for two industrial companies, filed a patent with her advisors titled 'Method and systems for generating power from low and mid-temperature heat sources', published several articles on accredited journals including *Sustainable and Renewable Energy Reviews* and *Energy*, and presented her thesis and dissertation research findings at national and international venues. She graduates with a Doctor of Philosophy in Chemical Engineering from the University of South Florida in 2010 where she wrote a dissertation on the conversion of low-grade heat into power using supercritical Rankine cycles.